The k - meson nucleon interaction & the hadron – nucleus interaction

David Budgen

THE K^- - MESON NUCLEON INTERACTION

&

THE HADRON - NUCLEUS INTERACTION

THESIS SUBMITTED TO THE

UNIVERSITY OF DURHAM

BY

DAVID BUDGEN B.Sc. (DUNELM)

FOR THE DEGREE OF DOCTOR OF PHILOSOPHY

Department of Physics

University of Durham

Date. September 1972

TO

MY PARENTS

ABSTRACT

In the first part two inelastic two-body channels of the $\bar{K}N$ system are examined in energy-dependent partial wave analyses in which each non-resonant partial amplitude is expanded in an orthogonal series of polynomials over a normalised energy-dependent variable. The resonances known to be present in these channels are investigated as well as any possible new resonant states. It is found that the existing resonances are generally adequate to describe the available data for the two channels and that for $K^-p \longrightarrow \Lambda\pi$ in particular, the present fits form a statistically good solution with little new structure other than in the background phases.

In the second part two particular examples of hadron-nucleus elastic scattering are studied using Glaubers multiple-scattering series. The first of these is the scattering of negative pi-mesons from Helium-4, which is studied in detail at medium and high energy. A complete spin and isospin dependent set of πN amplitudes are used together with a number of forms for the nuclear densities. It is found that the use of more elaborate forms does not provide any significantly better description than the more simple forms available and it is concluded that more realistic nuclear densities may be needed to describe the wide-angle data adequately.

The second case studied is the scattering of medium-energy protons from Carbon-12 and a modified form of Glauber series is used with the nucleus described as a state formed from three alpha-particles. Different forms of distribution for these are examined but are generally found to give little improvement over the simple harmonic oscillator densities. An improved α-particle density is proposed which may combine the best properties of the different forms used while retaining simplicity of calculation.

ACKNOWLEDGEMENTS

I would like to thank Dr.A. D. Martin for his supervision and encouragement during the work on the first part of this thesis and express my gratitude to him for initially introducing me to this subject and continually encouraging my interest.

I would also like to thank Professor B.H. Bransden for his supervision and encouragement throughout this work and for his many helpful suggestions and ideas and also Dr. F.D. Gault for his continued encouragement.

Finally I would like to thank the Science Research Council for the award of a Research Studentship which enabled me to carry out this work together with their assistance in allowing me the use of the Computing facilities at the Rutherford Laboratory.

C O N T E N T S

INTRODUCTION

At the present time, it is usually accepted that the forces which act between the so-called ' elementary particles ' may be broadly divided into four classes. In ascending orders of coupling strength these are, first the gravitational interaction, second the weak interaction, third the electromagnetic and fourth the so-called strong interaction. The effects of the first of these is quite unknown and of the remaining three the electromagnetic interaction is the only one where theory is able to match experiment.

For nuclear physics in general , and particularly the associated high-energy particle interactions the dominant force is usually the strong interaction of which the main features would appear to be its independence of electrical charge (e.g. it does not appear to differentiate between say a proton and a neutron) and its short range, characteristically of the order of 10^{-13} cm. Since such dimensions lie beyond the range of any ' optical ' investigations , knowledge of the details of these forces must come from experiments upon the scattering between incident beams of particles upon particle or nuclear targets.

Since the early days of the subject and particularly since the advent of the large accelerators, the spectrum of known 'elementary' particles has greatly increased, at a rate unfortunately not matched by any corresponding increase in success of the theories advanced to describe these, and which remain largely phenomenological in form. Most of the recently formed states have been classed as resonances, where the difference between a resonance and a particle lies simply in that the former may decay by the strong interaction, being therefore characterised by a much shorter lifetime. Of the 'particles' found in

nature very few are in fact stable although some possess relatively long lifetimes by nuclear standards. The different particles and resonances are generally recognised by their different masses and the values which are assigned to their internal quantum numbers such as Baryon number, strangeness and parity.

By means of these quantum numbers the particles (and resonances) may be divided into a number of groups, characterised by some common form taken by their quantum numbers. The first of such divisions is that of spin, those of half-integer spin being termed fermions, such as p , $e^{\pm}$ and $\mu^{\pm}$ and those of integral spin termed bosons, such as π , $K^{\pm}$ and ρ . Another (and distinct) division is into those particles which are affected by the strong interaction, termed hadrons and those not affected, termed the leptons, such as e, μ and ν . The latter are all fermions (so far) while the hadrons are further subdivided by spin into the baryons (of half-integral spin such as p, n, Λ) and the mesons (of integral spin such as π , ρ , K). These form the main divisions which are conveniently used and the studies which will be described are concerned with the strong interaction between mesons and baryons, both singly and collectively.

Due to the lack of any independent theory, the knowledge of the strong interaction has been largely acquired by phenomenological studies which attempt to utilise the general properties of the interaction as widely as possible. These generally rely upon ' conservation laws ' which refer to eigenvalues or quantum numbers which appear to be preserved by the strong interaction, for example the Partial Wave Analysis relies upon the conservation of total angular momentum during a collision between particles.

As yet little is understood of the Strong interaction other than such basic properties as these conservation laws enshrine and the current objects of theoretical studies of the interaction are generally to utilise such knowledge to best advantage in the attempts to better understand the laws which govern the Strong interaction.

PART I

THE K^- - MESON NUCLEON INTERACTION

CHAPTER 1 The Partial-Wave Analysis

1:1 Introduction

In the present state of our knowledge of the strong interaction, the Partial Wave Analysis[1] forms a convenient and successful means for examining and analysing the experimental data for processes of the form

$$a + B \longrightarrow c + D$$

where c and D are not necessarily different to a and B; up to energies in excess of 3 GeV, above which the large number of partial waves required becomes a problem. By this means we are able to analyse those processes which involve an intermediate state, and which take the form

$$a + B \longrightarrow X^* \longrightarrow c + D$$

known as "formation" processes, where the resonant state X^* with definite quantum numbers is formed from the channel aB, decaying into the channel cD. From such analysis we may determine both the quantum numbers and the parameters for such a resonance.

In its most ideal form the partial wave analysis, which is obtained by expanding the complete scattering amplitude in terms of a set of linearly independent eigenstates of the total angular momentum, provides an analysis which is free of any model-dependence or bias.

We are able to make and utilise such an expansion because of the conservation laws for angular momentum $\underline{L}$, where for a central force, characterised by its Hamiltonian H, we may show[2]

$$\left[H , \underline{L} \right] = 0 \qquad (1.1)$$

and L^2 is therefore a conserved quantity (constant of the motion) and it is then advantageous to work with the eigenstates of L^2 .

To date, an encouraging consistency has been observed between

results obtained by such analyses and those obtained from other forms such as the "production" processes, of the form

$$a + B \longrightarrow X^{*} + \text{other particles}$$

for the low-energy data, and also the ability of the Partial Wave Analysis to analyse and seperate the many short-lived resonant states of definite angular momentum[3] has proved of great use.

In making such an analysis, our object is to determine the magnitudes of the amplitudes corresponding to the angular momentum eigenstates and to determine their individual variation with the energy of the incident particle. In order to achieve this object we should therefore perform the analysis energy by energy, obtaining a set of solutions for each and selecting between these by the requirement of continuity[4].

Unfortunately in practice, one is rarely able to perform an analysis in this manner, due both to the limitations of the data available at each energy, and also to the volume of computing power required. To make an energy-independent analysis we require at each energy that the number of data points should be at least as large as the number of parameters and for the $\bar{K}N$ system this is rarely realised. In such a case therefore, where the data is insufficient for an energy-independent analysis, one must resort to some other means of utilising the available data, usually by assuming an energy--dependent parameterisation for the partial wave amplitudes. Unfortunately the variation with energy of the individual amplitudes forms one of the aims of the analysis and a major problem is to reconcile necessity with this aim.

There are many forms for such energy-dependent parameterisations, for example at low energies we may use the effective range method[5],

and in the high energy regions we may resort to parameterisation of the higher partial wave amplitudes by means of the high-energy approximations[6]. For the analyses presented here, all the results have been obtained by describing the energy-dependence of each amplitude as an expansion in orthogonal polynomials over a normalised energy variable[7], which hopefully forms the most flexible form of parameterisation in this region.

The problems outlined above, arise because of our lack of knowledge as to the form of the strong interaction, lacking any form of potential we must resort to purely phenomenological methods in analysing experiment. In the manner used here, the partial wave analysis permits the determination of the parameters of the resonant states encountered, and in particular of the $Y_1^*(1670)$ state which occurs in the channels considered.

1:2 The Partial Wave Expansion

In analysing two-body scattering processes we must include in the analysis provision for the spin (intrinsic angular momentum) of the particles involved, since those processes for which data currently exists usually involve at least one particle of non-zero spin. For the derivation of the expansion there is a choice of representations, including the helicity representation[8] commonly encountered at high energy, but in this section we have preferred an older form, using the wave-function approach which is the formalism usually incountered in the partial-wave analyses of $0^-\frac{1}{2}^+ \longrightarrow 0^-\frac{1}{2}^+$.

It is convenient to introduce the notation used by considering in outline the scattering of two spin zero particles, after which this may be extended to the scattering between spin 0 and spin $\frac{1}{2}$ particles[9].

We describe the incident particle as a plane-wave state, and choose the direction of incidence to be the z-axis, so that the incident state has the form,

$$\Psi_i(\underline{r}) = e^{i\underline{k}.\underline{r}} = e^{ikz} \qquad (1.2)$$

and after scattering, the final state has the asymptotic form,

$$\Psi_f(\underline{r}) \underset{r \to \infty}{=} e^{i\underline{k}.\underline{r}} + \frac{f(\theta,\Phi)}{r} e^{ikr} \qquad (1.3)$$

where the first term represents the unscattered part and the second term describes the scattered part in terms of a spherical wave-front originating at the scattering centre, $f(\theta,\Phi)$ being the scattering amplitude which represents the probability of scattering into θ and Φ so that the differential cross-section $\frac{d\sigma}{d\Omega}$ is given by

$$\frac{d\sigma}{d\Omega} = \left| f(\theta,\Phi) \right|^2 \qquad (1.4)$$

and for a cylindrically symmetric potential

$$f(\theta,\Phi) \longrightarrow f(\theta)$$

so that

$$\frac{d\sigma}{d\Omega} = \left| f(\theta) \right|^2 \qquad (1.5)$$

The method of partial waves consists of expanding Ψ_i and Ψ_f in terms of Legendre polynomials, which are eigenfunctions of L^2, so that

$$\begin{aligned} \Psi_i(\underline{r}) &= \sum_\ell r^{-1} v_\ell(r) P_\ell(\cos\theta) \\ \Psi_f(\underline{r}) &= \sum_\ell r^{-1} u_\ell(r) P_\ell(\cos\theta) \end{aligned} \qquad (1.6)$$

where $v_\ell(r)$ and $u_\ell(r)$ are solutions of the Shrödinger equation for a free particle

$$\frac{d^2 v_\ell(r)}{dr^2} + \left[k^2 - \frac{\ell(\ell+1)}{r^2} \right] v_\ell(r) = 0 \qquad (1.7)$$

and for scattering from a potential U(r)

$$\frac{d^2 u_\ell(r)}{dr^2} + \left[k^2 - U(r) - \frac{\ell(\ell+1)}{r^2} \right] u_\ell(r) = 0 \qquad (1.8)$$

Taking the asymptotic forms, since it is these that are observed, as $r \longrightarrow \infty$, we get

$$\Psi_i(\underline{r}) = e^{ikr\cos\theta} = e^{ikz}$$

$$= \frac{1}{2ikr} \sum_\ell (2\ell+1) \left\{ e^{ikr} - e^{i\ell\pi} - e^{-ikr} \right\} P_\ell(\cos\theta) \qquad (1.9)$$

and

$$\Psi_f(\underline{r}) = \frac{1}{2ikr} \sum_\ell (2\ell+1) \left\{ \eta_\ell e^{ikr+2i\delta_\ell} - e^{i\ell\pi} - e^{-ikr} \right\} P_\ell(\cos\theta) \qquad (1.10)$$

where the effect of the potential at large r is to alter the phase of the ℓ-th outgoing wave by $2\delta_\ell$ (the phase shift) and to attenuate it by a factor η_ℓ ($0 \leq \eta_\ell \leq 1$)

From these two expansions (1.9) and (1.10) we obtain $f(\theta)$ as

$$f(\theta) = \frac{1}{2ik} \sum_\ell (2\ell+1) \left\{ \eta_\ell e^{2i\delta_\ell} - 1 \right\} P_\ell(\cos\theta) \qquad (1.11)$$

so that

$$\left.\frac{d\sigma}{d\Omega}\right|_{el} = |f(\theta)|^2 = \lambda^2 \left| \sum_\ell (2\ell+1) \left\{ \frac{\eta_\ell e^{2i\delta_\ell} - 1}{2i} \right\} P_\ell(\cos\theta) \right|^2 \qquad (1.12)$$

where $\lambda = 1/k$ is referred to as the wave number.

In terms of the more compact S-matrix notation, for elastic scattering we define the ℓ-th element of S to be

$$S_\ell = \eta_\ell \exp\left[2i\delta_\ell \right] \qquad (1.13)$$

where

$$S^+S = SS^+ = I$$

and defining the transition matrix T in the usual manner

$$S = I + 2iT \tag{1.14}$$

we obtain from (1.12)

$$\left.\frac{d\sigma}{d\Omega}\right|_{el} = \lambda^2 \left| \sum_{\ell} (2\ell + 1)\, T_\ell\, P_\ell(\cos\theta) \right|^2 \tag{1.15}$$

For physical cases of scattering we must now extend this to include spin, as those to be considered will involve the scattering of spin 0 particles from spin $\frac{1}{2}$ targets, although the formalism is unaltered if these are reversed since we work in the centre of mass system.

In this case both the total angular momentum $\underline{J} = \underline{L} + \underline{S}$ and the orbital angular momentum $\underline{L}$ are conserved, and an expansion is required in eigenfunctions of both $\underline{J}$ and $\underline{L}$.

To include the effect of spin, we modify the description of the initial state of the system to describe the spin state $\chi_s^{m_s}$, where s is the spin, and m_s its third component, so that

$$\Psi_i \longrightarrow e^{ikz}\, \chi_s^{m_s} \tag{1.16}$$

and expanding as before

$$\Psi_i = \chi_s^{m_s} \sum_{\ell} r^{-1} f_\ell(r)\, P_\ell(\cos\theta) \tag{1.17}$$

For a complete description, this should be averaged over all values of m_s for an unpolarised target or beam, but it is more convenient to deal with only one spin state and leave the averaging until later.

To expand this in terms of $\underline{J}$, the total angular momentum, we must first consider the rules for combining angular momentum and the eigenfunctions of the operators[10].

Let $Y_{j_1}^{m_1}$ be the normalised eigenfunction for a state characterised by j_1 and m_1 . Then for a total angular momentum $\underline{J} = \underline{j}_1 + \underline{j}_2$,

the product function $Y^{m_1}_{j_1} Y^{m_2}_{j_2}$ is an eigenfunction of the third component $M = m_1 + m_2$ but not in general a simultaneous eigenfunction of J^2, whose eigenfunction we denote by $Z^M_{J j_1 j_2}$. We require therefore an expression for the product $Y^{m_1}_{j_1} Y^{m_2}_{j_2}$ in terms of the Z's, which we obtain using the usual Clebsch-Gordan coefficients C , given by

$$Z^M_{J j_1 j_2} = \sum_{m_1=-j_1}^{j_1} \sum_{m_2=-j_2}^{j_2} C_{j_1 j_2}(J, M; m_1 m_2)\, Y^{m_1}_{j_1} Y^{m_2}_{j_2} \qquad (1.18)$$

and since the Z's and Y's form orthonormal sets we use the relation

$$\sum_{m_1=-j_1}^{j_1} \sum_{m_2=-j_2}^{j_2} C_{j_1 j_2}(J, M; m_1 m_2)\, C_{j_1 j_2}(J', M'; m_1 m_2) = \delta_{JJ'}\, \delta_{MM'} \qquad (1.19)$$

to obtain from (1.18) the expansion

$$Y^{m_1}_{j_1} Y^{m_2}_{j_2} = \sum_{J=|j_1-j_2|}^{j_1+j_2} \sum_{M=-J}^{J} C_{j_1 j_2}(J, M; m_1 m_2)\, Z^M_{J j_1 j_2} \qquad (1.20)$$

The $C_{j_1 j_2}$'s are well-known functions[10] and Table I gives their values for $j_1 = \frac{1}{2} = s$

	$m_s = +\frac{1}{2}$	$m_s = -\frac{1}{2}$
$J = +\frac{1}{2}$	$\left(\frac{+ M + \frac{1}{2}}{2 + 1}\right)^{\frac{1}{2}}$	$\left(\frac{- M + 1/2}{2 + 1}\right)^{\frac{1}{2}}$
$J = -\frac{1}{2}$	$-\left(\frac{- M + 1/2}{2 + 1}\right)^{\frac{1}{2}}$	$\left(\frac{+ M + 1/2}{2 + 1}\right)^{\frac{1}{2}}$

Table I

Values of Clebsch-Gordan Coefficients for $j_1 = \frac{1}{2}$

In this case the Y^m_j's are the normalised spherical harmonics

and we may write

$$P_\ell(\cos\theta)\ \chi^m_s = \left(\frac{4\pi}{2\ell+1}\right)^{\frac{1}{2}} Y^0_\ell(\theta)\ \chi^m_s$$

$$= \left(\frac{4\pi}{2\ell+1}\right)^{\frac{1}{2}} \sum_{J=|\ell-s|}^{\ell+s} C_{\ell s}(J, M=m_s; 0 m_s)\ Z^{m_s}_{J\ell s} \qquad (1.21)$$

so that the incident state becomes

$$\Psi_i = e^{ikz}\ \chi^m_s$$

$$= (4\pi)^{\frac{1}{2}} \sum_{J_{min}} \sum_{\ell=|J-s|}^{J+s} (2\ell+1)^{\frac{1}{2}} f_\ell(r)\ C_{\ell s}(J, M=m_s; 0\ m_s)\ Z^m_{J\ell s} \qquad (1.22)$$

and the final state similarly takes the form

$$\Psi_f = (4\pi)^{\frac{1}{2}} \sum_{J_{min}} \sum_{\ell=|J-s|}^{J+s} (2\ell+1)^{\frac{1}{2}} g_\ell(r)\ C_{\ell s}(J, M=m_s; 0\ m_s)\ Z^m_{J\ell s} \qquad (1.23)$$

and the asymptotic form of the scattered wave becomes

$$\Psi_{scatt} \xrightarrow[r \to \infty]{} \frac{e^{ikr}}{r}\left(\frac{\pi^{\frac{1}{2}}}{ik}\right) \sum_{J_{min}} \sum_{\ell=|J-s|}^{J+s} (2\ell+1)^{\frac{1}{2}}\ C_{\ell s}(J, M=m_s; 0\ m_s)\ x$$

$$x \left\{ \exp\left[2i\delta^{Jm}_\ell\right] - 1 \right\} Z^{m_s}_{J\ell s} \qquad (1.24)$$

At this point, we must average over all the spin states occuring for an unpolarised target or beam, and writing for brevity the two spin states involved for $s = \frac{1}{2}$ as

$$\chi^{\frac{1}{2}}_{\frac{1}{2}} = \alpha \qquad \text{and} \qquad \chi^{-\frac{1}{2}}_{\frac{1}{2}} = \beta$$

we have (from Table I) for $m_s = +\frac{1}{2}$

$$Z^{\frac{1}{2}}_{\ell+\frac{1}{2},\ell,\frac{1}{2}} = (4\pi)^{-\frac{1}{2}} \left\{ (\ell+1)^{\frac{1}{2}} P_\ell(\cos\theta)\alpha - (\ell+1)^{-\frac{1}{2}} P^1_\ell(\cos\theta)\ e^{i\Phi}\ \beta \right\}$$

(1.25)

$$Z^{\frac{1}{2}}_{\ell-\frac{1}{2},\ell,\frac{1}{2}} = -(4\pi)^{-\frac{1}{2}} \left\{ \ell^{\frac{1}{2}} P_\ell(\cos\theta)\alpha + \ell^{-\frac{1}{2}} P^1_\ell(\cos\theta)\ e^{i\Phi}\ \beta \right\}$$

and also

$$C_{\ell,\frac{1}{2}}(\ell+\tfrac{1}{2},\tfrac{1}{2};\ 0,\ \tfrac{1}{2}) = \left(\ \ell+1/\ 2\ell+1\ \right)^{\frac{1}{2}}$$

$$C_{\ell,\frac{1}{2}}(\ell-\tfrac{1}{2},\tfrac{1}{2};\ 0\ \tfrac{1}{2}) = -\left(\ \ell/\ 2\ell+1\ \right)^{\frac{1}{2}} \tag{1.26}$$

so that (1.24) becomes

$$\Psi_{scatt} \longrightarrow\quad r^{-1}\ e^{ikr}\ (\ f(\theta)\ \alpha\ -\ g(\theta)\ e^{i\Phi}\beta\ ) \tag{1.27}$$

where

$$f(\theta) = \frac{1}{2ik}\sum_{\ell}\left[(\ell+1)\left\{e^{2i\delta_\ell^{\ell+\frac{1}{2}}}-1\right\} + \ell\left\{e^{2i\delta_\ell^{\ell-\frac{1}{2}}}-1\right\}\right]P_\ell(\cos\theta)$$

$$g(\theta) = \frac{1}{2ik}\sum_{\ell}\left[\ e^{2i\delta_\ell^{\ell+\frac{1}{2}}} - e^{2i\delta_\ell^{\ell-\frac{1}{2}}}\ \right]P_\ell^1(\cos\theta) \tag{1.28}$$

and in terms of the T-matrix introduced earlier, we may write

$$T_\ell^+ = \frac{1}{2i}\left\{e^{2i\delta_\ell^{\ell+\frac{1}{2}}}-1\right\}$$

$$T_\ell^- = \frac{1}{2i}\left\{e^{2i\delta_\ell^{\ell-\frac{1}{2}}}-1\right\}$$

so that (1.28) become

$$f(\theta) = \frac{1}{k}\sum_{\ell}\left\{(\ell+1)\ T_\ell^+ + \ell T_\ell^-\right\}P_\ell(\cos\theta)$$

$$g(\theta) = \frac{1}{k}\sum_{\ell}\left\{T_\ell^+ - T_\ell^-\right\}P_\ell^1(\cos\theta) \tag{1.29}$$

and for $m_s = -1/2$, we obtain

$$\Psi_{scatt} \longrightarrow\quad r^{-1}\ e^{ikr}\ (\ f(\theta)\ \beta\ +\ g(\theta)\ e^{i\Phi}\alpha\ ) \tag{1.30}$$

and averaging over the spin co-ordinates we then obtain

$$\frac{d\sigma}{d\Omega} = \left|f(\theta)\right|^2 + \left|g(\theta)\right|^2 \tag{1.31}$$

where $f(\theta)$ is referred to as the non-spin-flip amplitude and $g(\theta)$ as the spin-flip amplitude.

In the presence of spin, it is possible to make measurements

of the final state polarisation, and the polarisation $\underline{P}$ is defined by

$$\underline{P} = \underline{n} \frac{2\,\mathrm{Im}(\, f^{*}(\theta)\, g(\theta)\,)}{|f(\theta)|^{2} + |g(\theta)|^{2}} \qquad (1.32)$$

so that

$$\underline{P}\frac{d\sigma}{d\Omega} = \underline{n}\, 2\,\mathrm{Im}(\, f^{*}(\theta)\, g(\theta)\,) \qquad (1.33)$$

where $\underline{n}$ is a unit vector perpendicular to the plane of scattering. Measurement of the polarised differential cross-section is therefore of use in determining $f(\theta)$ and $g(\theta)$ and in resolving the Minami ambiguity[11] which arises for this case.

This is because under parity exchange for the same J, e.g. $f_{l+} \longleftrightarrow f_{l-}$, $d\sigma / d\Omega$ remains invariant for the $0^{-}\frac{1}{2}^{+}$ reactions, but as discussed further in Chapter IV, the value of $\underline{P}\, d\sigma / d\Omega$ does change sign under parity exchange and can therefore be used to resolve this ambiguity.

The Partial Wave analysis must also be extended to cover the inelastic reactions where in terms of the S-matrix, scattering from channel α into channel β is described by an off-diagonal matrix element $S_{\beta\alpha}$ where

$$S^{J}_{\beta\alpha} = S^{J}_{\alpha\beta} = \eta^{J}_{\alpha\beta} \exp(\, 2i\, \delta^{J}_{\alpha\beta}\,) \qquad (1.34)$$

so that the T-matrix for elastic and inelastic scattering will take the forms from (1.14) of

$$T^{J}_{\alpha\alpha} = \left\{ \eta^{J}_{\alpha\alpha} \exp(2i\, \delta^{J}_{\alpha\alpha}) - 1 \right\} / 2i \qquad (1.35)$$

and

$$T^{J}_{\alpha\beta} = \eta^{J}_{\alpha\beta} \exp(2i\, \delta^{J}_{\alpha\beta}) / 2i \qquad (1.36)$$

so that the real and imaginary parts of $T^{J}_{\alpha\beta}$ are given by

$$\text{Re } T^J_{\alpha\beta} = 1/2 \ \eta^J_{\alpha\beta} \sin 2\delta^J_{\alpha\beta}$$

$$\text{Im } T^J_{\alpha\beta} = -1/2 \ \eta^J_{\alpha\beta} \cos 2\delta^J_{\alpha\beta} \qquad (1.37)$$

and from the unitarity condition ($\underline{S}^+\underline{S} = \underline{I}$) we find that

$$T^J_{\alpha\beta} \leq 1/2$$

so that for the inelastic channels, $T^J_{\alpha\beta}$ is constrained to lie within a circle of radius 1/2, centred at the origin.

CHAPTER 2 The $\bar{K}N$ System

2:1 General features of the system

For a beam of negative K-mesons, incident upon a hydrogen target, a range of two and three body inelastic channels are open even at threshold, due to the system possessing a total hypercharge $Y = 0$, where the hypercharge Y is defined as

$$Y = B + S \qquad (2.1)$$

B being the baryon number and S, strangeness.

This forms a very distinctive and unique feature of the $\bar{K}N$ interaction. In Figure I we show the positions of the inelastic thresholds which lie below and around the K^-p threshold.

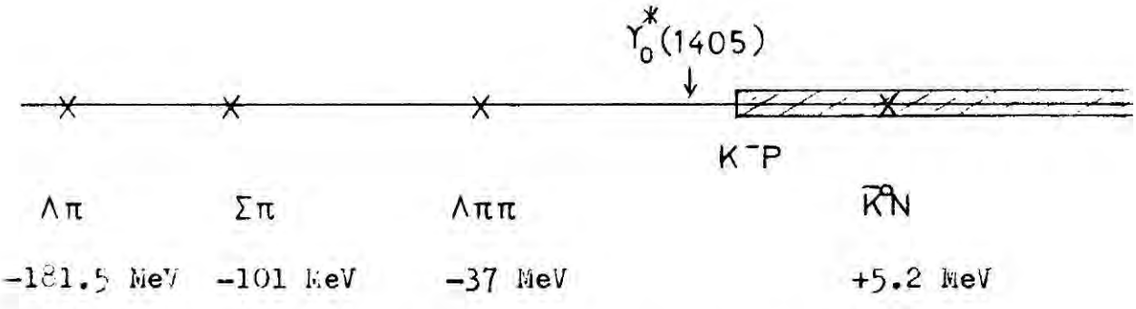

Figure I The $\bar{K}N$ thresholds

As an example, an experiment with K^- beam momentum around 500 MeV/c [12] lists data for six two-body channels, nine three-body channels and one four-body channel. Consequently seperation of the different reactions present may be difficult and the data and analyses from experiments in the $\bar{K}N$ system are rarely of high accuracy as compared with a system such as πN[4].

The $\bar{K}N$ system also possesses a large number of resonant states, the hyperon resonances of strangeness = -1, hypercharge = 0. As it is

a combination of isospin 0 and isospin 1 states, resonances of both isospin values are found and are conventionally denoted by either $Y_o^*(\text{mass})$ or $\Lambda(\text{mass})$ for the I = 0 resonances and $Y_1^*(\text{mass})$ or $\Sigma(\text{mass})$ for the I = 1 resonances. Many of these states have been found by partial wave analyses of formation experiments, the classic example being the $Y_o^*(1520)$ [13], a very well-established resonance[14]. Analyses of production experiments are also of great value, since many resonances are only weakly coupled to the two-body states, and in particular the parameters of the $Y_o^*(1405)$ [15] which lies below the K^-p threshold may only be determined in this way. From the nature of the data and the other features of the system one can see that the status of the Y^* resonances can vary greatly from the well established to the very doubtful.

2:2 The $\Lambda\pi$ and $\Sigma\pi$ channels

The two-body channels with which this analysis will be concerned are the $\Lambda\pi$ and $\Sigma\pi$ channels. The former has only one neutral mode $\Lambda\pi^o$, since the Λ has an isospin of zero while the latter possesses two charged ($\Sigma^+\pi^-$ and $\Sigma^-\pi^+$) and a neutral ($\Sigma^o\pi^o$) mode being a combination of both isospin states. Since the two-body channels of the $\bar{K}N$ system are $0^-\frac{1}{2}^+ \longrightarrow 0^-\frac{1}{2}^+$ the analysis uses the expansions described in Chapter 1.

The strong interaction does not mix states of different isospin values and so a set of phase-shifts is obtained for each of the isospin states present in a channel, so that each phase-shift and partial wave amplitude must be labelled by its value of isospin I in addition to its values of L and J, e.g. δ^I_{LJ} and $L_{I,2J}$, the latter being the spectroscopic notation by which the amplitudes are commonly labelled. Hence before being able to make a partial wave

expansion, the different channels must be decomposed into their constituent isospin states. Table II lists the values of I, I_3 and Y for the different particles concerned.

	I	I_3	Y
K^-	1/2	-1/2	-1
π^+	1	1	0
π^o	1	0	0
π^-	1	-1	0
p	1/2	1/2	1
Λ	0	0	0
Σ^+	1	1	0
Σ^o	1	0	0
Σ^-	1	-1	0

Table II - Values of I, I_3 and Y for $K^-p \longrightarrow \Lambda\pi,\ \Sigma\pi$

The decomposition of the amplitudes is made according to the same rules which govern angular momentum, using the expansion

$$|\alpha;I',I^2;I\ I_3\rangle = |\alpha;I',I^2;I_3'\ I_3^2\rangle \times \langle \alpha;I',I^2;I_3'I_3^2 | \alpha;I',I^2;I\ I_3\rangle \qquad (2.2)$$

We follow the SU(3) convention that $I' \longleftrightarrow$ baryon, and that $I^2 \longleftrightarrow$ meson [16], with the constraint on the third component

$$I_3^{K^-} + I_3^p = 0 = I_3' + I_3^2 \qquad (2.3)$$

The isospin states are denoted by $|\Phi_i^I\rangle$ where $I \longleftrightarrow$ isospin and i denotes the channel (1 = $\bar{K}N$, 2 = $\Sigma\pi$, 3 = $\Lambda\pi$). Considering

each channel in turn;

$\underline{\bar{K}N}$:

$$|1,0\rangle = (\tfrac{1}{2})^{\frac{1}{2}}|\bar{K}^0 n\rangle + (\tfrac{1}{2})^{\frac{1}{2}}|K^- p\rangle = |\Phi_1^1\rangle$$

$$|0,0\rangle = -(\tfrac{1}{2})^{\frac{1}{2}}|\bar{K}^0 n\rangle + (\tfrac{1}{2})^{\frac{1}{2}}|K^- p\rangle = |\Phi_1^0\rangle$$

so that

$$|K^- p\rangle = (\tfrac{1}{2})^{\frac{1}{2}}\left\{|\Phi_1^1\rangle + |\Phi_1^0\rangle\right\} \tag{2.4}$$

$\underline{\Sigma\pi}$:

$$|2,0\rangle = \frac{1}{\sqrt{6}}|\Sigma^+\pi^-\rangle + \sqrt{\frac{2}{3}}|\Sigma^0\pi^0\rangle + \frac{1}{\sqrt{6}}|\Sigma^-\pi^+\rangle = |\Phi_2^2\rangle$$

$$|1,0\rangle = \frac{1}{\sqrt{2}}|\Sigma^+\pi^-\rangle - \frac{1}{\sqrt{2}}|\Sigma^-\pi^+\rangle = |\Phi_2^1\rangle$$

$$|0,0\rangle = \frac{1}{\sqrt{3}}|\Sigma^+\pi^-\rangle - \frac{1}{\sqrt{3}}|\Sigma^0\pi^0\rangle + \frac{1}{\sqrt{3}}|\Sigma^-\pi^+\rangle = |\Phi_2^0\rangle$$

so that

$$\begin{aligned}
|\Sigma^0\pi^0\rangle &= \sqrt{\tfrac{2}{3}}\,|\Phi_2^2\rangle - \tfrac{1}{\sqrt{3}}\,|\Phi_2^0\rangle \\
|\Sigma^+\pi^-\rangle &= \tfrac{1}{\sqrt{6}}\,|\Phi_2^2\rangle + \tfrac{1}{\sqrt{2}}\,|\Phi_2^1\rangle + \tfrac{1}{\sqrt{3}}\,|\Phi_2^0\rangle \\
|\Sigma^-\pi^+\rangle &= \tfrac{1}{\sqrt{6}}\,|\Phi_2^2\rangle - \tfrac{1}{\sqrt{2}}\,|\Phi_2^1\rangle + \tfrac{1}{\sqrt{2}}\,|\Phi_2^0\rangle
\end{aligned} \tag{2.5}$$

$\underline{\Lambda\pi}$:

$$|1,0\rangle = |\Lambda^0\pi^0\rangle = |\Phi_3^1\rangle \tag{2.6}$$

and denoting the T-matrix elements as $T^I_{\alpha\beta}$, these are

$$\begin{aligned}
\langle \Sigma^0\pi^0|T|K^- p\rangle &= -\tfrac{1}{\sqrt{6}}\,T^0_{12} \\
\langle \Sigma^+\pi^-|T|K^- p\rangle &= \tfrac{1}{\sqrt{6}}\,T^0_{12} + \tfrac{1}{2}\,T^1_{12} \\
\langle \Sigma^-\pi^+|T|K^- p\rangle &= \tfrac{1}{\sqrt{6}}\,T^0_{12} - \tfrac{1}{2}\,T^1_{12} \\
\langle \Lambda^0\pi^0|T|K^- p\rangle &= \tfrac{1}{\sqrt{2}}\,T^1_{13}
\end{aligned} \tag{2.7}$$

From these it can be seen that the reaction $K^-p \longrightarrow \Lambda\pi$ is completely described by the $I = 1$ amplitudes while the $K^-p \longrightarrow \Sigma\pi$ channel requires both $I = 0$ and $I = 1$ amplitudes for its description.

Our analyses cover a centre of mass energy range of approximately 1600 - 1700 MeV in which there are three well established resonances present, two of $I = 0$, the $Y_0^*(1670)$ in the S_{01} amplitude and the $Y_0^*(1690)$ in the D_{03} amplitude, and one of $I = 1$, the $Y_1^*(1670)$ in the D_{13} amplitude. Of these the latter resonance is the most controversial and the situation in this energy region for the $I = 1$ states is far from clear[3], with discrepancies apparently arising between the formation and production experiments and analyses.

One hypothesis which has been advanced to explain these suggests the existence of two Y_1^*'s in this region, with the same spin-parity assignments[17], but decaying by different channels. Unfortunately the present state of knowledge makes this difficult to examine[18].

A major aim of these analyses was to make a further determination of the parameters of the $Y_1^*(1670)$, and to investigate the possibility of there being other resonant states in this region. The analyses of the $\Sigma\pi$ channel also allowed a further determination of the parameters of the two known Y_0^* resonances.

Table III shows the current states of the $I = 0$ and $I = 1$ resonances in the region 1600 - 1700 MeV and their status.

	Amplitude	Resonant Energy (MeV)	Comment
I = 0	S_{01}	1670	Well established
	D_{03}	1690	Well established
I = 1	S_{11}	1620	Weakly coupled, suggested by Kim's K-matrix analysis[19].
	P_{11}	1620	From $K^- p \longrightarrow \Sigma \pi$ and $\bar{K}^o n$, but only reported twice[19,20].
	?	1620	Production experiments suggest structure in this region which may correspond to the above states[18].
	D_{13}	1670	Well established but discrepancies between branching ratios from production and formation analyses.
	?	1690	Seen in production experiments[3]; may be linked to the problems in the D_{13} resonance above.

Table III

Resonances in the c.m. energy region 1600 - 1700 MeV.

CHAPTER 3 Parameterisation of the Partial Wave Amplitudes

3:1 Choice of parameterisation

As described in Chapter 1, the phase shifts may rarely be determined at each energy independently and some form of energy - - dependence must be used to interpolate over the range of energies. The $\Lambda\pi$ and $\Sigma\pi$ channels are such a case, since at the energies considered the number of variables required is larger than the volume of available data for each energy, so requiring some form of interpolation.

For the purposes of the analysis, the partial wave amplitudes are divided into two distinct groups, (i) those which are not known or believed to be resonant and (ii) those known or believed to be resonant. Since the parameterisation used in each case takes a very different form, each case is considered seperately in detail.

3:2 Non - resonant Amplitudes

In the absence of any model for $T^I_{LJ}(E)$, a number of empirical means of extrapolating the amplitudes have been developed, each of which stands purely by its sucdess in a consistent interpretation of the data[21]. Some of these are briefly reviewed here and the form used in our own analyses is described.

At low energies, around the $\bar{K}N$ threshold, the scattering-length (effective range) formalism[5] is often used, particularly for those analyses which include all open channels simultaneously. Assuming that the S-wave is the dominant amplitude, this assumes the form for phase - shift δ and momentum k of

$$k \cot \delta = (-1/a) + \tfrac{1}{2} r_o k^2 \qquad (3.1)$$

where a is termed the 'scattering length' and r_o the 'effective range'. The latter may be calculated for a given form of potential being dependent only on the width and depth, but not shape, of the potential. For higher ℓ-values a similar expression may still be obtained though the interpretation is more difficult[22].

For the higher energies where more amplitudes are needed, a more flexible form is required, a typical example is that of Smart[23] for $\bar{K}N \longrightarrow \Lambda\pi$

$$T_\ell = (A_\ell + B_\ell k + C_\ell k^2) \exp(i(D_\ell + E_\ell k + F_\ell k^2)) \qquad (3.2)$$

for $\quad A_\ell + B_\ell k + C_\ell k^2 \leq 0$

and that of Lea, Martin and Oades[24] for K^+p scattering

$$\delta_\ell = q^{2\ell+1} (A_\ell + B_\ell q^2 + C_\ell q^4) \qquad (3.3)$$

The CERN - Heidelberg - Saclay Collaboration who have made many of the measurements of $\bar{K}N$ interactions for these regions[12] have used a form which is linear in momentum p[25]

$$T_\ell = a_\ell + b_\ell (p - p_o) \qquad (3.4)$$

a_ℓ and b_ℓ complex, and for larger energy ranges have sometimes modified (3.4) to a two line fit in the complex plane, joining at momentum p_f

$$\begin{aligned} T_\ell &= a_\ell + b_1 (p - p_f) \quad p \geq p_f \\ T_\ell &= a_\ell + b_2 (p - p_f) \quad p \leq p_f \end{aligned} \qquad (3.5)$$

All these forms (3.2) - (3.5) are essentially empirical in nature, the choice of form being the particular preference of the worker.

For the analyses presented here, a more general and we believe more flexible form has been preferred, although again with no strong theoretical justification. This form was first introduced by Litchfield[7], when analysing all the available $\Lambda\pi$ data, and subsequently been used to analyse other channels[26].

In this form, the real and imaginary part of each amplitude is expanded as a series of orthogonal polynomials of a linear function of the incident momentum which is normalised in the region (-1,1) over the range of momenta considered, so that the amplitudes take the form

$$\begin{aligned} \text{Real } T^I_{LJ} &= \sum_{K}^{K_{max}} a^I_{LJK} P_K(x) \\ \text{Imag } T^I_{LJ} &= \sum_{M}^{M_{max}} b^I_{LJM} P_M(x) \end{aligned} \qquad (3.6)$$

where $x = -1$ at a value 10 MeV/c below the minimum value of the laboratory momentum and $x = +1$ at 10 MeV/c above the maximum value for the interval considered. The a's and b's provide the parameters of the fit, with K_{max} and M_{max} being determined for each amplitude as described in Chapter 4.

By the use of this form it was hoped that any energy - dependence of T_ℓ encountered could be described, with the advantage when fitting that removal of a higher polynomial should not greatly affect the lower coefficients from the orthogonality property of the polynomials.

3:3 Resonant Amplitudes

The concept of resonance may be formulated in several ways, and to show this, three definitions of resonance are given below, these are;

a) Resonance occurs when the Scattering Amplitude for a particular set of quantum numbers (spin, parity, etc.) is a maximum. For purely

elastic scattering this corresponds to δ passing through $\pi/2$. Ref.(27)

b) Resonance phenomena are associated with the existence of eigenstates of the complete Hamiltonian for which there are asymptotically only outgoing waves. Ref.(28)

c) In a region sufficiently 'small', and far from the branch point or three-particle threshold, then the S-matrix may be parameterised as a set of poles plus an analytic part, equivalent to a constant. Ref.(29)

In each case a Breit-Wigner resonance form may be derived from the definition given, by means of suitable interpretation of the forms obtained. As an example we outline the derivation following definition a), which most closely corresponds to the concepts involved in the partial wave analysis. From scattering theory[1] we may obtain the expression, for momentum k and complex scattering length a

$$\cot \delta \;=\; 1/ka \;+\; \ldots. \;=\; f(k) \qquad (3.7)$$

At resonance $\delta = \pi/2$, $f(k) \longrightarrow 0$, so expanding about E_R the resonance energy

$$f \;=\; 0 \;+\; (E_R - E) \frac{d}{dE}(f)_{E_R} \;+\; \ldots$$

and defining

$$\frac{d}{dE}(f)_{E_R} \;=\; 2 / \Gamma \qquad (3.8)$$

then using the relation

$$T \;=\; \frac{ka}{1 \;-\; ika}$$

we get

$$T \;=\; \frac{1}{2(E_R - E)/ \;-\; i\Gamma}$$

$$T \;=\; \frac{\Gamma/2}{(E_R - E) - i\,\Gamma/2} \qquad (3.9)$$

the well-known Breit-Wigner resonance form[30].

For the case when there are a number of open channels this becomes

$$T_{\alpha\beta} = \frac{\frac{1}{2}\,\Gamma_\alpha\,\Gamma_\beta}{(E_R - E) - i\,\Gamma/2} \qquad (3.10)$$

A more rigourous derivation of this form in terms of the S-matrix definition c) is given in Appendix A following the derivation given in reference(29).

For phenomenological purposes, the behaviour of the amplitudes in the argand plane is used as a means of detecting possible resonant behaviour. Considering the cases of (i) elastic and (ii) inelastic scattering, and writing

$$\varepsilon = 2(E_R - E)/\Gamma$$

then for the elastic case, from (3.9)

$$T_e = \frac{1}{\varepsilon - i} \qquad (3.11)$$

so

$$T_e = \frac{\varepsilon}{\varepsilon^2 + 1} + \frac{i}{\varepsilon^2 + 1} = u + iv \qquad (3.12)$$

which is a solution of the equation describing a circle in the argand plane

$$u^2 + (v - \tfrac{1}{2})^2 = 1/4 \qquad (3.13)$$

where the direction of rotation is determined by the Wigner condition[31]. Some typical plots are shown in figure II for elastic scattering with values of $\eta = 1$ and $\eta = 1/2$.

For the inelastic case, the branching ratio x_i is written as

$$x_i = \Gamma_i / \Gamma$$

to get

$$T_{a\beta} = \frac{\pm \sqrt{x_\beta x_a}}{\varepsilon - 1} \qquad (3.14)$$

and figure III shows typical behaviour of $T_{a\beta}$

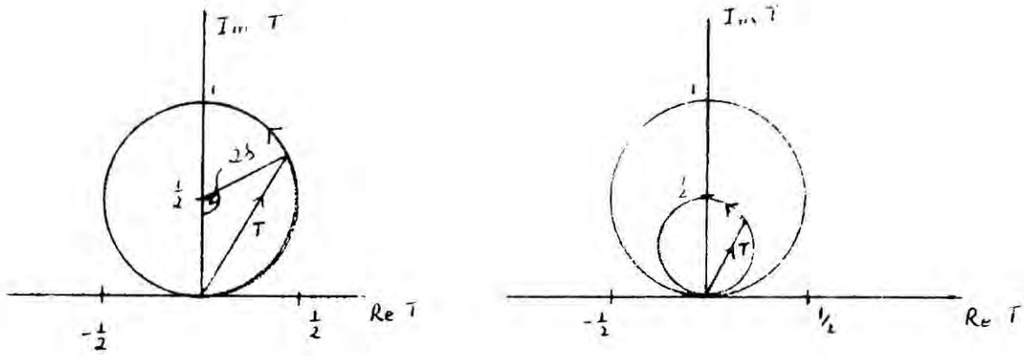

$\eta = 1$ $\eta = 1/2$

Figure II Elastic Resonant Amplitudes.

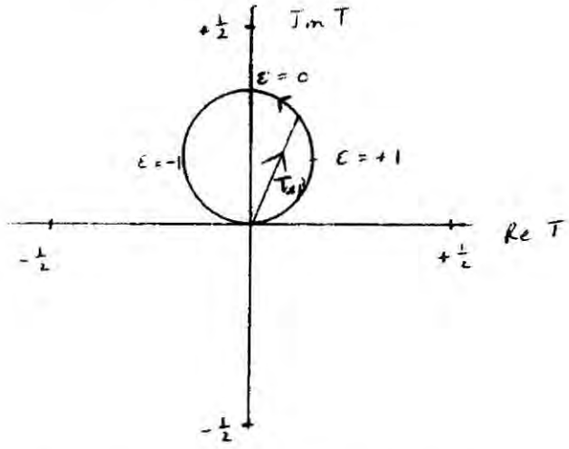

Figure III Inelastic Resonant Amplitudes.

Before analysing the argand plots, the effect of non-resonant background scattering should be included[28,32], making the usual assumptions for the S-matrix that;

a) $S = S_B S_R$

b) S_B varies slowly

so that

$$S = e^{2i(\delta_B + \delta_R)}$$

$$= e^{2i\delta_B}(1 + 2iT_R) = 1 + 2iT$$

$$T = T_B + e^{2i\delta_B} T_R \qquad (3.15)$$

so that the background phase produces a distortion in T_R as shown in figure IV for the elastic case.

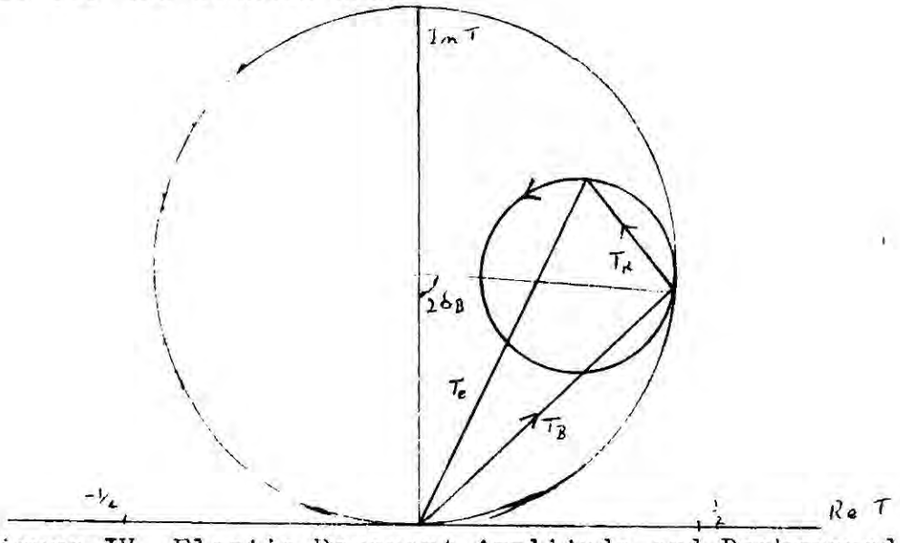

Figure IV Elastic Resonant Amplitude and Background.

In making the analyses, the resonant amplitudes have been parameterised with the form of (3.10), which becomes

$$T_R = \frac{\Gamma/2\ \sqrt{xx'}}{(E - E_R) - i\Gamma/2} \qquad (3.16)$$

and wherever possible a background phase has been included, although it is necessary to fix one phase and determine others relative to this. The energy-dependence of $\Gamma(E)$ has been introduced in two ways (i) the barrier penetration formula of Blatt and Weisskopf[33] and (ii) the empirical form of Glashow and Rosenfeld[34] and these are described in Chapter 4 where the details of the fits are given.

Chapter 4 Results and Conclusions

4:1 The $\Lambda\pi$ and $\Sigma\pi$ data

The data was presented in two forms, a) partial cross-sections for the two-body channels at each value of the incident K^- momentum and b) values of the differential and polarised differential cross-sections over a full angular distribution at each value of the K^- momentum. At each momentum the differential cross-sections were expanded in the forms

$$\frac{d\sigma}{d\Omega}(\theta) = \lambda\!\!\!^{-2} \sum_{n=0}^{n_{max}} A_n P_n(\cos\theta) \qquad (4.1)$$

$$\underline{P}\frac{d\sigma}{d\Omega}(\theta) = \underline{n}\ \lambda\!\!\!^{-2} \sum_{k=1}^{k_{max}} B_k P_k^1(\cos\theta) \qquad (4.2)$$

where the $P_n(\cos\theta)$ and $P_k^1(\cos\theta)$ were the usual Legendre and first associated Legendre polynomials, $\lambda\!\!\!^{-}$ the reduced wavelength $= 1/k$ and $\underline{n}$ the unit normal vector to the scattering plane. No correction was made for the electromagnetic interaction which is very slight for most of the data and would have considerably increased computational requirements[24].

The values of n_{max} and k_{max} were determined by the most adequate fits to $d\sigma/d\Omega$ and $\underline{P}\, d\sigma/d\Omega$ obtained by matrix inversion procedures. As the criteria for selection the χ^2 probability distribution function $P(\chi^2)$ was used[35], and allowance was made in this for continuity of the A_n's and B_k's with energy. In the case of the $\Lambda\pi$ channel the published values of A_n and B_k[12] were used, but for the $\Sigma\pi$ channel, the data for the range of interest was refitted and a number of improved fits were obtained for the $\Sigma^-\pi^+$ data. Data for the $\Sigma^{\pm}\pi^{\mp}$ channels was also obtained for

K^- momentum of 806 MeV/c and was included to give a more balanced cover of the energy range of interest, and thus reduce edge effects for the Breit-Wigner forms.

The coefficients A_n and B_k may be expressed in terms of the partial amplitudes T_ℓ, and the method of derivation for these is described in Appendix B, where the expressions are tabulated.

From these expressions, the nature of the ambiguities mentioned earlier may easily be observed. For the Minami ambiguity, interchanging parity for the same J-value, this corresponds to the interchange of the amplitudes $S_1 \longleftrightarrow P_1$, $P_3 \longleftrightarrow D_3$ etc. and from table B.I this can be seen to leave $d\sigma/d\Omega$ unaltered, whilst from table B.II the sign of $\underline{P}\, d\sigma/d\Omega$ is changed by -1.

It may further be observed that the operation of complex conjugation applied to all the amplitudes would similarly leave $d\sigma/d\Omega$ unaltered while changing the sign of $\underline{P}\, d\sigma/d\Omega$ and in practice this is resolved by establishing the phase using the Wigner condition while fixing the overall $SU(3)$ phase by one of the resonance terms.

The cross-sections σ, can be expressed in terms of the amplitudes by observing that

$$\sigma = \frac{4\pi}{k^2} A_o \qquad (4.3)$$

and to reduce errors of normalisation[7], the fitted data points were the values of σ, A_n/A_o and B_k/A_o at each energy. Minimisation was by the CERN program MINUIT[36] as detailed in Appendix C.

For the non-resonant amplitudes the parameters of the fits were taken to be the a^I_{JLK}'s and b^I_{JLM}'s of equations (3.6), with K_{max} and M_{max} determined only by the need for a good fit. The resonant amplitudes had the Breit-Wigner parameters E_R, Γ, $\sqrt{xx'}$ and the background phase Φ_B.

Provision was also made for a linear background in each resonant amplitude.

4:2 Details of the fitting procedure

For the $\Lambda\pi$ channel, the values of n_{max} and k_{max} in (4.1) and (4.2) were taken as 3 and initial fits were made with amplitudes of l-value up to 3 (S-F), but as in no fit was any but a neglegible F-wave present these were subsequently taken to be zero for all later fits. Since the channel is isosinglet with $I = 1$, the $Y_1^*(1670)$ is the only known resonance in the region analysed and with the exception of a few trial fits this was parameterised as a Breit-Wigner form.

The energy dependence of the resonance width $\Gamma(E)$ [37] was parameterised in two ways. The first by using the non-relativistic angular momentum barrier penetration factor[33], took the form for $l = 2$ of

$$\Gamma(E) = \Gamma_o\left(\frac{q}{q_R}\right)^5 \left\{\frac{9 + 3q_R^2r^2 + q_R^4r^4}{9 + 3q^2r^2 + q^4r^4}\right\} \qquad (4.4)$$

where q = c.m. momentum of the outgoing particles, q_R is the value of q at resonance and r the interaction radius. The second form used was an empirical dependence first used by Glashow and Rosenfeld[34], which had the form

$$\Gamma(E) \qquad \Gamma_o\left(\frac{q}{q_R}\right)^5 \left(\frac{q_R^2 + X^2}{q^2 + X^2}\right)^3 \qquad (4.5)$$

where X had a value of 350 MeV/c, determined empirically. Little difference could be detected between the fits obtained using the two forms and the first form was retained in all later fits.

Apart from the $Y_1^*(1670)$ the other amplitudes were parameterised

by the parametric form (3.6), and for the polynomial series, both Legendre polynomials, as in previous analyses[7,26], and Tchebyscheff polynomials were used, the latter being the optimum expansion[38] for the reduction of end effects. However as no expansion above three terms was ever required, and as the first two polynomials of each kind are identical, no difference could be adequately investigated.

Previous analyses of this region have preferred to fix the overall phase by the tail of the D_{15} resonance $Y_1^*(1765)$ [25], but we found that a better fit was obtained if the overall phase were fixed using the $Y_1^*(1670)$.

The analysis of the $\Sigma\pi$ channel was performed in a similar overall manner, with the advantage of the experiences gained from the $\Lambda\pi$ analysis. However the differences between the two channels made this a far less tractable problem and consequently the results should be treated with caution. The most significant differences lay in the poorer quality of the data, particularly for the $\Sigma^o\pi^o$ channel where events are difficult to seperate[12], and in the need for a much larger number of parameters (85) due to the two isospin states, with subsequent complications for minimisation.

The centre of mass energy region considered contained three known resonances, $Y_1^*(1670)$ as before, and two $I = 0$ resonances $Y_o^*(1670)$ in the S-wave and $Y_o^*(1690)$ in the D_3 wave. As for the $\Lambda\pi$ channel, the overall phase was fixed using the $Y_1^*(1670)$. The resonance width for the $Y_o^*(1690)$ was given the energy-dependence of (4.4) and that of the $Y_o^*(1670)$ was taken to be constant with energy. All other amplitudes were parameterised by the form (3.6) and provision was made for the inclusion of a trial resonant form in any chosen amplitude.

The criteria for the goodness of fit was taken to be the reduced χ^2- value for the particular fit, where for N_D data points the χ^2- value is defined as

$$\chi^2 = \sum_{i=1}^{N_D} \left\{ \frac{\xi_i^{\text{calculated}} - \xi_i^{\text{expt}}}{\Delta\xi_i} \right\}^2$$

where ξ_i is the i - th data point, $\Delta\xi_i$ the error; and the reduced χ^2- value, χ^2_{NDF} is defined as

$$\chi^2_{NDF} = \chi^2 / (N_D - N_P)$$

where N_P is the number of parameters used in the fit, i.e. (N_D - N_P) = no of degrees of freedom for the fit. For an optimum fit the value of χ^2_{NDF} should be 1.0 [35].

With the methods described in Appendix C, a number of fits to the data were obtained for each channel and in both cases it was possible to select one fit which was better than the others obtained. This was then used as a basis for a search for possible resonances present, although we found, as noted by Litchfield[7], that the method of adding resonance forms to the amplitudes is rather unstable, even for well-established resonances, and that unless the parameter values are initially close to their accepted values convergence is unlikely.

4:3 Results for $K^- p \longrightarrow \Lambda\pi$

These have been published elsewhere[39] and are repeated for completeness. This channel was analysed over a centre of mass region of 1615 - 1696 MeV with a number of fits extending into the region

below 1615 MeV, where however the Breit-Wigner description of the D_{13} amplitude is no longer reliable. An adequate description was obtained with amplitudes of $\ell = 2$ and little evidence could be found to suggest any further resonant structure, although for completeness fits were made with a trial resonance to investigate any possibilities. The best fit obtained had a value of $\chi^2 = 72.4$ for 90 data points and 18 parameters giving a value of $\chi^2_{NDF} = 1.01$ and was statistically more significant than any other fit found.

Figure V shows the amplitudes for the fit together with those obtained from other analyses in this region. Discussing the amplitudes in turn it was observed that:

D_{15}: It was necessary to include a linear form for this amplitude, which might be expected since the tail of $Y_1^*(1765)$ should extend to this region. A number of initial fits were made fixing the overall phase by this resonance, as done elsewhere[25] but this was found less satisfactory than using the D_{13}, probably because the Breit-Wigner form is only intended to describe the region close to resonance.

Unlike reference(24) it was unnecessary to fix the form of this amplitude for a good fit and no vanishing was observed for a free parameterisation. For the form used the behaviour is consistent with an interpretation as the low-energy tail of the $Y_1^*(1765)$ with a phase relative to $Y_1^*(1670)$ in agreement with SU(3) prediction[16].

D_{13}: If the form (3.6) were used for this amplitude, a resonant form was strongly suggested, as required if the expansion were to be of use. In the fits presented the amplitude was described by the forms (3.16) and (4.4) with the interaction radius r taken to be 0.8 fermi[40].

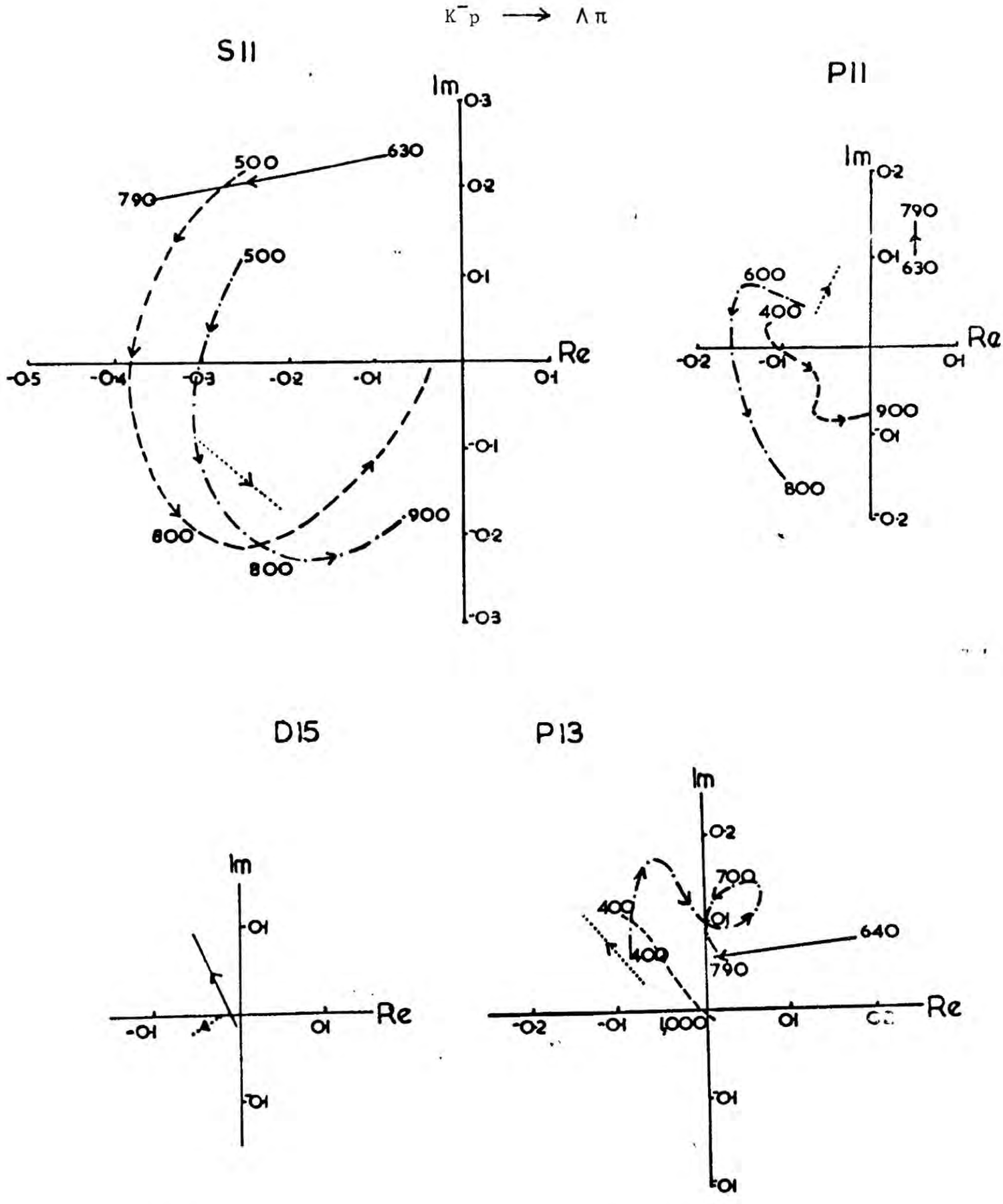

Figure V The solid line is our fit, over the interval 634 - 793 MeV/c, the dotted line is taken from Ref.(42) and covers the interval 450 - 670 MeV/c. The curves shown as dashed and dot-dashed lines are from References (19) and (20) over the same region as our fit.

From the fits the parameters of $Y_1^*(1670)$ were determined to be

$$E_R = 1676.5 \pm 2.0 \text{ MeV} \qquad \Gamma_o = 59 \pm 4.5 \text{ MeV} \qquad \sqrt{xx'} = 0.165 \pm 0.01$$

When compared with other results[3] the value of Γ_o is seen to be a little higher, but this may be a consequence of the free parameterisation of the D_{15} amplitude in our fit, since there is a close correlation between the two D - waves.

P_{13}: There is little to suggest any structure in this amplitude[41] in the region investigated, although an extension to the lower energy regions required some small extra structure. The amplitude is quite adequately described by a linear form an varies rapidly with energy.

P_{11}: This amplitude showed least sign of any structure at all, and over the range used could be parameterised as a complex constant with only very small movement in the Argand plane if the fit were extended to a larger range.

S_{11}: Initial results suggested that this was the most likely amplitude to possess a resonant structure in this region, but attempts to impose a Breit - Wigner proved unavailing, if included this gave resonance parameters

$$E_R = 1670 \text{ MeV} \qquad \Gamma_o = 106 \text{ MeV} \qquad \sqrt{xx'} = 0.18$$

with a value of $\chi^2_{NDF} = 1.26$. As mentioned earlier this method was unstable and the values obtained very unreliable. Despite the rapid variation with energy a satisfactory fit required only a complex linear form.

Table IV shows the parameters of the best fit obtained, for the non-resonant amplitudes.

	a^1_{LJ1}	b^1_{LJ1}	a^1_{LJ2}	b^1_{LJ2}	a^1_{LJ3}
S_{11}	-0.194	0.200	-0.160	-0.019	-
P_{11}	0.062	0.153	-	-	-
P_{13}	0.101	0.067	-0.081	-0.018	-0.038
D_{15}	-0.022	0.019	-0.011	0.064	-

Table IV Parameter values for $K^- p \longrightarrow \Lambda \pi$

In figure V we also show the fits made by Kim[19] and the C.H.S. collaboration in this region, and that of Wong[42] in the adjoining region below. The fits use either $Y_1^*(1765)$ or $Y_o^*(1520)$ to fix the overall phase, no other fit using $Y_1^*(1670)$.

Comparing with these, it can be observed that the magnitudes of our amplitudes are generally in agreement although they possess an overall clockwise rotation when compared with those from the other fits. As observed in Chapter 3, this may be an effect of a background present in either the D_{13} or D_{15} amplitudes (or both) if the solutions are to agree. Another consideration may be the inadequacy of the Breit - Wigner form used to describe the variation away from resonance.

4:4 Results for $K^- p \longrightarrow \Sigma \pi$

The $\Sigma\pi$ channel was analysed over a c.m. energy range of 1615 - 1702 MeV, giving a slightly better distribution around the region of interest, and as for the $\Lambda\pi$ analysis the overall phase was fixed by the $Y_1^*(1670)$, and amplitudes with ℓ-values of up to 2 were required.

Like Reference (25c) we found that, despite many attempts, no very satisfactory fit could be found and the best value of χ^2 was 291.0 for 244 data points and 43 parameters, corresponding to $\chi^2_{NDF} = 1.45$ (compared to $\chi^2_{NDF} = 1.49$ for a larger range of data in Reference (25c)).

The data is not very sensitive to the input, since a number of fits which were started with the wrong SU(3) phases for the Y_o^* resonances were able to converge to a best value of $\chi^2_{NDF} = 1.75$ and gave reasonable parameters for the resonances involved! Consequently any deductions from this data should be treated with great care. In figures VI and VII the amplitudes finally obtained are shown together with those of the C.H.S. collaboration.

Again discussing each amplitude in turn, one observes:

D_{15}: A small complex constant amplitude was adequate, reasonably showing no sign of the $Y_1^*(1765)$ which is only weakly coupled to the $\Sigma\pi$ channel.

D_{13}: As for the $\Lambda\pi$ channel this was adequately parameterised by the Breit - Wigner form and the parameters obtained were in good agreement with other fits to this channel, these were

$E_R = 1665.1 \pm 1.6$ MeV $\quad \Gamma_o = 43.2 \pm 2.4$ MeV $\quad \sqrt{xx'} = 0.139 \pm 0.007$

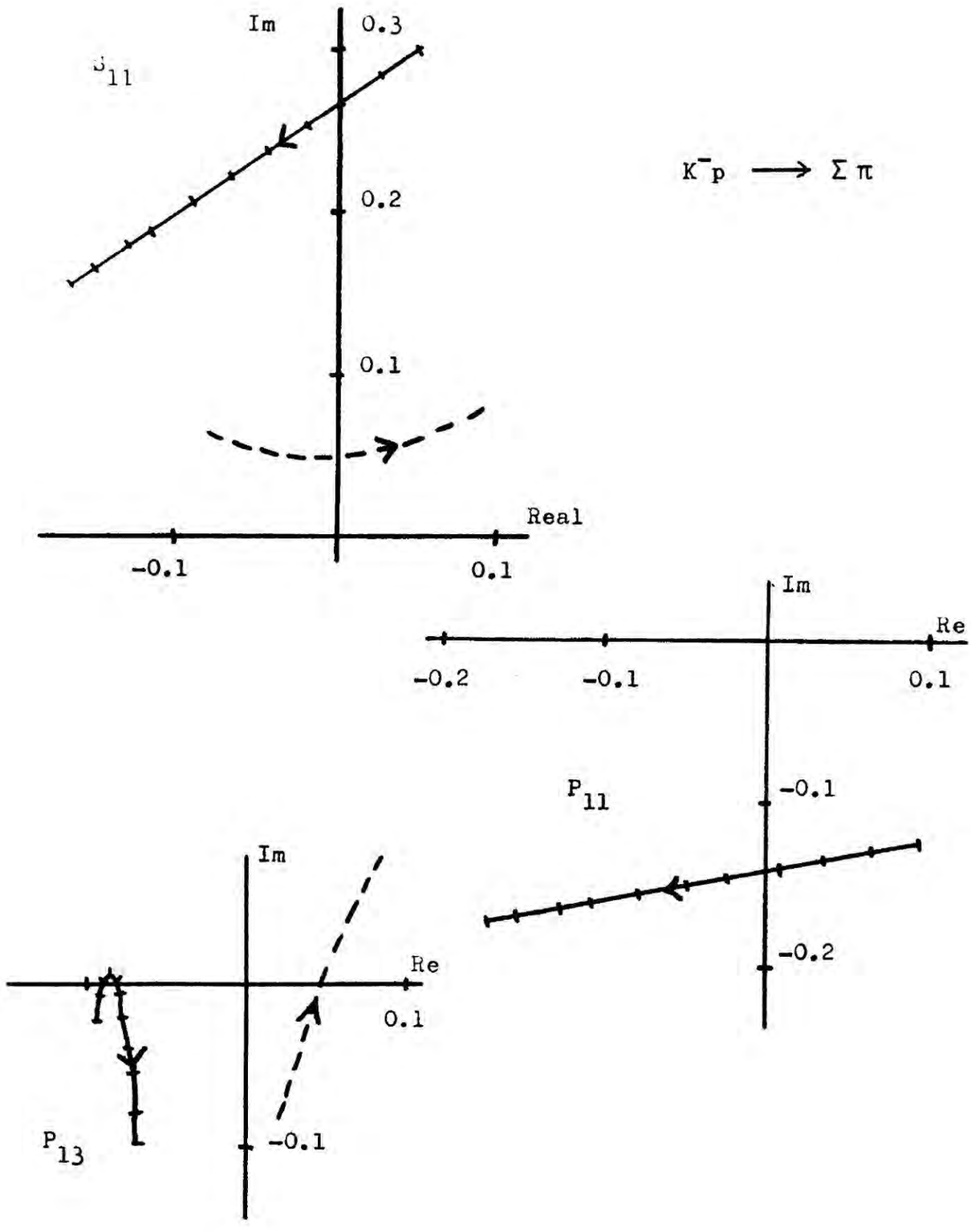

Figure VI The $I = 1$ amplitudes for $K^- p \longrightarrow \Sigma \pi$. The solid line is our fit over the interval 617 - 806 MeV/c and the broken lines are taken from Reference(20).

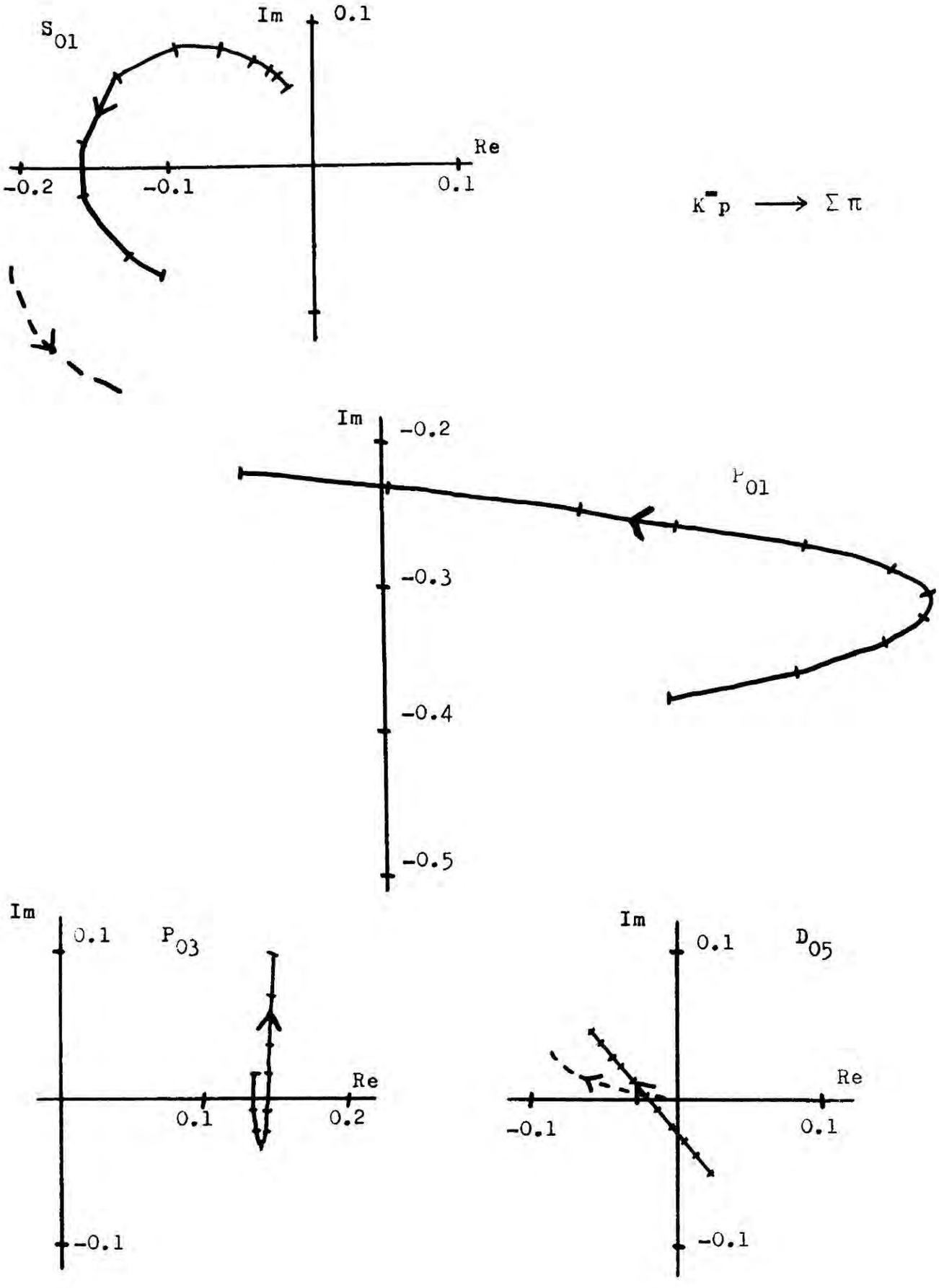

Figure VII The $I = 0$ amplitudes for $K^- p \longrightarrow \Sigma \pi$. The solid line is our fit over the interval 617 - 806 MeV/c and the broken lines are taken from Reference(20).

P_{13}: This amplitude was best described by a non-linear form although reduction to a linear form produced only a small rise in χ^2. The amplitude was small with no particular features.

P_{11}: A complex linear form was again quite adequate and as in the $\Lambda\pi$ analysis this showed no sign of any structure at all in this region.

S_{11}: Unlike the $\Lambda\pi$ analysis no fits showed any structure in this amplitude which could be quite adequately described by a linear form.

D_{05}: Again no sign of any structure, a linear parameterisation being adequate with only small movement in the amplitude.

D_{03}: This appeared to be adequately described by the Breit - Wigner form used with little indication of background present. An interaction radius of 0.8 f [40] was used in (4.4) and the resonance parameters were found to be

$$E_R = 1683.9 \pm 1.6 \text{ MeV} \qquad \Gamma_o = 78.6 \pm 4.8 \text{ MeV} \qquad \sqrt{xx'} = -0.342 \pm 0.007$$

with a phase angle of $\Phi_D = 0.068 \pm 0.01$ rad. These above parameters are in good agreement with other analyses, particularly for the $\Sigma\pi$ channel.

P_{03}: Very slight signs of structure were shown but reduction to a complex linear form produced only a relatively small increase in χ^2.

P_{01}: A more extensive form of parameterisation was required for this amplitude and could not be further reduced without a large rise in χ^2. A fit with Breit-Wigner form and a large constant background gave parameters of

$$E_R = 1650 \text{ MeV} \qquad \Gamma_o = 41.6 \text{ MeV} \qquad \sqrt{xx'} = -0.075$$

for a value of $\chi^2 = 340.2$, $\chi^2_{NDF} = 1.68$. This was the only

amplitude to show any sign of resonant structure.

S_{01}: Although this was parameterised by a Breit - Wigner, a slightly improved solution required a background term. Two solutions were then obtained for this amplitude with and without a constant background amplitude. For the solution with a constant background the resonance parameters were

$E_R = 1682.8 \pm 2.5$ MeV $\quad \Gamma_o = 35.3 \pm 3.4$ MeV $\quad \sqrt{xx'} = -0.144 \pm 0.012$

where the coupling to the $\Sigma\pi$ channel is smaller than usually obtained. For the solution without a background the parameters were

$E_R = 1682.3 \pm 2.5$ MeV $\quad \Gamma_o = 50.5 \pm 3.5$ MeV $\quad \sqrt{xx'} = -0.164 \pm 0.012$

the width being increased. Other fits to this resonance have included a background amplitude [25c].

A large background phase was also found, with the value of $\Phi_S = -1.66 \pm 0.10$ rad. Table V gives the values of the parameters for the non-resonant amplitudes obtained with minimum structure possible, $\chi^2_{NDF} = 1.48$.

There is less to observe in making comparison between fits for the $\Sigma\pi$ channel since the data is not adequate for any remotely definitive results or determinations. There is no obvious connection between this and any other solutions other than that the amplitudes are generally of similar magnitude.

	a^I_{LJ1}	b^I_{LJ1}	a^I_{LJ2}	b^I_{LJ2}	a^I_{LJ3}	b^I_{LJ3}
P_{01}	0.236	-0.301	-0.160	0.089	-0.256	-
P_{03}	0.140	0.007	0.006	0.046	-	0.069
D_{05}	-0.018	-0.001	-0.045	0.052	-	-
S_{11}	-0.058	0.227	-0.119	-0.082	-	-
P_{11}	-0.038	-0.150	-0.147	-0.028	-	-
P_{13}	-0.080	-0.026	0.015	-0.043	-	-0.048
D_{15}	0.004	0.057	-	-	-	-

Table V Parameters for $K^-p \longrightarrow \Sigma\pi$

4:5 Conclusions

Our investigation of the $\Lambda\pi$ and $\Sigma\pi$ channels of the $\bar{K}N$ system in the c.m. energy region 1600 - 1700 MeV has indicated no need for any new resonances, while values have been obtained for the known resonances which are in good general agreement with those previously found[3] from formation experiments.

The results from the analysis of $K^-p \longrightarrow \Lambda\pi$ concur in general with previous analyses while leaving the question of background in need of clarification. A statistically significant fit to the existing data could be obtained with no new resonances nor

any significant structure in any of the amplitudes.

In the case of the $\Sigma\pi$ analysis, agreement with other solutions is slight and confusion arises for the resonance in the P_{01} amplitude, its background and the strength of the coupling differing quite considerably from previous values. There is again little to suggest a need for any new resonance states but the best fit obtained was statistically much less impressive. Since the χ^2 value is found to come fairly uniformly from the data points better data is probably needed before any conclusions may be drawn from any analyses of this channel.

Unfortunately little light has been shed on the confusion of $Y_1^*(1670)$, but it would seem worth considering that the description from the $\Lambda\pi$ channel seemed statistically adequate implying that in the event of another resonance being present, its coupling to the $\Lambda\pi$ channel must be very weak.

The parameterisation selected was not fully utilised in the sense of describing any forms of pronounced structure since none could be found, but particularly for the $\Lambda\pi$ channel the parameterisation was able to give an adequate description and to demonstrate that no significant structure was present, thus showing that the form of the parameterisation need not be the source of any apparent structure[7].

In conclusion these two channels of the $\bar{K}N$ system would appear reasonably well described by the amplitudes obtained in these solutions, but the problem of 'background' in these analyses remains unclarified and will probably require improved data (or theory) for its description.

PART II

THE HADRON - NUCLEUS INTERACTION

CHAPTER 5 The scattering of hadrons from nucleons and nuclei

5:1 Introduction

The study of the interaction between hadrons and nuclei has proved to be a subject of interest to both nuclear and particle physics, providing a common region of study which utilised many of the interesting features of these two branches of physics. For the nuclear physicist, hadron scattering and electron scattering at high energy are able to provide details of the mass and charge distributions of nuclei, and test details of nuclear models; while for the particle physicist the nucleus provides a means of studying the scattering off unstable particles and of measuring cross-sections for reactions such as πn or pn which are otherwise unobtainable. With a reliable model for scattering from nuclei there is the further advantage of testing the input data for such details as normalisation or of selecting between different solutions available.

At high energies the rather complicated problem for a hadron scattering from a many-nucleon target is greatly simplified since the effects of the internucleon forces are much reduced, so that the scattering may be treated as a simple sum of two-body collisions between the incident particle and the nucleons of the target, with the incident particle propogating freely between collisions. The approximation by which the scattering from a bound nucleon is equated with the scattering from a free nucleon is generally referred to as the 'Impulse approximation'. A model to describe such a situation has been developed by Glauber[46-48] and extensively used to study the interactions of high-energy protons and π-mesons with nuclei[49-81], with results frequently in excess of expectation.

When comparing predictions with the data one of the main

attractions of this model is its absence of free parameters, the results being dependent only upon the input from hadron-nucleon and electron-nucleus scattering experiments.

In the next section some features of high-energy scattering are discussed and a model to describe the high-energy elastic scattering from nucleons is given. Section 3 describes some of the different models used for hadron-nucleus scattering and their regions of validity and in section 4 the Glauber multiple scattering series is derived. In Chapter 6 this is used in a study of the elastic scattering of π^- mesons from Helium-4 and comparison is made with the available data for high and medium-energy scattering with the object of examining different forms of nuclear input and their effect. Chapter 7 describes a more unusual use, describing the elastic scattering of π^- mesons and protons from Carbon-12 using an α-particle model for the C^{12} nucleus,[82] and in Chapter 8 the Glauber model is briefly surveyed along with the conclusions from these calculations.

5:2 The Eikonal Approximation for high-energy scattering

The first derivations of the Glauber multiple-scattering model were made using the non-relativistic eikonal approximation for high-energy two-body scattering. A review of the eikonal formalism and its origins has been given by Schiff[83] and there have been many more recent additions to this topic[84-93]. More recent derivations of the multiple-scattering series[94-96] have imposed fewer restrictions on its range of validity and an extensive discussion of the constraints of the eikonal has been given by Osborn[94].

This section outlines the eikonal approximation in the potential model[47] along with some results from the operator formalism, describing the approximations made together with the constraints

which they impose upon the multiple-scattering series.

Unlike the description of scattering given in Chapter 1, elastic scattering at high energy is greatly simplified by the approximations which may be used, the main ones of which are (i) the spin-flip amplitude may generally be neglected, (ii) the scattering is mainly in the forward direction and (iii) the large values of ℓ required to describe the forward peak make it possible to replace the summation over ℓ by an integration over the impact parameter b. As will be described, the resultant multiple-scattering model may still give a good description even when some or even all of these conditions fail to hold.

In the potential model, the scattering from a localised potential V(r) is assumed to be described by the Schrödinger equation, and to possess, for an incident plane wave of momentum $\underline{k}$, an integral solution for the outgoing state $\Psi_{\underline{k}}(\underline{r})$ of

$$\Psi_{\underline{k}}(\underline{r}) = e^{i\underline{k}.\underline{r}} - \frac{2m}{4\pi\hbar^2}\int \frac{e^{ik|\underline{r}-\underline{r}'|}}{|\underline{r}-\underline{r}'|} V(\underline{r}')\Psi_{\underline{k}}(\underline{r}')\, d\underline{r}' \qquad (5.1)$$

In the asymptotic region, this may be compared with the expression (1.3) by observing that

$$|\underline{r}-\underline{r}'| \underset{r\longrightarrow\infty}{\longrightarrow} r - \frac{\underline{r}'.\underline{r}}{r}$$

and defining a propogation vector $\underline{k}_r = |\underline{k}|\frac{\underline{r}}{r} = k\frac{\underline{r}}{r}$, equation(5.1) becomes

$$\Psi_{\underline{k}}(\underline{r}) \underset{r\longrightarrow\infty}{\longrightarrow} e^{i\underline{k}.\underline{r}} - \frac{2m}{4\pi\hbar^2}\frac{e^{ikr}}{r}\int e^{-i\underline{k}_r.\underline{r}'} V(\underline{r}')\Psi_{\underline{k}}(\underline{r}')\, d\underline{r}' \qquad (5.2)$$

so that the scattering amplitude $f(\underline{k}',\underline{k}) \equiv f(\theta)$ for scattering from $\underline{k} \longrightarrow \underline{k}'$ where $|\underline{k}| = |\underline{k}'|$ is defined by

$$f(\underline{k}',\underline{k}) = -\frac{2m}{4\pi\hbar^2}\int e^{-i\underline{k}'.\underline{r}}\, V(\underline{r})\Psi_k(\underline{r})\, d\underline{r} \qquad (5.3)$$

At this point, it should be noted that (5.1) is an exact expression for the scattering process, the eikonal solution being then obtained by factorising $\Psi_k(\underline{r})$

$$\Psi_k(\underline{r}) = e^{i\underline{k}.\underline{r}}\, \Phi(\underline{r}) \qquad (5.4)$$

so that $\Psi(\underline{r})$ is seperated into a product of an incident plane wave and a modulating factor $\Phi(\underline{r})$, so that from (5.1)

$$\Phi(\underline{r}) = 1 - \frac{2m}{4\pi\hbar^2}\int \frac{e^{ik|\underline{r}-\underline{r}'|} - i\underline{k}.(\underline{r}-\underline{r}')}{|\underline{r}-\underline{r}'|}\, V(\underline{r}')\Phi(\underline{r}')\, d\underline{r}' \qquad (5.5)$$

and defining $\underline{r}'' = \underline{r} - \underline{r}'$ this becomes

$$\Phi(\underline{r}) = 1 - \frac{2m}{4\pi h^2}\int \frac{e^{i(kr'' - \underline{k}.\underline{r}'')}}{r''}\, V(\underline{r}-\underline{r}'')\Phi(\underline{r}-\underline{r}'')\, d\underline{r}'' \qquad (5.6)$$

Making the assumptions that the scattering is weak, with $V/E \ll 1$ and that the particle wavelength is much smaller than the width of the potential $ka \ll 1$, then if $\Phi(\underline{r})$ varies slowly within the particle wavelength $\lambda = 1/k$ and varies appreciably only within a distance d, the integral of (5.6) may be performed using polar co-ordinates so that

$$d\underline{r}'' = r''^2\, dr''\, d\beta\, d\alpha$$

with $\beta = \cos(\underline{k},\underline{r})$ and α the aximuthal angle, to get

$$\Phi(\underline{r}) = 1 + \frac{2m}{4\pi h^2}\int r''^2 dr'' d\alpha \left[\frac{e^{ikr''(1-\mu)}}{ikr''} V(r-r')\Phi(\underline{r}-\underline{r}')\right]_{-1}^{+1} + O(\frac{1}{kd}) \tag{5.7}$$

Since the limit $\mu = -1$ corresponds to $\underline{r}''$ antiparallel to $\underline{k}$, the contribution from this limit is $O(\frac{1}{kd})$ and is neglected, leaving

$$\Phi(\underline{r}) = 1 - \frac{i}{\hbar v}\int_0 V(r-r'')\Phi(\underline{r}-\underline{r}'')\Big|_{r/\!/k} dr'' \tag{5.8}$$

where v = velocity. This equation is better expressed in cartesian co-ordinates choosing $\underline{k}$ to lie along the z-axis so becoming

$$\Phi(x,y,z) = 1 - \frac{i}{\hbar v}\int_{-\infty}^{z} V(x,y,z')\,\Phi(x,y,z')\,dz' \tag{5.9}$$

which has a solution of form

$$\Phi(x,y,z) = \exp\left[\frac{-i}{\hbar v}\int_{-\infty}^{z} V(x,y,z')\,dz'\right] \tag{5.10}$$

and so, substituting back into (5.4), the eikonal wave function is then

$$\Psi(x,y,z) = \exp\left[ikz - \frac{i}{\hbar v}\int_{-\infty}^{z} V(x,y,z')\,dz'\right] \tag{5.11}$$

so that the scattering amplitude (5.3) becomes

$$f(\underline{k}',\underline{k}) = -\frac{2m}{4\pi\hbar^2}\int e^{-i\underline{k}.\underline{r}'} V(\underline{r}) \exp\left[i\underline{k}.\underline{r} - \frac{i}{\hbar v}\int_{-\infty}^{z} V(\underline{b}+\underline{n}z')dz'\right] dz d^2b \tag{5.12}$$

where the impact parameter $\underline{b}$ lies in the xy plane, perpendicular to the incident momentum, and $\underline{n}$ is the unit vector along z as shown

in Figure VIII

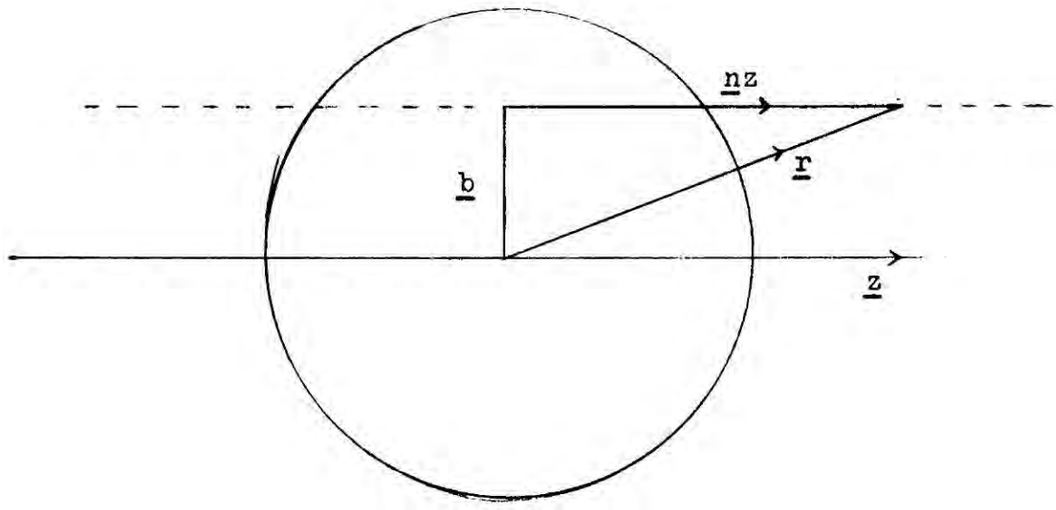

Figure VIII Impact parameter co-ordinates

Rewriting (5.12) as

$$f(\underline{k}',\underline{k}) = -\frac{2m}{4\pi\hbar^2}\int e^{i(\underline{k}-\underline{k}').(\underline{b}+\underline{n}z)}\, V(\underline{b}+\underline{n}z)\, e^{-\frac{i}{\hbar v}\int_{-\infty}^{z} V(\underline{b}+\underline{n}z')\,dz'}\, dz\, d^2b \qquad (5.13)$$

and further approximating for small angles

$$\exp\left[\, i(\underline{k}-\underline{k}').\underline{n}z \,\right] = 1 \qquad (5.14)$$

$f(\underline{k}',\underline{k})$ is finally described by

$$f(\underline{k}',\underline{k}) = \frac{k}{2\pi i}\int e^{i(\underline{k}-\underline{k}').\underline{b}}\left\{ e^{-\frac{i}{\hbar v}\int_{-\infty}^{\infty} V(\underline{b}+\underline{n}z')dz'} - 1 \right\} d^2\underline{b} \qquad (5.15)$$

From (5.15), an eikonal phase shift is generally defined in the form

$$\chi(\underline{b}) = -\frac{1}{\hbar v}\int_{-\infty}^{\infty} V(\underline{b}+\underline{n}z')dz' \qquad (5.16)$$

so that

$$f(\underline{k}',\underline{k}) = \frac{k}{2\pi i}\int e^{i(\underline{k}-\underline{k}').\underline{b}}\ \left(e^{i\chi(\underline{b})} - 1 \right) d^2\underline{b} \qquad (5.17)$$

For a central potential this may be further reduced by making the small angle approximation

$$(\underline{k}-\underline{k}').\underline{b} = kb\theta\cos\Phi \qquad (5.18)$$

so that

$$f(\underline{k}',\underline{k}) = \frac{k}{i}\int_0^\infty J_0(kb\theta)\left(e^{i\chi(\underline{b})} - 1 \right) b\, db \qquad (5.19)$$

It is possible to show that (5.19) is in fact an exact representation of the scattering amplitude[97], the approximation being in (5.16). The impact parameter may be related to the usual angular momentum l by the limiting relations for large l of

$$kb \longleftrightarrow l + 1/2$$

$$d^2\underline{b} \longleftrightarrow \sum_l$$

so that the eikonal phase shift is related to the phase shifts by

$$\chi\left(\frac{l+1/2}{k}\right) \longleftrightarrow 2\delta_l \qquad (5.20)$$

The derivation of (5.17) required a number of assuptions, chiefly of $V/E \ll 1$ for small angle scattering and throughout the derivation, $\underline{k}$ and $\underline{k}'$ are taken to be very little different. In the one-dimensional case, it can be easily shown[47] that the approximations made in obtaining (5.8) correspond to the linearisation of the Schrödinger equation, by neglecting the term $\frac{d^2}{dr^2}$, and from the

form of this the operator formalism for obtaining an eikonal Hamiltonian follows directly. The basic form for the amplitude, which is utilised in formulating the multiple-scattering expansion is provided by equation(5.17).

Other forms of eikonal expansions have been obtained[83-89], generally with better behaviour at large angle, together with relativistic forms[90,91] and these and their differences have been well reviewed in the literature[89]. For our purposes the form obtained is adequate, although for completeness a short description of the form of the approximation in operator formalism is included.

Denoting the incident c.m. momentum by $\underline{k}$, and the reduced mass of the projectile as μ, for a collision between two high - - energy particles the non-interacting Hamiltonian H_o may be written as

$$H_0 = \underline{p}^2 / 2\mu \qquad (5.21)$$

where $\underline{p}$ is the momentum operator in the c.m. frame. This may also be expressed as

$$H_o = \frac{1}{2\mu} (\underline{p} - \underline{k}).(\underline{p} + \underline{k}) + \frac{1}{2\mu} k^2 \qquad (5.22)$$

and the eikonal form is obtained by linearising this form, as described for $\Phi(\underline{r})$ previously, assuming that all the important contributions have values of $\underline{p}$ close to $\underline{k}$, since the angles are small, so that one may approximate

$$\underline{p} + \underline{k} = 2\underline{k} \qquad (5.23)$$

and obtain the eikonal Hamiltonian

$$H_0^{eik} = \frac{\underline{k}}{\mu} .(\underline{p} - \underline{k}) + \frac{1}{2\mu} k^2 \qquad (5.24)$$

An extensive discussion of (5.24) and its consequences has been given by Osborn[94], one of whose findings is repeated without proof to illustrate the nature of the eikonal more fully. A characteristic of H_o^{eik} is that it is not diagonal in energy and so does not conserve energy during a collision, instead conserving the component of $\underline{p}$ which is parallel to $\underline{k}$, denoted $\underline{p}_{//}$.

As a consequence, the Greens function in momentum space for the exact and eikonal Hamiltonians may be shown to possess very different singularity surfaces corresponding to this non-conservation of energy. The Greens functions are

$$\langle \underline{p} \mid G_o^{eik}\left(\frac{k^2}{2\mu} + i\varepsilon \right) \mid \underline{p}' \rangle = \frac{\delta^3(\underline{p} - \underline{p}')}{(2\underline{k}/2\mu).(\underline{p}-\underline{k}) - i\varepsilon} \qquad (5.25)$$

$$\langle \underline{p} \mid G_o \left(\frac{k^2}{2\mu} + i\varepsilon \right) \mid \underline{p}' \rangle = \frac{\delta^3(\underline{p} - \underline{p}')}{p^2/2\mu - k^2/2\mu - i\varepsilon} \qquad (5.26)$$

These are shown in Figure IX, where the components of $\underline{p}$ parallel to $\underline{k}$ and perpendicular to $\underline{k}$ are denoted by $\underline{p}_{//}$ and $\underline{p}_{\perp}$.

Figure IX Singularity surfaces of the Greens functions.

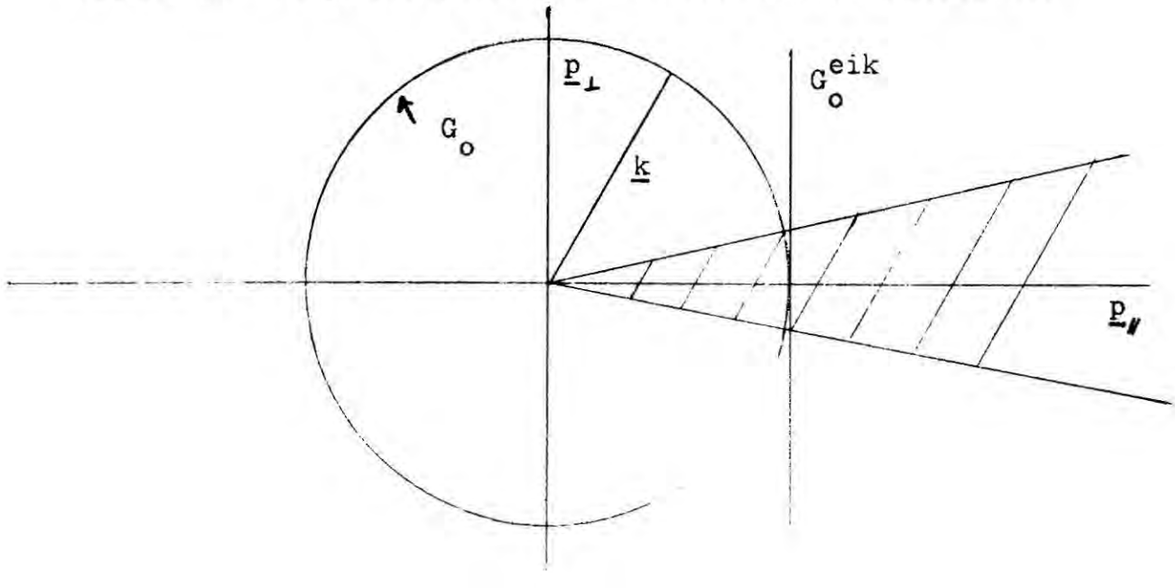

As may be seen, the region where G_o^{eik} should well approximate G_o is the region of small momentum transfer and small angle, where most of the scattering is concentrated.

5:3 Scattering from Nuclei

One reason for studying the scattering of hadrons at high energies is the simplification which is created for the many-body problem which results. However methods do exist for calculating the scattering of low-energy and medium-energy particles and these are briefly outlined in this section.

Much of the early work on hadron-nucleus scattering was performed using the semiphenomenological Optical Model[98-100] which treats the nucleus as a continuous media rather than an assembly of point particles, and obtains the phase-shifts by solving some experimentally determined potential. However even at relatively low energies, diffraction-type patterns emerge in elastic scattering and the optical model has great difficulty in explaining these and was, for example, quite unable to explain much of the Brookhaven data at 1 BeV[81], which is well described by Glaubers model[69].

An improved optical model is provided by Kisslingers model[101] and has been used to describe π^- - 12C scattering well above the expected validity range with some success[102]. It has also been observed that the Glauber series also possesses an optical limit[47] under suitable approximations.

An exact description of the multiple-scattering from nuclei is provided by the Watson model[103-105] in terms of a series. However calculations using this series must cope with the problems arising from the facts that,(i) all terms after the first involve off-shell

amplitudes which cannot be measured from two-body experiment and (ii) the convergence of the Watson series may be slow.

To obtain this series, the nuclear Hamiltonian is denoted by H_N and the kinetic energy operator for the incoming particle as K_o to give a total Hamiltonian

$$H_o = H_N + K_o \tag{5.27}$$

For a target nucleus of A nucleons, the interaction potential between incident particle and target takes the form

$$V = \sum_{i=1}^{A} V_i(\underline{r} - \underline{r}_i) \tag{5.28}$$

Then using the Lippmann-Schwinger equation for the total transition operator

$$T = V + VG_oT \tag{5.29}$$

where the propogator G_o for energy E is given by

$$G_o = (E - H_o + i\varepsilon)^{-1} \tag{5.30}$$

Watson was able to obtain the infinite series for T

$$T = \sum_{i=1}^{A} t_i + \sum_{i \neq j}^{A} t_iG_ot_j + \sum_{i \neq j \neq k}^{A} t_iG_ot_jG_ot_k + \ldots\ldots \tag{5.31}$$

where the hadron nucleon operator t_i is defined by

$$t_i = V_i + V_iG_ot_i \tag{5.32}$$

and where t_i differs from the free scattering amplitude for hadron - - nucleon scattering in that G_o is the propogator for the total

Hamiltonian and energy and not those for the incident hadron and the nucleon.

As may be seen from the form of (5.31) , the evaluation of the Watson series is a complicated procedure. The Glauber series (which is finite) may be derived from the Watson series[96] but the connection is neither simple nor direct.

5:4 The Glauber Multiple-Scattering Model

The Glauber model was originally formulated with the aim of extracting the high-energy pn and πn cross-sections from deuterium[46,50,51], and to account for the cross-section 'defect' of deuterium where the total cross-section was slightly less than the sum of the two individual cross-sections by means of a 'shadowing' correction by which one nucleon could shadow the other. From this, the extension to differential cross-sections was direct as was the extension of the model to other nuclei.

An early problem of the model was that the calculated differential cross-section for deuterium, as for other spin-zero nuclei showed a dip in the region where the single and double - scatterings interfered, whereas the data for deuterium showed only a shoulder, while the measurements on other nuclei agreed well with prediction. This problem was eventually resolved by the inclusion of the deuteron D-state[55], which, although only 4% of the deuteron state, was able to give the required features.

Since Glaubers original derivation[47] of the series, other forms of derivation have been formulated, including the operator formalism method[94] and the graph method[95]. The derivation presented in this section follows the original formulation for a spin zero nucleus of A nucleons, the inclusion of the spin and isospin of the incident

particle being left for the next chapter.

Defining the momentum transfer $\underline{q}$ as

$$\underline{q} = \underline{k} - \underline{k}'$$

expression (5.17) becomes

$$f(\underline{q}) = \frac{ik}{2\pi} \int e^{i\underline{q}.\underline{b}} \left(1 - e^{i\chi(\underline{b})} \right) d^2\underline{b} \qquad (5.33)$$

The profile function $\Gamma(\underline{b})$ is then defined as

$$\Gamma(\underline{b}) = 1 - e^{i\chi(\underline{b})} \qquad (5.34)$$

so that $f(\underline{q})$ forms the Fourier transform of $\Gamma(\underline{b})$

$$f(\underline{q}) = \frac{ik}{2\pi} \int e^{i\underline{q}.\underline{b}} \Gamma(\underline{b}) \, d^2\underline{b} \qquad (5.35)$$

and $\Gamma(\underline{b})$ may be obtained by the inverse Fourier transform as

$$\Gamma(\underline{b}) = \frac{1}{2\pi ik} \int e^{-i\underline{q}.\underline{b}} f(\underline{q}) \, d^2\underline{q} \qquad (5.36)$$

The compound system of A nucleons are taken to have position vectors $\underline{r}_1, \ldots \underline{r}_A$ with components $\underline{s}_1, \ldots, \underline{s}_A$ in the impact parameter plane, relative to the axis of collision as shown in Figure X.

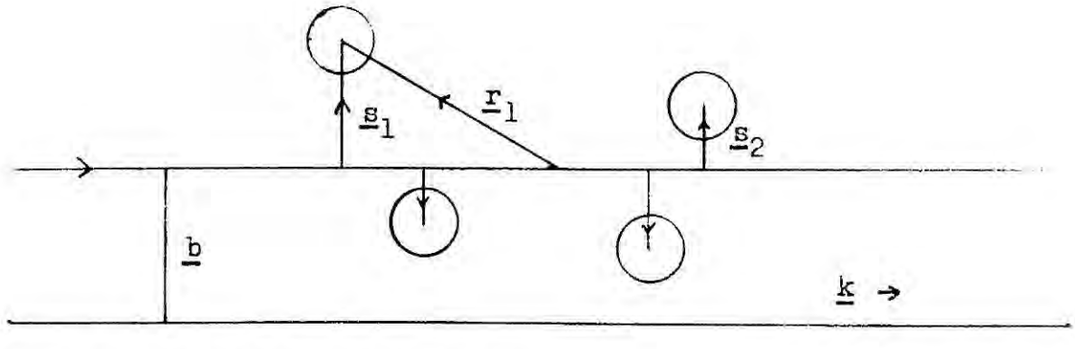

Figure X Impact-parameter representation of the position of the nucleons in the nucleus.

At high energy, the Fermi motion of the nucleons may be taken as neglegible and so it is assumed that these do not move during the time of the collision. A further simplifying assumption is made that the trajectory of the incident particle does not significantly deviate from a straight line, reducing the path integral to a simple summation. The main and fundamental assumption is then made that the phase-shifts are additive (i.e. the potentials are additive) so that the total eikonal phase-shift for the nucleus is equal to the sum of the individual phase-shifts, and together with the previous assumption gives

$$\chi(\underline{b},\underline{s}_1,\ldots,\underline{s}_A) = \chi_1(\underline{b}-\underline{s}_1) + \chi_2(\underline{b}-\underline{s}_2) + \ldots + \chi_A(\underline{b}-\underline{s}_A) \qquad (5.37)$$

The total profile function is then given by

$$\Gamma(\underline{b},\underline{s}_1,\ldots,\underline{s}_A) = 1 - e^{i\chi(\underline{b},\underline{s}_1,\ldots,\underline{s}_A)}$$

$$= 1 - \prod_{j=1}^{A} (1 - \Gamma_j(\underline{b}-\underline{s}_j)) \qquad (5.38)$$

To obtain the amplitude for scattering from an initial nuclear state $|i\rangle$ to a final state $|f\rangle$, a description of the final and initial nuclear states is substituted into (5.35) together with the expansion (5.38) for , to obtain the amplitude

$$F_{fi}(\underline{q}) = \frac{ik^*}{2\pi} \int e^{i\underline{q}.\underline{b}} \langle f| \Gamma(\underline{b},\underline{s}_1,\ldots,\underline{s}_A) |i\rangle \, d^2\underline{b} \qquad (5.39)$$

Equation (5.39) differs from (5.35) in two forms, firstly in the additional description of the nuclear state (an assumption), and also in the term k^*, where $\underline{k}^*$ is the momentum of the incident

particle relative to the whole nucleus. A further term is also required in (5.39) to account for the centre of mass constraint by means of the factor $\delta\left(\frac{1}{A}\sum_{i=1}^{A}\underline{r}_i\right)$ so that (5.39) becomes

$$F_{fi}(\underline{q}) = \frac{ik}{2\pi}^{*}\int e^{i\underline{q}.\underline{b}}\langle f|\ \delta(A^{-1}\sum_{i=1}^{A}\underline{r}_i)(1-\prod_{j=1}^{A}(1-\Gamma_j(\underline{b}-\underline{s}_j)))\ |i\rangle\, d^2\underline{b} \tag{5.40}$$

and using the inverse transform (5.36) this finally becomes

$$F_{fi}(\underline{q}) = \frac{ik}{2\pi}^{*}\int e^{i\underline{q}.\underline{b}}\langle f|\ \delta(A^{-1}\sum_{i=1}^{A}r_i)\ \times$$

$$\times\left\{1-\prod_{j=1}^{A}\left(1-\frac{1}{2\pi ik}\int e^{-i\underline{q}_j.(\underline{b}-\underline{s}_j)}f_j(\underline{q}_j)\,d^2\underline{q}_j\right)\right\}|i\rangle\, d^2\underline{b} \tag{5.41}$$

Franco and Glauber[50] have shown that (5.41) may represent the amplitude in either the laboratory or c.m. frame according to the values of $\underline{k}$ and $\underline{k}^{*}$ used. Since the quantity $F_{fi}(\underline{q})/k^{*}$ is invariant, this may be evaluated in either frame. In general, in the literature k and k^{*} are not differentiated between and this may lead to confusion, since working in the c.m. system, $\underline{k}$ is the momentum in the particle-nucleon centre of mass while $\underline{k}^{*}$ is that in the particle-nucleus centre of mass.

The expansion (5.41) provides a description of the scattering amplitude as a series of up to A-fold collisions with no nucleon twice acting as the scattering centre. The alternate signs of the multiple-scattering terms is of importance since this provides the

interference forms which characterise π-A and p-A scattering.

The chief difference between Glaubers series and that of Watson lies in Glaubers summing of the phases (or potentials) rather than the amplitudes and thus being able to obtain a closed form in a finite series. The eikonal approximation contributes only to the additivity assumption for the phase-shifts and Osborn has shown[94] that starting from an approximation that is unitary and includes the impulse approximation a Glauber-type series will be obtained.

For a small nucleus such as He^4, the delta-function in (5.41) may be explicitly included in the calculations, but for large nuclei this becomes too complicated, and may be removed from the integral signs by means of the Gartenhaus-Schwartz transformation[106] although this is only simple for a simple-harmonic oscillator type of nuclear wave-function[107], where the removal of the δ-function corresponds to multiplying the amplitude by a factor of

$$R(\underline{q}) = e^{-q^2/4A\alpha^2} \qquad (5.42)$$

α being the spring constant.

For small angles, the effects of coulomb scattering are important and these may be included[48,78,108] by a suitable addition to the eikonal phase shift so that

$$\chi_{tot}(\underline{b}) = \chi_c(\underline{b}) + \chi_s(\underline{b}) \qquad (5.43)$$

where $\chi_c(\underline{b})$ is the coulomb phase-shift and $\chi_s(\underline{b})$ is the usual strong interaction phase-shift. In the calculations that follow, the coulomb interaction has been neglected since we are chiefly interested at angles away from the coulomb region.

CHAPTER 6 The Elastic Scattering of Pions from Helium-4

6:1 The Pion-Nucleon system

As an important preliminary to studying scattering from nuclei, the form of the free particle-nucleon scattering should be examined. This section reviews some general features of the pion-nucleon system and of the kinematics used in the analysis of high-energy scattering processes, which may be applied also to the case of elastic pion - - nucleus scattering.

So far the experiments performed in hadron-nucleus scattering have been with beams of protons or pi-mesons[56,57,66,67,76,81,109]. This chapter is limited to the study of pion scattering chiefly because the free π-nucleon amplitudes are much less complex than for the case of protons, requiring only two complex amplitudes for their description as opposed to five for the more complex spin dependence of the latter. In addition the π-nucleon interaction is not so strong as that of the proton-nucleon so that altogether the π-nucleon system is better known than the proton-nucleon and a greater accuracy is obtainable for the input. Thus for a comprehensive attempt to compare calculation with experimental result, it is preferable to use the best-known input and to make a comparison between different nuclear models a reliable hadron-nucleon input to equation (5.41) is very useful.

The πN system has been comprehensively studied and reviewed[110]. The features that are of concern to the following calculations are the description of forward angle scattering, since most hadron-nucleus scattering measurements are at forward angles, and the decomposition of the π-nucleon amplitudes in terms of spin and isospin.

The π-nucleon interaction, like the $\bar{K}N$ interaction, is of the form

$0^-\frac{1}{2}^+ \longrightarrow 0^-\frac{1}{2}^+$ but differs in that there is not the wealth of inelastic two-body channels. For the π^-p case, the only open two - - body channel is the charge exchange reaction to $\pi^0 n$ while π^+p has no other two-body channels. In the manner described in Chapter 1, the πN amplitude may be decomposed into the form

$$F_{\pi N}(\theta) = f(\theta) + g(\theta)\, \underline{\sigma}.\underline{n} \qquad (6.1)$$

with the spin-flip and non-spin-flip amplitudes being further decomposed into isospin states.

In the work that follows, it is convenient to work in terms of the relativistic invariant t, rather than θ, where the Mandalstam variables s,t,u are defined for the reaction $1\ 2 \longrightarrow 3\ 4$ by the following relations

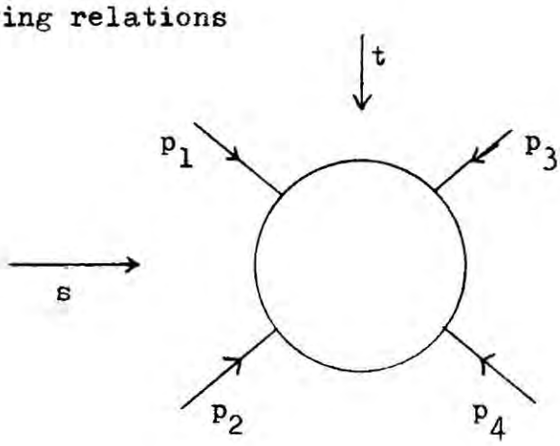

$$\begin{aligned} s &= (p_1 + p_2)^2 \\ t &= (p_1 + p_3)^2 \\ u &= (p_1 + p_4)^2 \end{aligned} \qquad (6.2)$$

where p_i is the 4 - vector for particle i defined by

$$p_i = (E_i, \underline{p}_i) \qquad (6.3)$$

The variable s corresponds to the square of the c.m. energy, t is the square of the 4 - momentum transfer and u is the square of

the 4 - momentum transfer in the crossed channel. s,t,u are related by the relation

$$s + t + u = \sum_i m_i^2 \qquad (6.4)$$

and for elastic scattering, t may be related to the c.m. scattering angle θ by the relation

$$t = -2k^2 (1 - \cos\theta) \qquad (6.5)$$

where k is the incident c.m. momentum. It is common to compare calculations with data for the invariant differential cross-section $d\sigma/dt$ defined as

$$d\sigma/dt = \frac{\pi}{k_1 k_2} \left(\frac{d\sigma}{d\Omega} \right) \qquad (6.6)$$

where $\underline{k}_1$ is the incident c.m. momentum, $\underline{k}_2$ the final c.m. momentum. The comparison is generally made by plotting $d\sigma/dt$ or $d\sigma/d\Omega$ against $-t$.

In multiple-scattering calculations, using series of the form (5.41) at small angle, the eikonal conservation of the forward component of the momentum leads to the approximate relation for the momentum transfer $\underline{q} = \underline{k} - \underline{k}'$ of

$$q^2 = -t \qquad (6.7)$$

which is commonly used for small-angle high-energy calculations of this type and relation (6.7) will be assumed for the latter part of this chapter.

Since the pions form an isotriplet and the nucleons an isodoublet the πN interaction is described by amplitudes of total isospin 1/2 and 3/2 . By an isospin decomposition of the form described in

Chapter 2, the amplitudes for the three measurable πN reactions take the form

$$\begin{aligned} \langle \pi^+ p \mid T \mid \pi^+ p \rangle &= T^{3/2} \\ \langle \pi^- p \mid T \mid \pi^- p \rangle &= \tfrac{1}{3} T^{3/2} + \tfrac{2}{3} T^{1/2} \\ \langle \pi^0 n \mid T \mid \pi^- p \rangle &= \tfrac{\sqrt{2}}{3} (T^{3/2} - T^{1/2}) \end{aligned} \qquad (6.8)$$

where $T^{1/2}$ and $T^{3/2}$ are the amplitudes for states of total isospin $1/2$ and $3/2$.

For the purposes of incorporating isospin into the multiple - - scattering series[64,65,111,112], it is convenient, as shown by Baier & Samaranayake in Reference(64) to work in terms of the isospin-non-flip and flip amplitudes rather than those of total isospin. These are constructed by observing that for $\pi N \longrightarrow \pi N$ reactions, for meson indices α and β the amplitude may be written as a matrix in the nucleon isospin space[113], and using the usual τ-matrices this takes the form

$$F_{\alpha\beta} = \delta_{\alpha\beta} F^+ + \tfrac{1}{2} \left[\tau_\alpha , \tau_\beta \right] F^- \qquad (6.9)$$

and if θ is the isospin operator for the π-meson the projection operators for $I = 3/2$ and $I = 1/2$ may be obtained by observing that

$$\underline{I} = \tfrac{1}{2} \underline{\tau} + \underline{\theta}$$

from which

$$\underline{\theta} . \underline{\tau} = I(I+1) - 2 - \tfrac{3}{4} \qquad (6.10)$$

so that the projection operators have the forms

$$P_{3/2} = \frac{2 + \underline{\tau}.\underline{\theta}}{3}$$

$$P_{1/2} = \frac{1 - \underline{\tau}.\underline{\theta}}{3} \qquad (6.11)$$

and

$$\delta_{\alpha\beta} = \left(P_{3/2} + P_{1/2} \right)_{\alpha\beta}$$

$$(\underline{\tau}.\underline{\theta})_{\alpha\beta} = \left(P_{3/2} - 2P_{1/2} \right)_{\alpha\beta} \qquad (6.12)$$

Finally by the relation

$$\frac{1}{2}\left[\tau_\alpha , \tau_\beta\right] = i\,\varepsilon_{\alpha\beta\gamma}\tau_\gamma = -\underline{\tau}.\underline{\theta}_{\alpha\beta} \qquad (6.13)$$

the total πN amplitude may be written from (6.9) and (6.13) as

$$F_{\pi N} = F^+ - F^-(\theta\tau) \qquad (6.14)$$

where F^+ and F^- are composed of non-spin-flip and spin-flip amplitudes as before, so that the total πN amplitude takes the form

$$F_{\pi N}(t) = f^+ - f^-(\theta\tau) + g^+(\underline{\sigma}.\underline{n}) - g^-(\underline{\sigma}.\underline{n})(\theta\tau) \qquad (6.15)$$

Using the projection operators (6.12), F^+ and F^- may be related to the amplitudes of total isospin as

$$F^+ = \frac{2}{3} F_{3/2} + \frac{1}{3} F_{1/2}$$

$$F^- = \frac{1}{3} F_{1/2} - \frac{1}{3} F_{3/2} \qquad (6.16)$$

so that

$$\langle \pi^- p \mid T \mid \pi^- p \rangle = F^+ + F^-$$
$$\langle \pi^+ p \mid T \mid \pi^+ p \rangle = F^+ - F^- \qquad (6.17)$$

Consequently, by means of these relations the amplitudes f^+, f^-, g^+, and g^- may be obtained from the amplitudes $f_{1/2}$, $f_{3/2}$, $g_{1/2}$, $g_{3/2}$ more usually found for πN scattering.

6:2 The Glauber series for Helium-4

The Helium-4 nucleus presents a very good target for the study of multiple-scattering effects since it has a total spin of zero, so that the elastic scattering may be described as spin zero - spin zero, and since the spin and isospin of the four nucleons label each individually. A further advantage lies in the relatively short series obtained from (5.41) so that the computational requirements of more elaborate input may be tolerated and furthermore the c.m. constraint may be explicitly included. Since the first excited state for the nucleus is rather high, the Helium nucleus offers a good opportunity to measure elastic scattering without excitation, simplifying the analysis required.

Although data for π-meson scattering from Helium-4 is only available in limited quantities[66,67,114] a considerable body of literature exists on its study as well as for the scattering of protons[58-69]. Hence it is possible to make quite extensive comparisons between the different forms used and their results.

The calculations of this chapter have been made using the formalism and derivation of Baier and Samaranayake[64,65], incorporating both spin and isospin into the series (5.41) and which is described below.

Denoting the π-meson states as $|\pi\rangle$ and the nuclear states as $|\alpha\rangle$, the expression (5.41) for the ^{4}He nucleus takes the form

$$F_{fi}(\underline{q}) = \langle\pi_f|\langle\alpha_f| \frac{ik}{2\pi}^* \int d^2\underline{b}\ e^{i\underline{q}.\underline{b}}\ \delta\Big(\frac{1}{4}\sum_{i=1}^{4}\underline{r}_i\Big)\ x$$

$$x\Big\{1 - \sum_{j=1}^{4}\Big(1 - \frac{1}{2\pi ik}\int d^2\underline{q}'_j\ e^{-i\underline{q}'_j.(\underline{b}-\underline{s}_j)}\ f_j(\underline{q}_j)\Big)\Big\}|\alpha_i\rangle|\pi_i\rangle \tag{6.18}$$

Since the discussion is restricted to elastic scattering, $|\pi_i\rangle = |\pi_f\rangle$ and $|\alpha_i\rangle = |\alpha_f\rangle$ represents the ground state for ^{4}He. It is convenient to resolve this into a product between a Slater determinant $|\Phi\rangle$ describing the antisymmetric spin-isospin state and a space part $|s\rangle$ which describes the spacial distribution of the nucleons as elaborated in the next section. So that

$$|\alpha\rangle = |\Phi\rangle|s\rangle$$

In obtaining (6.18), where the πN amplitudes $f_j(\underline{q}_j)$ are spin and isospin dependent, the products of the profile functions in (5.40) are not in general commutative and so the sum in (6.18) requires that the terms of the series allow for all possible orderings as further described in Appendix D.

Following Reference(64), the amplitude $f_j(\underline{q}_j)$ for the j-th nucleon in (6.18) is taken to be of the form

$$f_j(\underline{q}_j) = f^+ - f^-(\theta\tau_j) + g^+(\underline{\sigma}^j.\underline{n}^j) - g^-(\underline{\sigma}^j.\underline{n}^j)(\theta\tau_j) \tag{6.19}$$

where $\underline{\sigma}.\underline{n}$ and $\theta\tau$ operate on the spin-isospin part $|\Phi\rangle$ of the total wave-function of ^{4}He . Equation (6.18) may then be written

$$F_{el}(\underline{q}) = \frac{ik}{2\pi}^{*} \langle a | \int d^2\underline{b}\ e^{i\underline{q}.\underline{b}}\ \delta\left(\frac{1}{4}\sum_{i}^{4}\underline{r}_i\right) \sum_{j=1}^{4} \left\{(-1)^{j+1} \times \right.$$

$$\times \left(\frac{1}{2\pi ik}\right)^{j} \int d^2\underline{q}_1 .. d^2\underline{q}_j\ e^{-i\underline{q}_1.(\underline{b}-\underline{s}_1) - \ldots - i\underline{q}_j.(\underline{b}-\underline{s}_j)} \times$$

$$\left. \times \quad f_1(\underline{q}_1) \ldots . f_j(\underline{q}_j) \right\} | a \rangle \qquad (6.20)$$

and removing the spin and isospin dependent terms as described in Appendix D, this becomes

$$F_{el}(\underline{q}) = \frac{ik}{2\pi}^{*} \langle s | \int d^2\underline{b}\ e^{i\underline{q}.\underline{b}}\ \delta\left(\frac{1}{4}\sum_{i}\underline{r}_i\right) \sum_{j=1}^{4} (-1)^{j+1} \left(\frac{1}{2\pi ik}\right)^{j} \times$$

$$\times \int d^2\underline{q}_1 .. d^2\underline{q}_j\ e^{-i\underline{q}_1.(\underline{b}-\underline{s}_1) .. -i\underline{q}_j.(\underline{b}-\underline{s}_j)}\ G^{j}(\underline{q}_1,..,\underline{q}_j) | s \rangle \qquad (6.21)$$

where the forms of the terms G^j are listed in Appendix D. The remaining part of the evaluation of (6.21) may then be treated in the usual manner since the $G^j(\underline{q}_1,..\underline{q}_j)$ are functions only of the $\underline{q}_j$.

To describe the space part of the wave-function, $| s \rangle$, a probability function $\Psi(\underline{r}_1,\ldots,\underline{r}_4)$ is defined so that

$$\int |\Psi(\underline{r}_1,\ldots,\underline{r}_4)|^2\ d\underline{r}_1 .. d\underline{r}_4 = \langle s | s \rangle \qquad (6.22)$$

and so that (6.21) takes the final form

$$F_{el}(\underline{q}) = \frac{ik^*}{2\pi}\int d^2\underline{b}\; e^{i\underline{q}.\underline{b}}\int d\underline{r}_1..d\underline{r}_4|\Psi(\underline{r}_1,..,\underline{r}_4)|^2\;\delta(\tfrac{1}{4}\sum_i \underline{r}_i) \quad x$$

$$x \sum_{j=1}^{4}(-1)^{j+1}\left(\frac{1}{2\pi ik}\right)^j \int d^2\underline{q}_1..d^2\underline{q}_j\; e^{-i\underline{q}_1.(\underline{b}-\underline{s}_1)}\;..\;-i\underline{q}_j.(\underline{b}-\underline{s}_j) \quad x$$

$$x \quad G^j(\underline{q}_1,...,\underline{q}_j) \qquad (6.23)$$

In section (6:4) the results of evaluating (6.23) for different forms of $|\Psi|^2$ are shown and compared with the experimentally measured differential cross-sections by the usual form

$$d\sigma/d\Omega \quad = \left|F_{el}(\underline{q})\right|^2 \qquad (6.24)$$

As has been observed[64], it is often more convenient to use the amplitude

$$F'_{el}(\underline{q}) = F_{el}(\underline{q})/k^* \qquad (6.25)$$

since

$$\frac{d\sigma}{dt} = \pi\left|F'_{el}(\underline{q})\right|^2 \qquad (6.26)$$

and so when evaluating $F'_{el}(\underline{q})$, the right hand side is invariant and may be evaluated in either the laboratory or centre of mass frames. In those calculations which follow, the right hand side is generally evaluated in the c.m. frame.

6:3 Nuclear densities for Helium-4

To evaluate the amplitude of expression (6.23) the πN amplitudes are required and also a form for $|\Psi(\underline{r}_1,..,\underline{r}_4)|^2$, describing the distribution of the nucleons within the nucleus.

This is generally provided by selecting some parametric form for the density distribution $\rho(\underline{r}_1,..,\underline{r}_4) = |\Psi|^2$ and obtaining the parameter values from a fit to the high-energy electron scattering data in the form of the charge form factor $F(q^2)$, where this represents the ratio between the differential cross-section for scattering from a point-charge nucleus and the measured differential cross-section

$$|F(q^2)|^2 = \frac{d\sigma}{d\Omega}_{el} \Big/ \frac{d\sigma}{d\Omega}_{point} \tag{6.27}$$

where

$$\frac{d\sigma}{d\Omega}_{point} = \left(\frac{Ze^2}{2E_o}\right)^2 \frac{\cos^2(\theta/2)}{\sin^4(\theta/2)} \frac{1}{1+\frac{2E_o}{mc^2}\sin^2\theta/2} \tag{6.28}$$

so that

$$\frac{d\sigma}{d\Omega}_{el} = \left(\frac{Ze^2}{2E_o}\right)^2 \frac{\cos^2\theta/2}{\sin^4\theta/2} \frac{|F(q^2)|^2}{1+\frac{2E_o}{mc^2}\sin^2\theta/2} \tag{6.29}$$

and by means of the Born term, we may write approximately

$$F(q^2) = \int \rho_{ch}(\underline{r})\, e^{i\underline{q}.\underline{r}}\, d\underline{r} \tag{6.30}$$

To use the form of $\rho_{ch}(\underline{r})$ found in this way, the assumption is made that the neutron and proton distributions are the same so that

a knowledge of $\rho_{ch}(\underline{r})$ and the nucleon form factor is sufficient to obtain the mass density function $\rho(\underline{r})$.

The parametric form selected for $\rho(\underline{r})$ is usually considerably influenced by the desire that the integrals of (6.23) should be capable of analytic evaluation, and consequently many of the forms used involve combinations of gaussian terms. The most popular forms are briefly reviewed below, these generally incorporate the further assumption that $\rho(\underline{r}_1,\ldots,\underline{r}_4)$ may be factorised into a product of one-particle functions with the possible inclusion of nucleon-nucleon correlations.

The simplest of these models is to assume that $\rho(\underline{r})$ may be factorised into a product of simple gaussians to give

$$\rho(\underline{r}_1,\ldots,\underline{r}_4) = \rho_o \prod_{i=1}^{4} e^{-a^2 r_i^2} \qquad (6.31)$$

where ρ_o is the normalisation factor. This simple model can describe most of the features of electron and proton scattering[59,63] but is unable to provide a complete description.

An improved form was used by Bassel & Wilkin[69] and by Chou[58], describing $\rho(\underline{r})$ by a product form with a hard core to reduce the possibility of states with all the nucleons in the centre, using the form

$$\rho(\underline{r}_1,\ldots,\underline{r}_4) = \rho_o \prod_{i=1}^{4} \left(e^{-a^2 r_i^2} - C e^{-\gamma^2 r_i^2} \right) \qquad (6.32)$$

with three parameters to be determined from the electron data, a,γ,C .

To give a description of the spacing between nucleons a more complicated form has also been used, including the correlations by means of a Jastrow series[116] and thus, if a hard core is also used,

having the form

$$\rho(\underline{r}_1,..,\underline{r}_4) = \rho_o \prod_{i=1}^{4} (e^{-a^2 r_i^2} - C e^{-\gamma^2 r_i^2}) \prod_{\substack{j=1 \\ j\neq k}}^{4} (1 - f_{jk}) \qquad (6.33)$$

The Jastrow term f_{jk} has been described by a number of forms, but the most convenient is generally the gaussian form,

$$f_{ij} = \exp(-\mu^2 (\underline{r}_i - \underline{r}_j)^2) \qquad (6.34)$$

where again α, γ, μ, C form the parameters for the fit to the electron scattering data.

The possible importance of correlation effects for the regions where multiple-scattering is important has led to considerable analysis of the electron scattering data[117-121] using correlated wave-functions of this type. One of the objects of the calculations described in the next section was to investigate any correspondence between the results for the different forms of distribution when applied to both electron and π-meson scattering.

6:4 Calculations for $\pi^- - {}^4He$

At present the differential cross-section for $\pi^- - {}^4He$ elastic scattering is limited in quantity, having been measured only for π^- laboratory momenta of 257 MeV/c , 1.25 GeV/c and 7.76 GeV/c[114,66,67]. However, as can be seen, the existing data covers a considerable range where the validity of the model used is concerned. The low-energy data is much older than the other, with large errors, but is in good agreement with the preliminary results of more recent measurements[122], while the rest of the data is relatively recent and of higher accuracy.

Calculations have been made for comparison with the above data

using the forms described in the preceding sections, and these and their results for each set of data are given in the rest of this section.

1.25 GeV/c Despite the limitations applied to the range of Glaubers model by the derivations, the model has been used at much lower energies quite successfully in a number of cases[102,123,125], and was expected to give a good description of the main features of the data at this energy. Baier and Samaranayake have performed quite thorough calculations at 1 GeV/c [64], a similar approach being used here.

To obtain the complete πN amplitude (6.19), the amplitudes $f_{1/2}$, $f_{3/2}$, $g_{1/2}$, $g_{3/2}$ were reconstructed from the available phase-shift data[126] over a range of t-values, and the amplitude was then derived for each t-value by means of the relations (6.16) [127]

$$F^{+} = \frac{2}{3} F_{3/2} + \frac{1}{3} F_{1/2}$$

$$F^{-} = \frac{1}{3} F_{1/2} - \frac{1}{3} F_{3/2}$$

A parameterisation was then required for the full amplitude so that the multiple integrals of (6.23) could be evaluated analytically. It was also required that the angular range fitted by this form for the πN data should be large enough to describe the ^{4}He data, although as pointed out in reference(64), the former range need not equal the latter since the large-angle ^{4}He scattering is predominantly composed of multiple small-angle scatterings. To standardise the resultant integrals, a wholly gaussian parametric form was used and the form used was finally taken to be

$$f^+(t) = \mathrm{Re}f^+(0)\, e^{\alpha_1 t} + A_1(e^{\alpha_2 t} - e^{\alpha_3 t}) + i\,\mathrm{Im}\, f^+(0) e^{\alpha_4 t}$$

$$f^-(t) = \mathrm{Re}\, f^-(0) e^{\alpha_5 t} + A_2(e^{\alpha_6 t} - e^{\alpha_7 t}) + i\,\mathrm{Im} f^-(0) e^{\alpha_8 t} + A_3(e^{\alpha_9 t} - e^{\alpha_{10} t})$$

$$g^+(t) = A_4(e^{\alpha_{11} t} - e^{\alpha_{12} t}) + i A_5(e^{\alpha_{13} t} - e^{\alpha_{14} t})$$

$$g^-(t) = A_6(e^{\alpha_{15} t} - e^{\alpha_{16} t}) + iA_7(e^{\alpha_{17} t} - e^{\alpha_{18} t})$$

(6.35)

The parameters $A_1 - A_7$, $\alpha_1 - \alpha_{18}$ were then obtained by fitting these forms to the amplitudes derived from the phase-shifts, using the program MINUIT [36] as described in part I. The values obtained for the range $0 \leq -t \leq 0.50$ are listed in Table VI .

Table VI Parameters for πN scattering at 1.26 GeV/c.

Parameter	Value	Parameter	Value
A_1	-0.9213	α_6	0.1871
A_2	8.8007	α_7	0.4805
A_3	0.0	α_8	0.00
A_4	-1.8557	α_9	0.00
A_5	1.6335	α_{10}	0.00
A_6	-3.7077	α_{11}	2.9095
A_7	3.4746	α_{12}	5.3953
α_1	1.2783	α_{13}	2.6590
α_2	2.3460	α_{14}	21.6620
α_3	7.8795	α_{15}	10.9980
α_4	3.8566	α_{16}	13.1940
α_5	0.0579	α_{17}	8.1661
		α_{18}	5.5416

The differential cross-section over the range of t that was of interest was calculated from (6.23) and values obtained for the nuclear densities of (6.31) and (6.32). In addition a truncated form of (6.33) was used, in which only the singly correlated terms are retained in the latter part of the expression giving a form

$$\rho(\underline{r}) = \rho_o \prod_{i=1}^{4} (e^{-\alpha^2 r_i^2} - C e^{-\gamma^2 r_i^2})(1 - \sum_{\substack{j=1 \\ k \neq j}}^{4} f_{jk}) \qquad (6.36)$$

The manner of evaluation of the multiple-integrals of (6.23) is described in Appendix E together with a description of the program DSDT used to calculate the differential cross-sections. Since the gaussian forms used throughout allowed (6.23) to be evaluated analytically, the computing was chiefly reduced to an exercise in book-keeping.

In reference(64) it was found that even when the πN spin-flip term was most significant at 0.826 GeV/c, the effects of the spin--flip were neglegible in ^4He and so the calculations for 1.25 GeV/c were repeated with g^+ and g^- omitted to examine the effects at a slightly higher momentum value.

Querrou[61] has analysed this data using a nuclear density of the form (6.32) and similarly finds that the only effect from a neglect of spin dependence is a slight movement in the position of the dip. He has also calculated the effects of Fermi motion, which we neglect, and similarly found this to be small. One of the objects of his analysis was to compare different sets of input data in the form of phase-shifts for πN which produce different results particularly in the region of the second maximum. The data itself is largely concentrated in this region, with only two points in the forward region so that any

detailed comparison may only be made in a small region.

Figure XI shows the results of the calculations made using the full πN amplitude and the hard-core nuclear density of (6.32), showing most divergence from the data in the region of the second maximum where the model is not expected to be so reliable in any case. Figure XIIA shows the results of a similar calculation using a simple gaussian nuclear density (6.31) which gives a poorer description of the forward peak, removing the conviction from the apparently better description of the second peak. In both cases the neglect of the spin-flip terms proved to have little effect beyond a slight shifting of the dip.

The calculations made with the singly-correlated form(6.36) proved to be very close to those made using the uncorrelated form suggesting that single correlations are of little significance at this energy. A discussion of the conclusions that might be drawn from these results is given in Chapter 8.

257 MeV/c To see if the type of calculation described above would work at lower energy, an attempt was made to describe the $\pi^- - {}^4He$ data at 257 MeV/c obtained by Budagov et al.[114]. As before the πN amplitudes were obtained from the phase-shift data and the differential cross-sections were obtained in the same manner.

However to fit the πN data over an acceptable angular range proved much more difficult, since the differential cross-section at low energies is less easily described by gaussian forms and is dominated by the presence of the (3,3) resonance, so that the fits obtained with the forms of (6.35) were far from satisfactory. The subsequent calculation of the differential cross-section was unsuccessful, the resultant multiple-scattering series being very

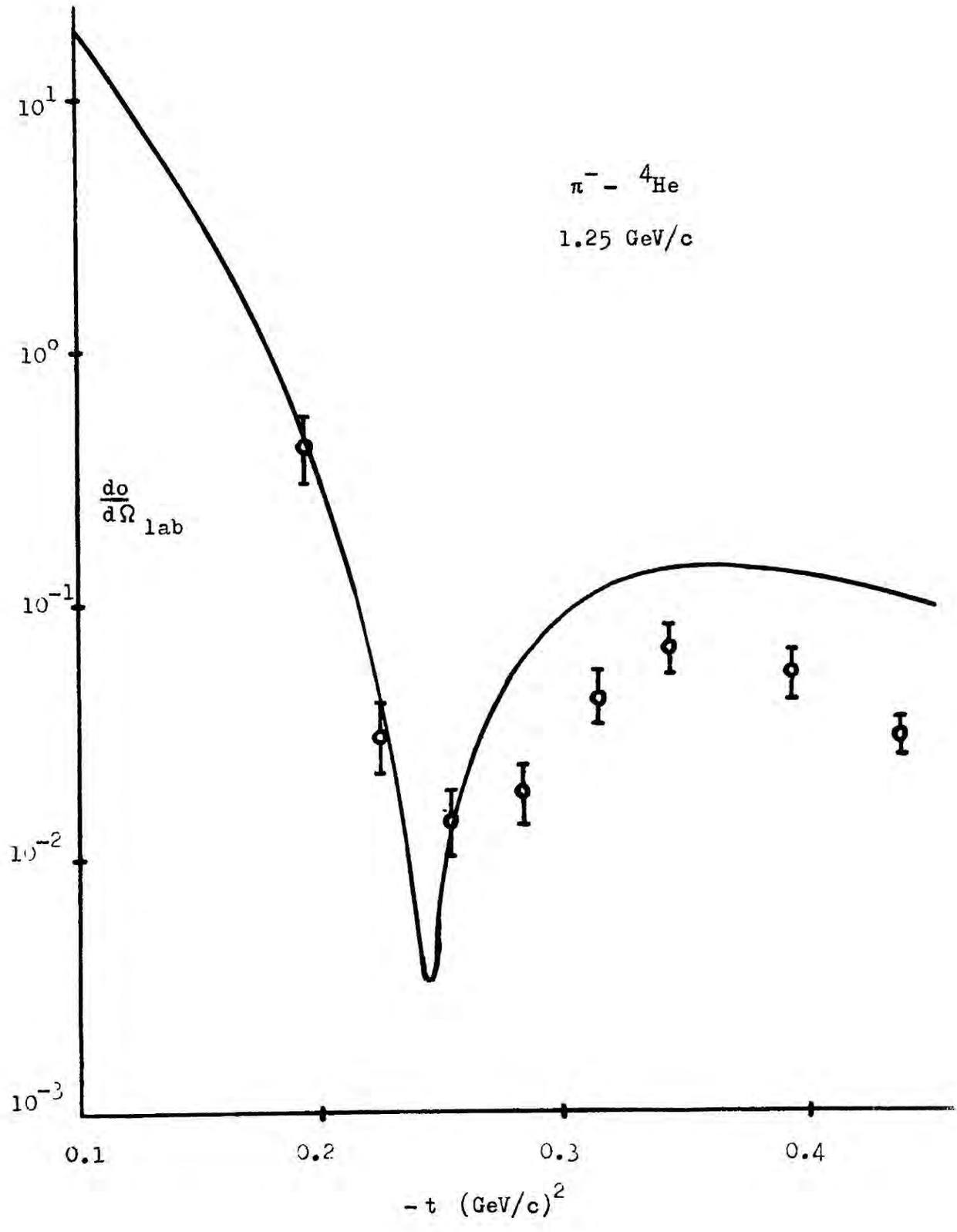

Figure XI $d\sigma/d\Omega_{lab}$ for $\pi^- - {}^4He$ at 1.25 GeV/c using the full πN amplitude and the nuclear density of Reference(58).

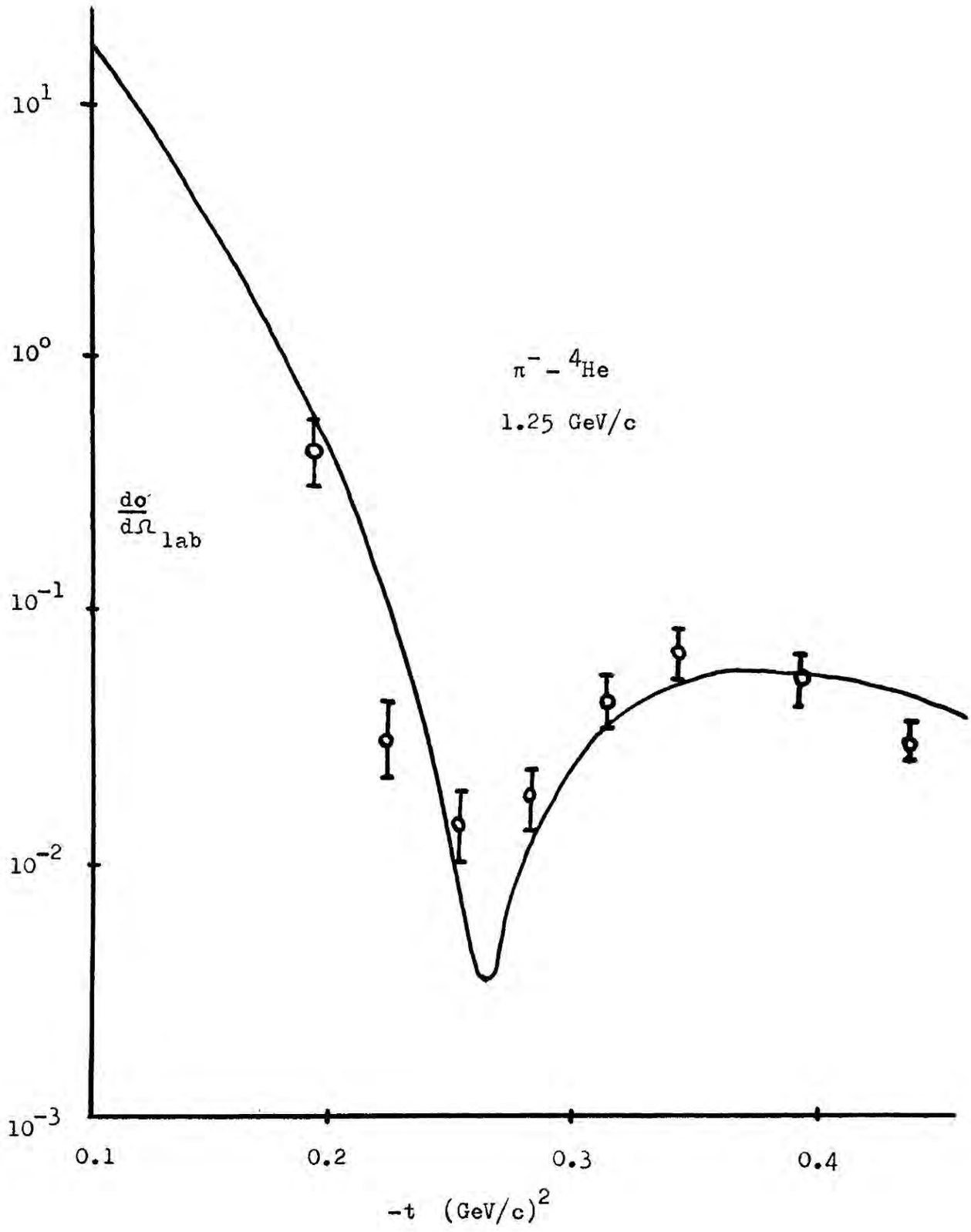

Figure XIIA $d\sigma/d\Omega_{lab}$ for $\pi^- - {}^4He$ at 1.25 GeV/c using the full πN amplitude and a simple gaussian nuclear density.

unstable and no recognisable form being obtained.

7.76 GeV/c It is for energies such as this that the Glauber model may be expected to give its best results and so the data for this energy was investigated as thoroughly as possible. The main observations from this investigation have been published elsewhere[128] and the details are given again here.

The differential cross-section data of Ekelof et al.[67,129] covers a wide range from the forward peak to the tail of the second peak, and is therefore much more complete than the data for 1.25 GeV/c which covers mainly the second peak.

At these energies the πN differential cross-sections are well described by a gaussian form and so the program used to evaluate the scattering at 1.25 GeV/c was easily able to make the calculations for this energy. Taking the πN differential cross-sections as

$$\frac{d\sigma}{dt} = A e^{-bt} \qquad (6.37)$$

and neglecting the spin-flip as neglegible at this energy, the elastic πN amplitudes may be parameterised by the form

$$f_{\pi^{\pm}p}(t) = \frac{ik\sigma_{\pm}}{4\pi} (1 + i\alpha_{\pm}) \exp(-\tfrac{1}{2} b^{\pm} t) \qquad (6.38)$$

where $\sigma_{\pm}$ and $\alpha_{\pm}$ are the total cross-sections and the ratios of real part / imaginary part respectively for $\pi^{-}p$ and $\pi^{+}p$. These values have been determined for 7.76 GeV/c [130] and were taken from the literature. The values of the slope parameters $b^{\pm}$ were not available for this energy, but were obtained by a least-squares fit to the wide-angle differential cross-section data at 8.5 GeV/c[131], the values obtained being in agreement with those published.

To obtain the total amplitude $F_{\pi N}$, which by neglect of spin--flip is reduced to the form

$$F_{\pi N}(t) = f^{+}(t) - f^{-}(t)(\theta\tau) \qquad (6.39)$$

the relations (6.18) were used whereby

$$f_{\pi^- p} = f^{+} + f^{-}$$

$$f_{\pi^+ p} = f^{+} - f^{-}$$

so that by inverting these relations, f^{+} and f^{-} could be obtained as a sum of gaussians in t, these taking the form

$$\begin{aligned}
\mathrm{Re}\, f^{+}(t) &= \frac{ik}{8\pi}\left\{\sigma_{-}\exp(-\tfrac{1}{2}b^{-}t) + \sigma_{+}\exp(-\tfrac{1}{2}b^{+}t)\right\} \\
\mathrm{Im}\, f^{+}(t) &= \frac{ik}{8\pi}\left\{\alpha_{-}\sigma_{-}\exp(-\tfrac{1}{2}b^{-}t) + \alpha_{+}\sigma_{+}\exp(-\tfrac{1}{2}b^{+}t)\right\} \\
\mathrm{Re}\, f^{-}(t) &= \frac{ik}{8\pi}\left\{\sigma_{-}\exp(-\tfrac{1}{2}b^{-}t) - \sigma_{+}\exp(-\tfrac{1}{2}b^{+}t)\right\} \\
\mathrm{Im}\, f^{-}(t) &= \frac{ik}{8\pi}\left\{\alpha_{-}\sigma_{-}\exp(-\tfrac{1}{2}b^{-}t) - \alpha_{+}\sigma_{+}\exp(-\tfrac{1}{2}b^{+}t)\right\}
\end{aligned} \qquad (6.40)$$

In addition, some of the calculations of Ekelof et al.[67] were repeated using a spin and isospin independent amplitude of the form

$$F_{\pi N} = \frac{ik\sigma}{4\pi}(1 + i\alpha)\exp(-\tfrac{1}{2}bt) \qquad (6.41)$$

and using $\sigma = 26.6$ mb and $b = 7.15$ $(\mathrm{GeV/c})^{-2}$. These were repeated for a number of values of α .

The shorter form of the πN input used at this energy allowed the inclusion of the more elaborate nuclear density functions, so that it was possible to calculate $d\sigma/dt$ using the density functions of (6.31), (6.32) and (6.33), and also the form (6.36) with correlation terms above first-order neglected.

By so doing, comparison could be made between the $\pi^- - {}^4He$ calculations, with and without correlations, and the analyses of the electron scattering experiments which have made investigations of correlation effects[117-120] in the nucleus.

In order to be able to make detailed comparison with the structure of the data, this was renormalised to the most forward measured value of $-t$, since the errors of normalisation were found to be quite considerable. Table VII gives some values of $d\sigma/dt$ calculated for different cases at several values of t as well as the normalised values, and from this it can be seen that the different forms of nuclear density produce only small changes in the results.

Figures XII and XIII show the measured values for $d\sigma/dt$ and the calculated values using the hard-core density (6.32) and the simple gaussian $F_{\pi N}$ and the complete form (6.40) respectively. Figure XIV shows the results for the complete form of $F_{\pi N}$ and the simple gaussian nuclear density.

The parameters for the different nuclear density functions used in the calculations at 1.25 GeV/c and 7.76 GeV/c were taken from the papers of (i) Czyż and Lesniak[63] for (6.31), (ii) Chou[58] for (6.32) and (iii) Bassel & Wilkin[69] for (6.33) and (6.36).

A discussion of the forms of the different results and the conclusions that may be drawn are given in the final chapter where the successes and failures of the model are reviewed.

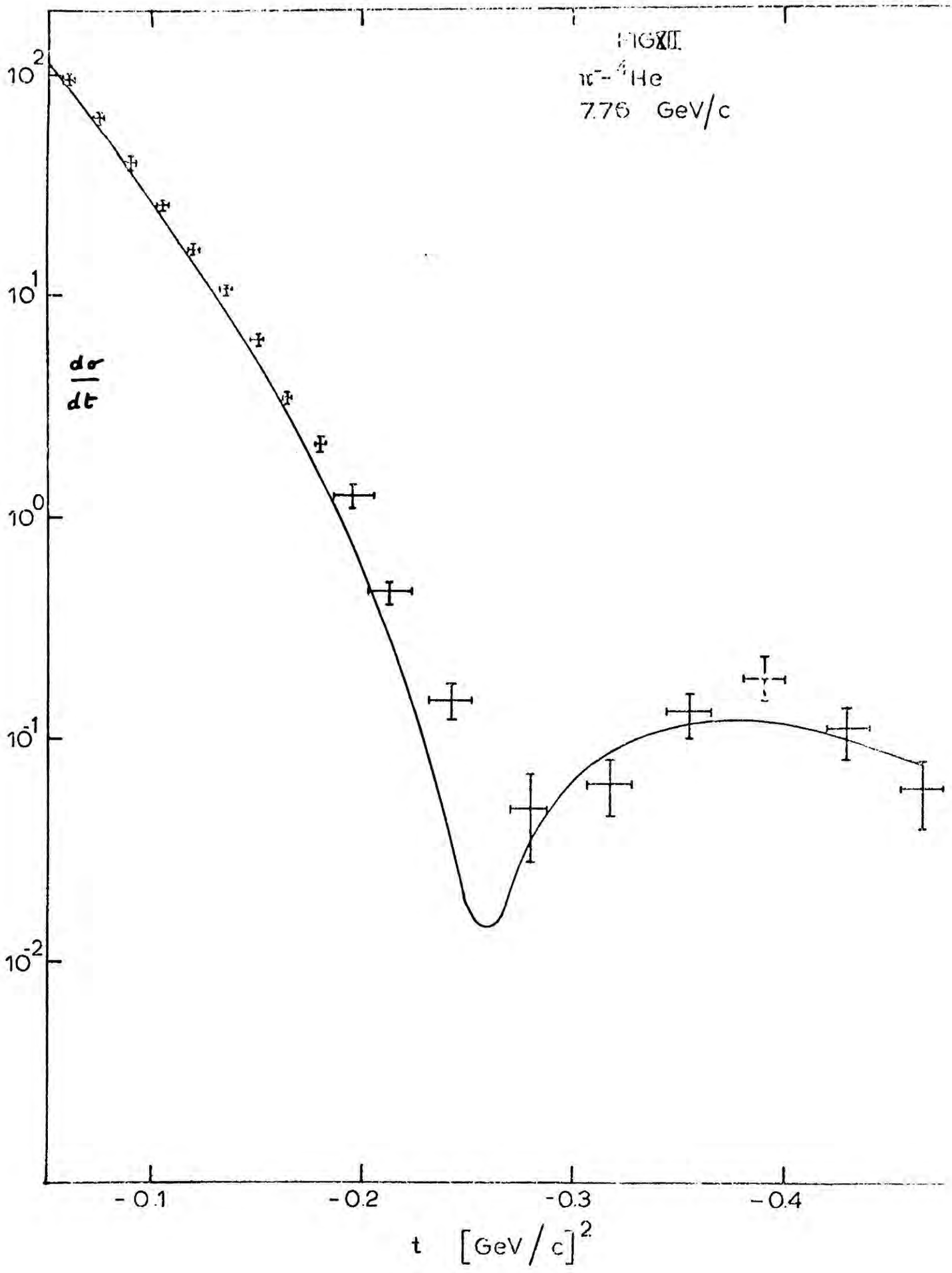

Figure XII $d\sigma/dt$ in $mb/(GeV/c)^2$ against t at 7.76 GeV/c using the simple gaussian form of $F_{\pi N}$ with $\alpha = -0.2$, and the nuclear density of Ref.(58) . The data has been normalised to the forward point.

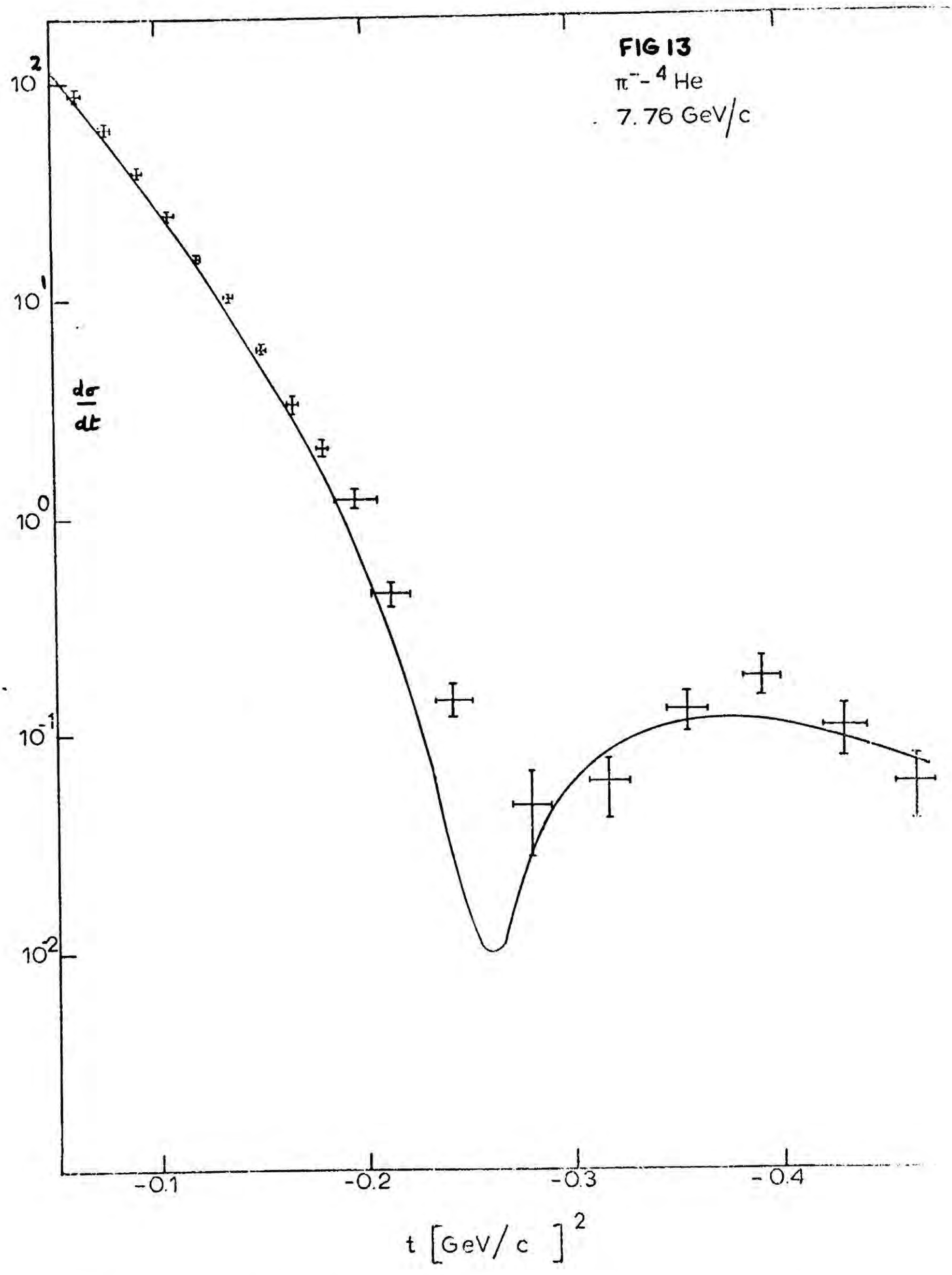

Figure XIII $d\sigma/dt$ in $mb/(GeV/c)^2$ against t at 7.76 GeV/c using the full πN amplitude and the nuclear density of Ref.(58). The data has been normalised to the forward point.

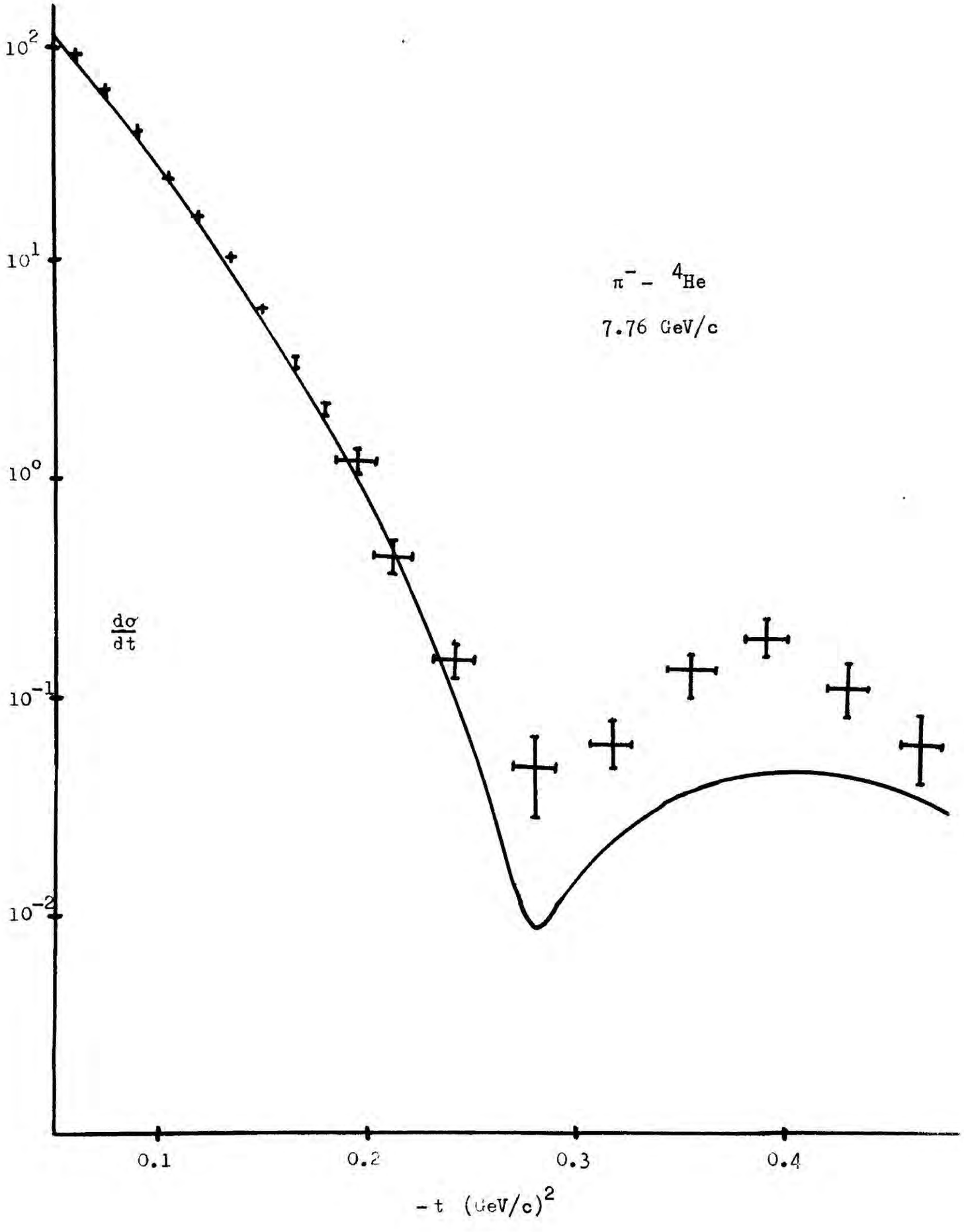

Figure XIV $d\sigma/dt$ in mb/(GeV/c)^2 against t at 7.76 GeV/c with full πN amplitude and a simple gaussian nuclear density.

$-t$ $(GeV/c)^2$	Measured values of $d\sigma/dt$	$d\sigma/dt^{(a)}$	$d\sigma/dt^{(b)}$	$d\sigma/dt^{(c)}$	$d\sigma/dt^{(d)}$
0.104	24.95 ± 1.8	24.23	23.58	20.81	25.41
0.149	6.1 ± 0.24	5.39	5.19	4.67	5.79
0.212	0.46 ± 0.05	0.33	0.31	0.28	0.37
0.280	0.048 ± 0.022	0.033	0.029	0.031	0.029
0.466	0.06 ± 0.026	0.081	0.076	0.078	0.09

Table VII Some calculated values of $d\sigma/dt$ compared with the measured values.

a) Simple gaussian $F_{\pi N}$, with $\alpha = -0.2$, and density of (6.32)

b) Full form of $F_{\pi N}$ and nuclear density (6.32)

c) Full form of $F_{\pi N}$ and singly-correlated density (6.36)

d) Full form of $F_{\pi N}$ and fully-correlated density (6.33)

CHAPTER 7 The α-particle model and Glauber's Theory for Carbon-12

7:1 π^- - ^{12}C and p - ^{12}C Scattering in Glauber Theory

The Carbon-12 nucleus has been less well-examined in experiment than has the Helium-4 nucleus described in the previous chapter, the only available data for elastic differential cross-sections being the 1 GeV proton scattering measurements of Palevsky et al.[81] and the low-energy π^- scattering measurements made by Binon et al.[109]

A number of papers have applied Glaubers multiple-scattering model in defferent forms to describe these measurements[69-74,82] with various degrees of success. The problem is made more complicated because, although the Carbon-12 nucleus is of spin zero, it is also known to be deformed and it has been shown that those calculations made for p-^{12}C scattering assuming that the nucleus is spherical are inadequate quantitatively, although the simple harmonic oscillator model describes similar data for ^{16}O extremely well[69]. From this the conclusion has been drawn that a better description for the nuclear density of ^{12}C is required.

Leśniak and Leśniak were able to show that a better description of the π^- - ^{12}C data could be obtained by the use of an oblately deformed simple harmonic oscillator density, but although this is in good agreement with the results of Hartree-Fock-like calculation, a later paper by Ciofi Degli Atti and Guardiola[72] has shown that such a deformation is not consistent with the high-energy electron and proton scattering data.

Another interesting suggestion for improving the description of the ^{12}C nucleus has been to use a description of the α-particle clustering effect which is known to be quite significant in ^{12}C and

Ahmad[82] has made some quite successful calculations of the p- ^{12}C differential cross-section using a very simple form of α-particle density. In this chapter this model is used to predict the π^-- ^{12}C differential cross-sections at 8 GeV/c by using the results of the preceding chapter, and in addition other forms of α-density are tried and the resultant calculations for proton scattering are compared with those from this simple form and with the available data.

7:2 The α-particle model

This model has quite a long history, being originated as far back as 1929 by Gamow to describe those nuclei having 4N configurations. Despite its later replacement by the more successful shell-model and other models it has enjoyed renewal in different forms, including the resonating group method and the Cluster model, which are reviewed in references (132) and (133) .

For the case of Carbon-12 the α-model in its different forms has proved of considerable popularity and has received considerable attention in the recent literature on the study of nuclear levels[134]. These generally assume that the ground state of the Carbon-12 nucleus consists of three α-particles forming a triangle and retaining seperate identities, descriptions of the excited nuclear levels being connected to the dilations and rotations of the triangle and the rearrangement of the α-particles.

In this chapter the elastic scattering of pions and protons from the Carbon-12 nucleus is taken to be described by a form of Glauber series in which the three α-particles act as the scattering centres and the resultant scattering is described by a sum of single, double and triple scatterings from these α's. The basic π-α and p-α amplitudes are obtained from a normal Glauber series for Helium-4.

The main approximations involved in the use of the α-particle model are (i) the α-particles are assumed to retain their identities throughout the scattering process, (ii) for the purposes of the calculation each α is treated as a spinless boson and (iii) the α-particles within the nucleus are usually (but not necessarily) taken to have the same parameters as a free α-particle. In addition the usual assumptions for a Glauber series are required. As will be seen, the α-model can give quite a good description of the scattering of protons from ^{12}C, which is the case which will be examined since the data is the most close to that energy region where Glaubers model may be expected to work well.

7:3 Elastic scattering with a simple model for ^{12}C

Probably the most simple model available is that adopted by Ahmad in his calculations[82] in which the three α-particles are constrained to a rigid equilateral triangle, of side d , which is free to assume any orientation. The elastic scattering amplitude may then be written as

$$F(\underline{q}) = \frac{k^*}{k} \langle 0 | F_1(\underline{q}) + F_2(\underline{q}) + F_3(\underline{q}) | 0 \rangle \qquad (7.1)$$

where the single, double and triple-scattering amplitudes have the forms

$$F_1(\underline{q}) = F_\alpha(\underline{q}) \sum_{j=1}^{3} \exp\left[i\underline{q}.\underline{s}_1\right] \qquad (7.2)$$

$$F_2(\underline{q}) = \frac{i}{2\pi k} \sum_{\ell \neq k}^{3} \int d\underline{q}_1 \, F_\alpha(\underline{q}_1) F_\alpha(\underline{q}-\underline{q}_1) \exp\left[i\underline{q}.\underline{s}_\ell + (\underline{q}-\underline{q}_1).\underline{s}_k\right] \qquad (7.3)$$

$$F_3(\underline{q}) = \left\{\frac{1}{2\pi ik}\right\}^2 \int d\underline{q}_1\, d\underline{q}_2\, F_\alpha(\underline{q}-\underline{q}_1-\underline{q}_2)\, F_\alpha(\underline{q}_1)\, F_\alpha(\underline{q}_2) \quad x$$

$$x \quad \exp\left[i(\underline{q}-\underline{q}_1-\underline{q}_2).\underline{s}_1 + \underline{q}_1.\underline{s}_2 + \underline{q}_2.\underline{s}_3 \right] \tag{7.4}$$

and where $F_\alpha(\underline{q})$ is the elastic amplitude for scattering from free ^4He.

Ahmad was able to obtain analytic expressions from this model[135] by assuming the form used by Czyż & Lesniak[63] for the amplitude $F_\alpha(\underline{q})$ as

$$F_\alpha(\underline{q}) = \sum_{j=1}^{4} A_j\, e^{-\alpha_j q^2} \tag{7.5}$$

where A_j and α_j are given by

$$\alpha_j = \frac{1}{4a^2}\left[\frac{1 + 2a^2\beta^2}{j} - \frac{1}{4}\right] \tag{7.6}$$

$$A_j = \frac{ik}{2}\left(\frac{1 + 2a^2\beta^2}{a^2}\right)\frac{(-1)^{j+1}}{j}\binom{4}{j}\left[\frac{\sigma(1 + i\rho)\,a^2}{2\pi(1 + 2a^2\beta^2)}\right]^j \tag{7.7}$$

and where σ is the average pN cross-section, β^2 the slope of the nucleon-nucleon elastic differential cross-section and ρ is the ratio of the real and imaginary parts of the amplitude. a^2 is the size parameter for the α-particle itself.

The values used were $\beta^2 = 5.97\ (GeV/c)^{-2}$, $a^2 = 0.0208\ (GeV/c)^2$ for the free α-particle and $a^2 = 0.0159\ (GeV/c)^2$ for the bound α-particle, $\rho = -0.13$ and $\sigma_{\pi N} = 44$ mb

The expressions for $F_1(\underline{q})$, $F_2(\underline{q})$ and $F_3(\underline{q})$ which result are relatively simple and allow a very quick computation of the differential cross-section. Ahmad found that a better description could be found by increasing the size of the bound α-particle due to α-α attraction and thus decreasing the parameter a^2 in (7.6) and (7.7), as was found for an analysis of high-energy electron scattering with the α-particle model[136].

Two typical calculations for $p - {}^{12}C$ at 1 GeV are shown in Figure XV, using in one case the free α-particle parameters and a triangle of side $d = 15.2\ (GeV/c)^{-1}$ and using an enlarged α-particle together with a triangle side of $d = 13.0\ (GeV/c)^{-1}$. As can be seen from the data, even such a crude model is able to show the main features of the differential cross-section.

Since a good description of the $\pi^- - \alpha$ scattering was obtained previously at 8.00 GeV/c, this has been utilised with the above model in order to make some predictions for $\pi^- - {}^{12}C$ scattering. For convenience the 1st to 4th order amplitudes for $\pi^- - \alpha$ were fitted by the form

$$F_j(\underline{q}) = A_j\, e^{-a_j q^2} \qquad (7.8)$$

to obtain an input of the same form as (7.5). The form (7.8) was fitted by means of the program MINUIT, described previously, and these parameters were used since no means were obtained for correcting for the bound state.

7:4 Elastic scattering with other forms of α-model

In view of the results which may be obtained using the rigid triangle of α's, it is of interest to briefly examine other simple

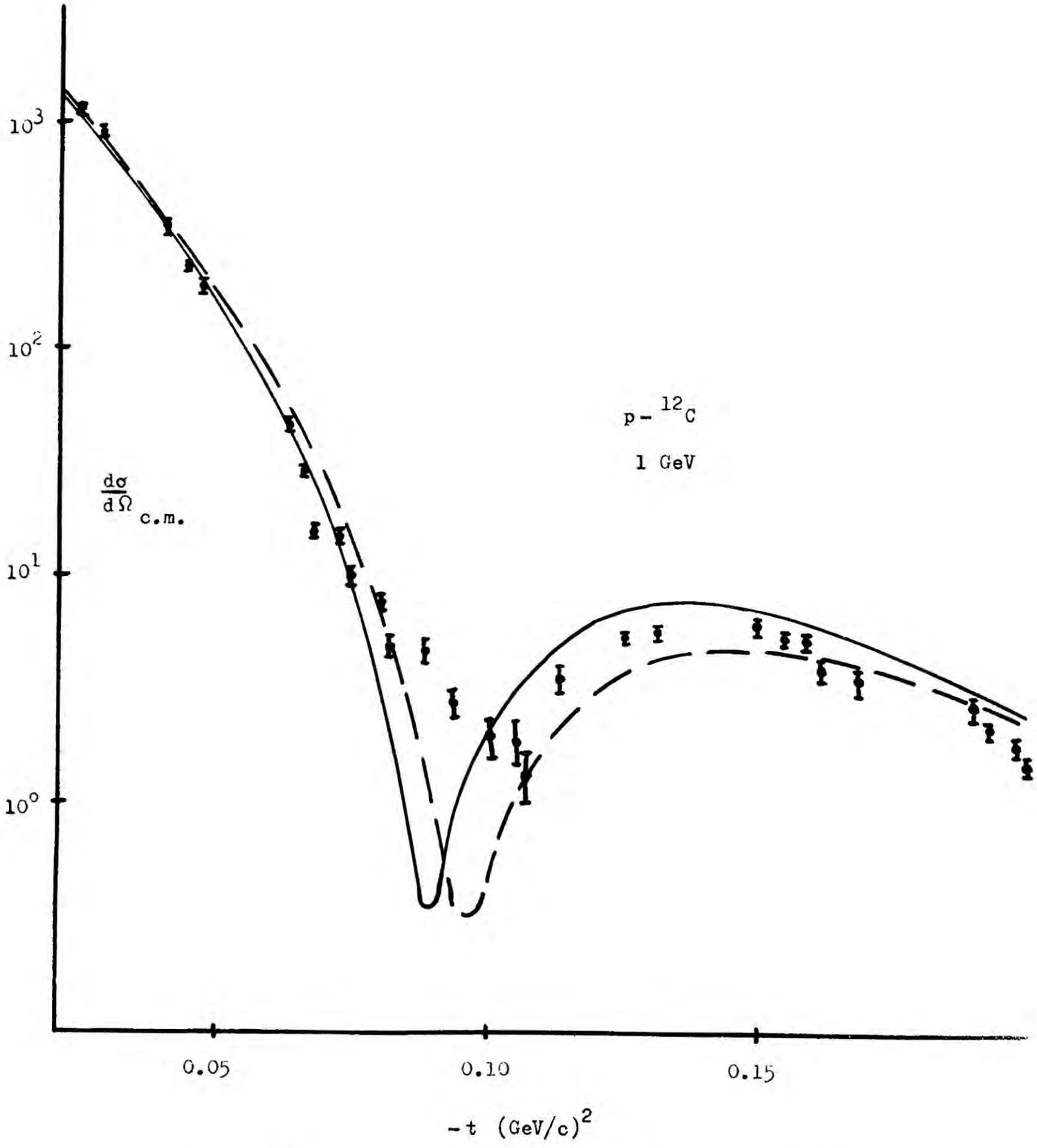

Figure XV $d\sigma/d\Omega_{c.m.}$ against t for p - ^{12}C at 1 GeV. The curves are computed using a rigid equilateral triangle of α-particles, the continuous line has parameter d = 15.2 $(GeV/c)^{-1}$ and free α-particle parameters while the broken line has d = 13.0 $(GeV/c)^{-1}$ and bound α-particle parameters.

distributions of α's for ^{12}C and to compare the results with those using the rigid triangle. In this section two other models are used to describe the configurations of the three α-particles and the resultant differential cross-sections are compared with both the experimental data and those previously calculated.

The most simple model available is to consider the spacial distribution to be described by a product wave function of gaussian form with no correlation between the α-particles. This leads to a density function of the form

$$\langle 0 \mid 0 \rangle = \rho_o \prod_{i=1}^{3} e^{-\alpha^2 R_i^2} \, d\underline{R}_i \qquad (7.9)$$

where $\underline{R}_i$ is the co-ordinate of the i-th α-particle from the centre of the nucleus. This simple form can easily be seen to correspond to a simple harmonic oscillator wave function with all nucleons in the s-shell and being unsymmeterised, since $R_i^2 = \sum_{j=1}^{4} r_{ij}^2$

where $\underline{r}_{ij}$ is the co-ordinate of the j-th nucleon within the i-th α-particle. Using the form (7.9) together with a c.m. constraint and the expressions (7.1) to (7.4), the resultant integrals may be performed in a similar manner to those described in Appendix E to give analytic forms for the amplitudes and the resultant differential cross-section.

To obtain the value of α^2 in (7.9), the expectation value of R^2 was calculated and led to the expression

$$\alpha^2 = \frac{1}{\langle R^2 \rangle} \qquad (7.10)$$

An analysis of the scattering of high-energy electrons from ^{12}C

using the α-particle model has been made by Inopin et al.[136] from which a value of R = 1.73 fermi was obtained for the mean distance of an α-particle from the centre of ^{12}C. Equating this with $\langle r^2 \rangle$ a value was obtained for a^2 of

$$a^2 \simeq 0.013$$

Subsequently calculations and comparison with the data for $p-^{12}C$ suggested a slightly larger value of $a^2 = 0.014$ or $a^2 = 0.015$, though these were selected by eye from comparisons with the data which had itself been obtained from a small graph.

Figure XVI shows the calculated curve for $a^2 = 0.015$ for $p-^{12}C$ at 1 GeV compared to the data. As with the rigid triangle form, calculations were made using α-particle parameters for both bound and free sizes. As may be seen from the figure, the simple gaussian form does not give a particularly good description of the data and is poorer than the rigid triangle. This is not altogether unreasonable since the total lack of interparticle correlation removes the salient feature of the previous model.

To try and combine some of the features of the two forms a little more, a third form was used of a nuclear density with an overall gaussian form but containing correlations between the α-particles. The form which resulted was similar to some which have been used for energy level calculation[137], taking the form

$$\langle 0 | 0 \rangle = \rho_0 \prod_{i=1}^{3} e^{-\beta^2 R_i^2} \prod_{\substack{j=1 \\ k \neq j}}^{3} e^{-\mu^2 R_{jk}^2} \qquad (7.11)$$

where $\underline{R}_{ij} = \underline{R}_i - \underline{R}_j$. Estimates of the parameters β^2 and μ^2 were again obtained by considering the mean radius for the α-particles and obtaining the relation

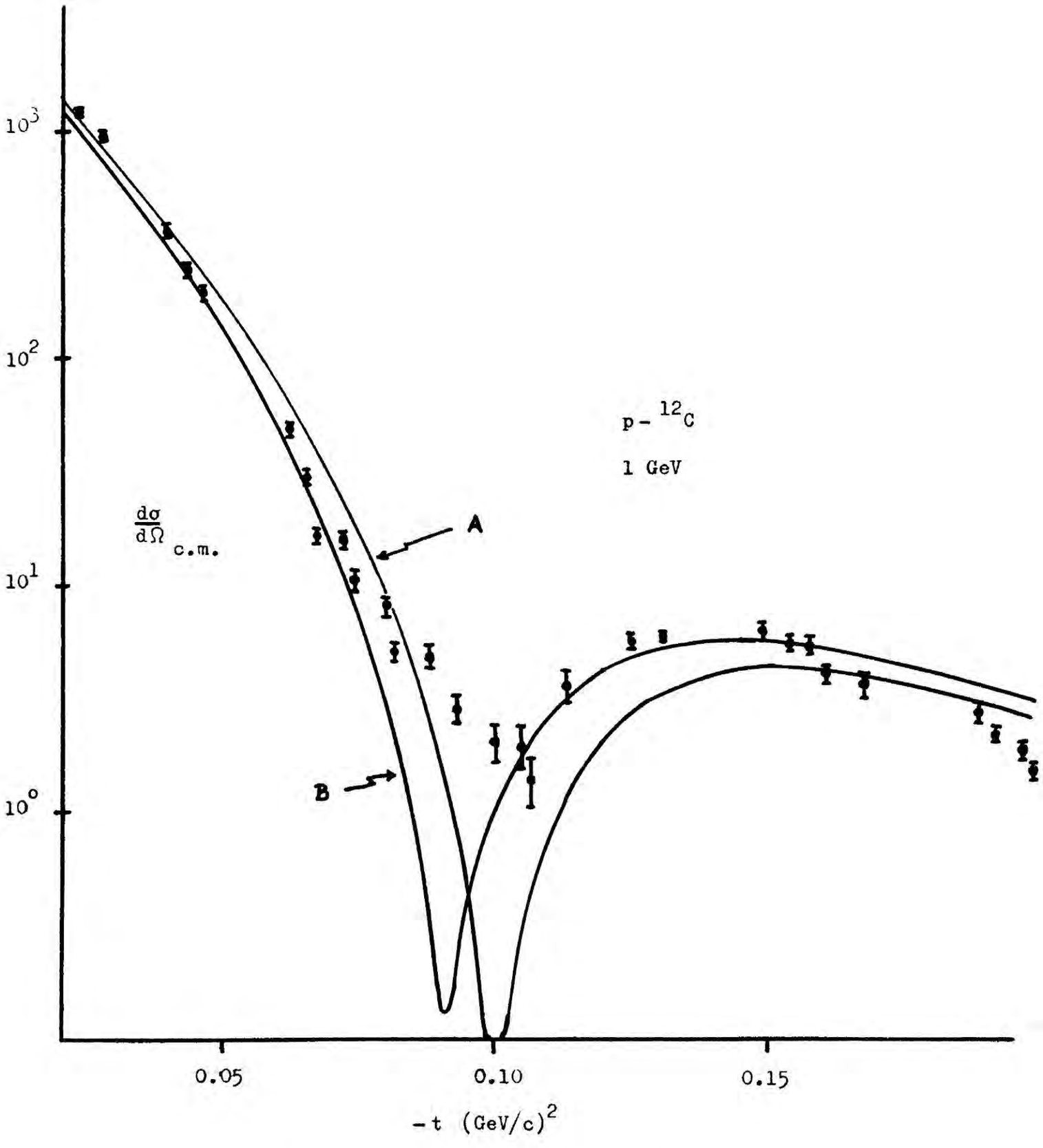

Figure XVI $d\sigma/d\Omega_{c.m.}$ against t for p - ^{12}C at 1 GeV. The curves are calculated using a gaussian distribution for the α-particles, with $a^2 = 0.015$. Curve A is calculated with the free α-particle parameters, curve B with bound α-particle parameters.

$$\alpha^2 = \frac{1}{\langle R^2 \rangle} = \beta^2 + 3\mu^2 \qquad (7.12)$$

In the absence of an electron-scattering analysis using this form no means could be devised to obtain seperate estimates of β^2 and μ^2 and so calculations were made for different values of β^2 and μ^2 which satisfied the relation (7.12) . However little variation occured between these calculations over a range $0.0005 \leq \mu^2 \leq 0.0040$ and little overall difference could be detected between these results and those using the simple gaussian form of (7.9) .

Some predictions have been made for $\pi^- - {}^{12}C$ differential cross-sections at 8 GeV/c using these forms together with the parameters obtained. The different curves are shown in Figure XVII for the two main forms of α-model and as can be seen, the differences for this case are more pronounced than for the lower energy proton case.

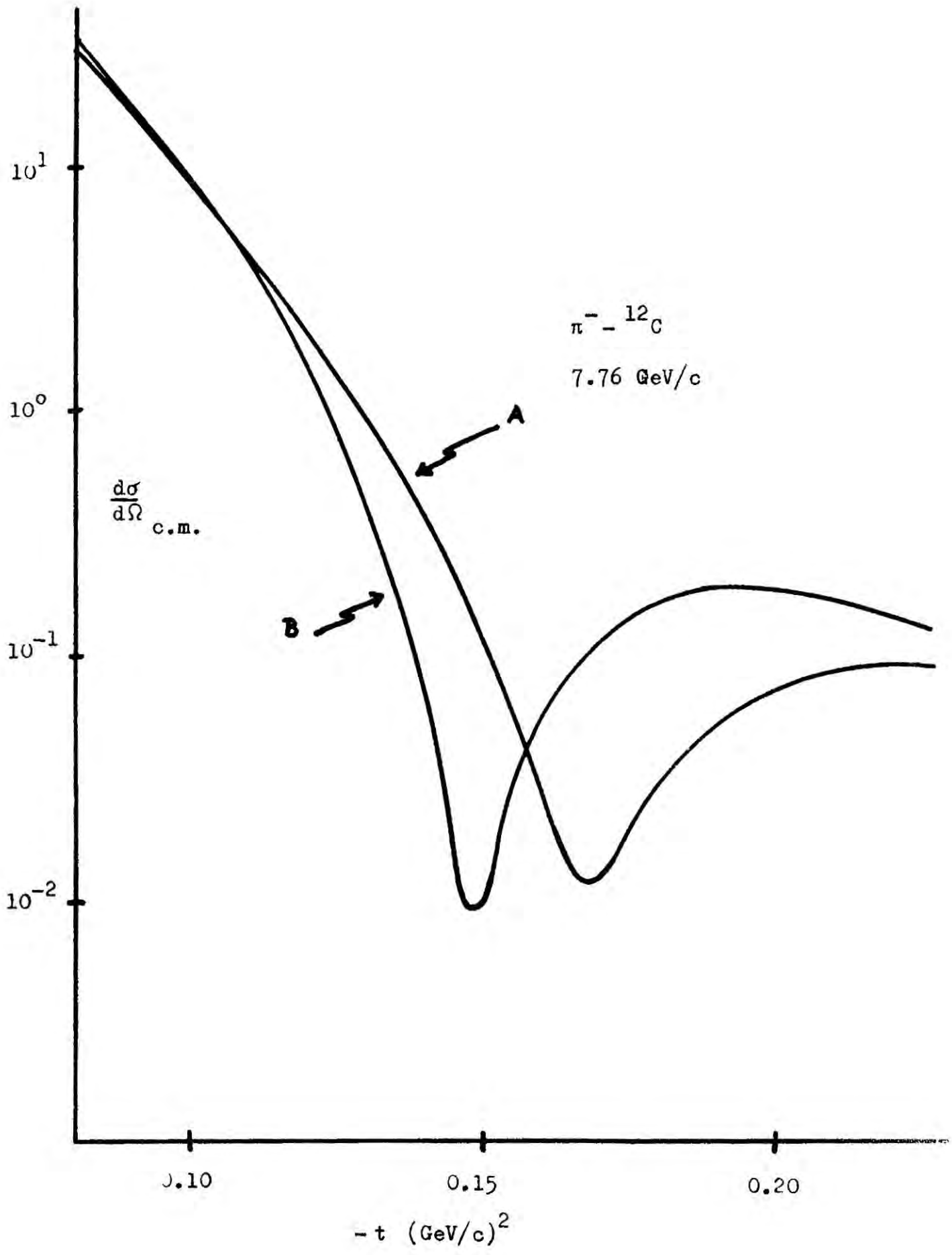

Figure XVII $d\sigma/d\Omega_{c.m.}$ against t for $\pi^- - {}^{12}C$ scattering at 8 GeV/c. Curve A is calculated for a gaussian distribution of a's, with $a^2 = 0.015$ and Curve B is calculated using a rigid triangle of a's, with parameter $d = 13.0\ (GeV/c)^{-1}$.

Chapter 8 Some Conclusions on the Glauber Model

8:1 Approximations made in the calculations

The basic Glauber model, as derived in Chapter 5, was applied in Chapters 6 and 7 to the elastic scattering of π-mesons from Helium-4 and of protons from Carbon-12. In evaluating numerically a series of the general form of (5.41) a number of convenient assumptions are made which are summarised in this section and in this Chapter some possible improvements to these are suggested.

For the scattering of π-mesons from Helium-4, the main computational problem lay in the calculations resulting from the multiple integrals, an example of which is described in Appendix E. In these integrals approximations were sometimes made about the limits involved, in order to obtain analytic solutions, and constraints were applied to the form of the input data.

The first of these approximations lies in the assumption of a gaussian form for the πN amplitudes, and as was shown in Chapter 6, this is by no means valid at lower energies although giving a good description in the high-energy region. The second approximation, which in some ways is a consequence of the first, is that in the integral over the momentum transfer $\underline{q}$, the upper limit is assumed to be ∞. Since $\underline{q}$ is bounded, $q_{max} = 2\underline{k}$ where $\underline{k}$ is the incident momentum, this is an approximation which is strictly limited only to fast falling gaussians in q^2. The necessity of this approximation may be seen however from an attempt to perform such an integral for a constant amplitude (the opposite extreme) leading to a great complexity due to the presence of the term $|\underline{b} - \underline{s}_i|$ in the integrand.

As described in Reference(97), the similar integral over $d^2\underline{b}$, the impact parameter plane does not contain any such approximation,

being instead an exact representation so that for this integral no approximation is involved.

A further approximation to the spin-dependent part of the calculation was mentioned in Appendix D, in the assumption that the scattering is coplanar, but as the effects of spin have been shown to be virtually neglegible the effects of this are assumed to be very slight, and certainly difficult to assess.

From the resultant calculations of Chapter 6, it is interesting to note that except at low energy these approximations do not seem to possess any particularly sizable effect (unless there exists some subtle form of cancellation) and in the regions where Glauber theory is expected to work these would seem to be very reasonable assumptions, though for the medium-energy region a more rigourous treatment of the upper bound of $\underline{q}$ might possibly be of some value. However before calling upon a comparison with the data to assess the effects of such approximations one should remember that their main effects are likely to lie in those regions where Glaubers model is itself an appreciable approximation.

Further approximations, which are common to both Chapters 6 and 7 occur in the assumption of gaussian densities and of the equality of charge and mass distributions. Certainly the former of these may be open to some degree of doubt although the second is probable quite reasonable, but in the present limits of computing power it is difficult to see any easy method of improving upon the forms used, although these may well have a large influence.

In the scattering of protons from Carbon-12, the chief remaining approximation is of course the α-particle model itself which has been used in the crudest possible forms and with virtually none of the

refinements which are possible due to the complications that these introduce. A further approximation is the gaussian p-α amplitudes which are used, and in particular it should be noted that these only provide a rough fit to the p-α data.

Apart from these the computational approximations lie in the form of the α-model and hence form a part of the investigation.

8:2 Conclusions from π^- - ^{4}He elastic scattering

In Chapter 6 the details were given of the calculations made at 1.25 GeV/c and 7.76 GeV/c while in the preceding section of this chapter some of the approximations involved have been described. This section discusses the comparisons between the different results obtained together with some of the conclusions that may be drawn from these.

At 1.25 GeV/c there is little that is new to be noted from the calculations. As has already been shown the effects of spin-flip are effectively neglegible[65] and the forms of input that were used were able to give a good description of the data when a realistic wave-function was used. (Strictly this wavefunction was not realistic since it had a hard core, a justification for this may be found in reference(69)). Unfortunately the data is limited to the region of the dip and second peak and so one cannot make simultaneous comparison with the forward peak as well but Querrou[61] has shown that the calculations of this form are in good agreement with older measurements of the differential cross-section at forward angles.

It is interesting to note that the effects of a first order Jastrow two-body nucleon-nucleon correlation were very small, expecially since the effects for such a form were found to be rather larger at 7.76 GeV/c. On the whole agreement at this energy is quite good,

particularly in the light of so many approximations and limitations.

It is possible to make some rather more detailed comparisons for 7.76 GeV/c, since this is a region possessing a much more simple πN input, so reducing computational time considerable and allowing a greater complexity of nuclear form. In addition the data covered a much wider angular range and so provided more features to aid a quantitative comparison.

In the absence of nucleon-nucleon correlations in the nuclear densities the isospin-dependent amplitude (6.39) led to a differential cross-section which differed very little from that obtained for the simple gaussian amplitude as in (6.41) so that the effects of isospin corrections could be seen to be very small. The two uncorrelated densities (6.31) and (6.32) did however give differing results, the simple gaussian form giving a much poorer description of the double-scattering peak in $d\sigma/dt$ so that like others[69] it may be concluded that a hard-core density is needed to describe ^{4}He.

When correlation effects between the nucleons were introduced by means of the Jastrow series (6.33), calculations with only the first order terms retained as in (6.36) produced a worsening of the agreement with the data for either form of the πN amplitude. This formed an interesting corroboration of the findings from high-energy electron scattering studies[118,119] where comparisons between different orders of Jastrow correlation have been made with the conclusion that the series does not stabilise for the inclusion of the first few orders. The data did not allow a direct comparison for each degree of correlation and so only the single term and complete form of correlation were calculated. For the fully correlated nuclear density (6.33), the differential cross-sections are very similar to those involving a completely uncorrelated form. The size of these effects

can be adequately seen from Table VII and this shows that the differences produced by different densities are small.

Hence at 7.76 GeV/c it would appear that neither a more rigourous form of $F_{\pi N}$, nor the inclusion of gaussian correlations into the nuclear densities are able to provide any large improvement in the already good agreement between experiment and the basic theory. In view of the difficulty in making any further improvements to $F_{\pi N}$ a better agreement would seem to be best obtained from an improved nuclear density, such a density would probable be non-gaussian in form, which also follows from the observations of the electron-scattering analyses where it is also found that ^4He is not adequately represented by any gaussian form for $\rho(\underline{r})$ (118).

In general the results of these calculations suggest that Glaubers model is well able to predict accurately the main features of the differential cross-section, a detailed numerical comparison probably needing more and better data. With regard to the form of the second peak, which is generally the region of poorest agreement, it is difficult to decide whether this is inadequacy of theory or of the nuclear densities until investigations have been made for non - - gaussian forms, although the computational problems for these may be considerable.

8:3 Conclusions on scattering from ^{12}C using the α-particle model

For the model of ^{12}C describing the nucleus as a rigid equilateral triangle of α-particles, the main claim by Ahmad(82) was that this model described the data in the region of the dip better than the simple harmonic oscillator model and so filled in the overdeep dip found in Reference(63). However our repeat of this form of calculation gave a rather deeper dip than shown in reference(82) although agreeing

with the curves shown there in all other details, a somewhat perplexing result. However the curve obtained still seems to produce a slightly better qualitative result than the simple harmonic oscillator and the calculation itself is of course much more simple.

The gaussian forms used to describe the α-distributions do not lead to any improvements over the simple rigid triangle but rather produce a worse agreement with the data. A detailed comparison was not however possible since the data was obtained from so small a graph that its reliability in all but a broad qualitative discussion was very questionable. The introduction of two-body correlations into the density did not appear to have any effect other than a very slight shifting of the dip. On the whole the failure of such forms was perhaps not totally unreasonable since a simple gaussian of α's may be expected to give similar results to the simple harmonic oscillator form which is known to be inadequate[69].

An interesting combination of the gaussian form and the inter - - particle spacing of the rigid triangle would be to use a density form for the α-particles similar to the ^{12}C wavefunction proposed long ago by Wheeler[138]. This contains terms to seperate the constituent α-particles and an overall central gaussian and having the form

$$\langle O \mid O \rangle = \rho_o \prod_{i=1}^{3} e^{-\alpha^2 R_i^2} \prod_{\substack{j=1 \\ k \neq j}}^{3} \left(e^{-\beta^2 R_{jk}^2} - e^{-\gamma^2 R_{jk}^2} \right)$$

Some trial calculations were attempted for such a form, but as there exists no electron scattering analysis using this form, one would first need to perform such an analysis before a good set of

parameter values could be obtained, and the attempts at estimating these proved unsuccessful. In many ways this would appear to provide a very promising form, since the property of the rigid triangle which produces the improved results is the built-in deformation, and many of the essential features of this are contained in this form. In addition the computational time required is not greatly increased.

In conclusion there would seem to be some agreement with the suggestions that the α-particle model may provide a better description of ^{12}C than the harmonic oscillator[69,82] particularly as even the use of a more complex density as above would still require less computational time than a calculation with the full simple harmonic oscillator form.

8:4 Some General Conclusions

The Glauber multiple-scattering model may now be regarded as a well established model and has been shown to possess great predictive powers. As has been shown here, the final form of the calculations is rarely very dependent upon other than the broad form of the input, the $\pi^- - ^4He$ data at 7.76 GeV/c for example being relatively insensitive to any but the outer forms of the πN amplitudes and the nuclear density. Of course all attempts to obtain more detailed agreements with experimental data must assume that the model is exact, and the successes of the model may well encourage an acceptance of this assumption in these cases, particularly at large angle, where it may be in doubt.

This assumption was implicit in the calculations of the last two chapters and no attempt has been made to introduce any form of correction term at wide angle, a procedure that would need great care since it has been shown by Harrington[85] that the Glauber series is a delicate

balance of terms. Certainly in the present state of the art it is probably better to try more variations of nuclear density than to modify the theory especially in such a case as ^{4}He where the nuclear density is known to be unsatisfactory, in its current forms.

In many ways it would seem from the present good agreement with data that is obtained that the model is probably better than is suggested by its derivations and it seems to be accepted that the model must contain something more fundamental than the simple summing of phases suggests. One can conclude that the Glauber model is in good form with so far no real difficulties in obtaining qualitative and usually quantitative descriptions of the available data, frequently at quite low energy, and one may well hope for better agreement yet to come.

APPENDIX A A derivation of the Breit - Wigner form

This derivation follows that of Coleman[29], and comes from the definition that he gives of resonance. This definition was

' In a region sufficiently "small" and sufficiently "far" from the branch point or the three-particle threshold we may parameterise the S-matrix as a sum of poles plus an analytic part which we may approximate as a constant.'

Hence from this definition we write the S-matrix as

$$S(z) = a + b/(z - z_1) \qquad (A.1)$$

$$= a(z - c)/(z - z_1)$$

and using the analyticity properties and the unitarity of the S-matrix we may write

$$S(z)S^{+}(z^*) = I = aa^*(z - c)(z - c^*)/(z - z_1)(z - z_1^*) \qquad (A.2)$$

and since this is a constant, and there are no poles, this implies that

$$c = z_1^*$$

$$aa^* = 1$$

and so we may write

$$a = S_B = \exp(2i\delta_B) \qquad (A.3)$$

termed the 'background' in the sense of being the limit of S away from the pole, that is, its asymptotic value. Equation (A.1) then becomes

$$S = S_B(z - z_1^*)/(z - z_1) \qquad (A.4)$$

If we then write

$$z_1 = E_1 - i\,\Gamma_1/2$$

with Γ_1 positive, since a pole term occurs only below the axis, (A.4) becomes

$$S = S_B \frac{E - E_1 - i\,\Gamma_1/2}{E - E_1 + i\,\Gamma_1/2} \qquad (A.5)$$

and if (for simplicity) $\delta_B \longrightarrow 0$, the T-matrix has the simple form

$$T = \frac{\Gamma}{2(E_R - E) - i\Gamma} \qquad (A.6)$$

which is the well-known Breit - Wigner resonance form (3.9).

For the case of inelastic scattering from channel α to channel β we get

$$T_{\alpha\beta} = \frac{-g_\alpha\, g_\beta^*}{2(E - E_R) + i\Gamma} \qquad (A.7)$$

where

$$\Gamma = \sum_\alpha |g_\alpha|^2$$

i.e. for n channels open

$$\Gamma = \Gamma_1 + \Gamma_2 + \ldots\ldots + \Gamma_n$$

APPENDIX B Evaluation of the coefficients A_n, B_n in terms of T-matrix amplitudes

The differential and polarised differential cross-sections are fitted by the expressions (4.1), (4.2)

$$\frac{d\sigma}{d\Omega} = \lambda^2 \sum_n A_n P_n(\cos\vartheta) \tag{B.1}$$

$$\underline{P}\frac{d\sigma}{d\Omega} = \underline{n}\,\lambda^2 \sum_k B_k P_k^1(\cos\vartheta) \tag{B.2}$$

where $d\sigma/d\Omega$ and $\underline{P}\,d\sigma/d\Omega$ are connected to the scattering amplitudes $f(\vartheta)$ and $g(\vartheta)$ by (1.31),(1.33)

$$\frac{d\sigma}{d\Omega} = |f(\vartheta)|^2 + |g(\vartheta)|^2 \tag{B.3}$$

$$\underline{P}\frac{d\sigma}{d\Omega} = \underline{n}\; 2\,\mathrm{Im}\left(f^*(\vartheta)\, g(\vartheta) \right) \tag{B.4}$$

and where $f(\vartheta)$ and $g(\vartheta)$ are given by the expansions (1.29) as

$$\begin{aligned} f(\vartheta) &= \frac{1}{k} \sum_\ell \left\{ (\ell+1)\, T_\ell^+ + \ell T_\ell^- \right\} P_\ell(\cos\vartheta) \\ g(\vartheta) &= \frac{1}{k} \sum_\ell \left\{ T_\ell^+ - T_\ell^- \right\} P_\ell^1(\cos\vartheta) \end{aligned} \tag{B.5}$$

writing $x = \cos\vartheta$, the Legendre Polynomials $P_n(x)$ and Associated Legendre Polynomials $P_n^1(x)$ obey the orthogonality relations[43]

$$\int_{-1}^{+1} P_n(x)\, P_m(x)\, dx = \delta_{mn} \frac{2}{2n+1} \tag{B.6}$$

$$\int_{-1}^{+1} P_n^1(x)\, P_m^1(x)\, dx = \delta_{mn} \frac{1}{2n+1} \tag{B.7}$$

thus from (B.1) and (B.7)

$$\int_{-1}^{+1} P_n(x) \frac{d\sigma}{d\Omega} \, dx = \frac{2}{2n+1} \lambda^2 A_n$$

so that

$$A_n = \frac{2n+1}{2\lambda^2} \int_{-1}^{+1} P_n(x) \frac{d\sigma}{d\Omega} \, dx \qquad (B.8)$$

and similarly

$$B_k = \frac{2k+1}{\lambda^2} \int_{-1}^{+1} P_k^1(x) \left(\pm \frac{d\sigma}{d\Omega} \right) dx \qquad (B.9)$$

If (B.3) and (B.5) are now substituted into (B.8), we may, after performing the requisite integral obtain A_n in terms of the T_ℓ's and similarly using (B.4) and (B.5) in (B.9) may obtain B_k in a likewise manner.

As an example, A_1 is evaluated assuming $\ell_{max} = 2$ for convenience of calculation, and describing the T_ℓ's by the spectroscopic notation L_{2J}. From (B.5) we get

$$f(\vartheta) = \lambda \left\{ S_1 P_o(x) + (2P_3 + P_1) P_1(x) + (3D_5 + 2D_3) P_2(x) \right\}$$

$$g(\vartheta) = \lambda \left\{ (P_3 - P_1) P_1^1(x) + (D_5 - D_3) P_2^1(x) \right\}$$

so that

$$|f(\vartheta)|^2 = \lambda^2 \left\{ |S_1|^2 + |2P_3 + P_1|^2 P_1(x)^2 + |3D_5 + 2D_3|^2 P_2(x)^2 \right.$$
$$+ 2\mathrm{Re}\left\{ S_1^* (2P_3 + P_1) \right\} P_1(x) + 2\mathrm{Re}\left\{ S_1^* (3D_5 + 2D_3) \right\} P_2(x)$$
$$\left. + 2\mathrm{Re}\left\{ (2P_3 + P_1)^* (3D_5 + D_3) \right\} P_1(x) P_2(x) \right\}$$

and

$$|g(\vartheta)|^2 = \lambda^2\Big\{ |P_3 - P_1|^2 \, P_1^1(x)^2 + |D_5 - D_3|^2 \, P_2^1(x)^2 + 2\mathrm{Re}\{ (P_3 - P_1)^*(D_5 - D_3)\} P_1^1(x) \, P_2^1(x) \Big\}$$

A useful relation in evaluating some of the integrals required when these expressions are substituted into (B.8) is given by[44]

$$\int_{-1}^{+1} P_a(x)P_b(x)P_c(x)\,dx = 2\begin{pmatrix} a & b & c \\ 0 & 0 & 0 \end{pmatrix}^2 \qquad \text{(B.10)}$$

where the 3-j symbols are related to the Clebsch - Gordon coefficients by the relation

$$\langle a\, b\, \alpha\, \beta \,|\, c\ -\gamma \rangle = (-1)^{a-b-\gamma}\,(2c+1)^{\frac{1}{2}} \begin{pmatrix} a & b & c \\ \alpha & \beta & \gamma \end{pmatrix} \qquad \text{(B.11)}$$

In evaluating A_1, we use the values of table B I , taken from Reference (44)

a	b	c	$\begin{pmatrix} a & b & c \\ 0 & 0 & 0 \end{pmatrix}^2$
0	2	2	1/5
2	2	2	2/35
1	1	2	2/15

Table B I

Performing the remaining integrals explicitly we obtain

$$A_1 = 2\mathrm{Re}\{S_1^*(2P_3 + P_1)\} + 4/5\mathrm{Re}\{(2P_3 + P_1)^*(3D_5 + 2D_3)\} +$$

$$+ \quad 12/5 \; \mathrm{Re}\left\{ \left(P_3 - P_1 \right)^* \left(D_5 - D_3 \right) \right\}$$

which is the required form.

Table B II gives the coefficients of $\frac{d\sigma}{d\Omega}$ in terms of the partial amplitudes and Table B III those of $\underline{P}\frac{d\sigma}{d\Omega}$ in like form.

Table B II The coefficients A_n expressed in Partial Waves.

	A_o	A_1	A_2	A_3
$S_1S_1 + P_1P_1$	1			
S_1P_1		2		
$S_1P_3 + P_1D_3$		4		
$S_1D_3 + P_1P_3$			4	
$S_1D_5 + P_1F_5$			6	
$S_1F_5 + P_1D_5$				6
S_1F_7				8
$P_3P_3 + D_3D_3$	2		2	
P_3D_3		4/5		36/5
$P_3D_5 + D_3F_5$		36/5		24/5
$P_3F_5 + D_3D_5$			12/7	
P_3F_7			72/7	
D_3F_7				8/3
$D_5D_5 + F_5F_5$	3		24/7	
D_5F_5		18/35		16/5
D_5F_7		72/7		8
F_5F_7			8/7	
F_7F_7	4		100/21	

where $S_1P_3 + P_1D_3 = \mathrm{Re}\,(S_1^*P_3 + P_1^*D_3)$ etc.

Table B III The coefficients B_n expressed in partial waves

	B_1	B_2	B_3
S_1P_1	2		
$S_1P_3 - P_1D_3$	-2		
$S_1D_3 - P_1P_3$		2	
$S_1D_5 - P_1F_5$		-2	
$S_1F_5 - P_1D_5$			2
S_1F_7			-2
P_3D_3	8/5		12/5
$P_3D_5 - D_3F_5$	-18/5		-2/5
$P_3F_5 - D_3D_5$		10/7	
P_3F_7		-24/7	
D_3F_7			4/3
D_5F_5	54/35		8/5
D_5F_7	-36/7		-2/3
F_5F_7		4/3	

where $S_1P_3 - P_1D_3 = \mathrm{Im}\,(S_1^* P_3 - P_1^* D_3)$

APPENDIX C The Method of Minimisation

To handle the large numbers of variables required for the partial wave analysis, the CERN program MINUIT[36] was used, which possesses three principal routines for minimisation of a problem, SEEK, TAUROS and MIGRAD. In this appendix these three routines are briefly described and the minimisation procedure used is outlined.

SEEK is a random-search routine using a Monte Carlo method and was found to be chiefly of value in finding start values of the parameters for the random starts. It was rarely found of use at any other time. The TAUROS routine, which uses the Rosenbrock method[45], an extension of the simple method of co-ordinate variation, proved to be the most useful routine and was used almost exclusively for the majority of the minimisation work. The third routine MIGRAD calculates the derivatives for χ^2 for each variable parameter and progresses by successive approximations to the covariance matrix. This was found unsuitable for more than about 15 parameters and away from minimum was much slower than TAUROS and so consequently this was used only in the final stages of a fit.

The procedure followed in each case was to vary only a few (up to ~ 25) of the parameters at a time, with each new minimisation starting from a previouly found minimum. The initial starts were generally made with all non-resonant amplitudes overparameterised and after a preliminary minimum was found the parameters for each amplitude were gradually reduced until a marked rise in the χ^2 -value occured for the removal of a parameter. In this way the optimum parameterisation for each amplitude was hopefully obtained, and the overall fit should possess the minimum structure. The orthogonality property of the Legendre Polynomials allowed the higher polynomials

to be removed without greatly affecting other coefficients and so allowing a rapid convergence in each subsequent fit.

For the $\Sigma\pi$ channel the above procedure proved very cumbersome since overparameterisation of the seven non-resonant amplitudes required a very large number of parameters (typically ~ 50) and so a number of the fits for this channel were made beginning with all amplitudes underparameterised so that all could be varied initially and then each amplitude was increased until all were thought to be overparameterised, after which the previous procedure was followed. By this method it was intended to reduce the bias that would have been initially introduced by being able to vary only a limited number of parameters at once, so favouring selected amplitudes.

For both channels, the complete range of data available was not used for two reasons, firstly the unreliability of the Breit - Wigner terms far from resonance and secondly because by treating fewer data points the processes of minimisation were much faster, an important detail in view of computational limitations.

Although MINUIT was selected chiefly for the flexibility available when handling large numbers of variables it was also found to give rapid convergence in most cases and most computing time was generally spent in searching the final minimum for any possible improvements.

To obtain the errors of the resonance parameters, a MINOS analysis was used where possible, which obtained the upper and lower bounds for each parameter specified to give a rise in χ^2 of 1.0 and these were taken to be the errors quoted for the parameters. However it was not possible to apply the MINOS routine to all parameters and so the errors for these were estimated form the range of fits around the minimum.

APPENDIX D Spin-isospin terms for ^{4}He

In Chapter 6, the spin and isospin-dependences were removed from the expression (6.20) leaving the $f_j(\underline{q}_j)$ as functions of $\underline{q}_j$ only. In this appendix the methods for this are shown and the first and second terms of (6.20) are evaluated, and the values of the $G^j(q_1,..,q_j)$ listed in table DI, the values of G^3 and G^4 being taken from Reference(64). Expression (6.20) took the form

$$F_{el}(\underline{q}) = \frac{ik}{2\pi}^{*} \langle \alpha | \int d^2\underline{b}\ e^{i\underline{q}.\underline{b}}\ \delta(\frac{1}{4}\sum_i^4 \underline{r}_i)\ \sum_{j=1}^{4} \left\{ (-1)^{j+1} \left(\frac{1}{2\pi ik}\right)^j \right. \quad x$$

$$x \left. \int d^2\underline{q}_1..d^2\underline{q}_j\ e^{-i\underline{q}_1.(\underline{b}-\underline{s}_1)..-i\underline{q}_j.(\underline{b}-\underline{s}_j)}\ f_1(\underline{q}_1)..f_j(\underline{q}_j) \right\} | \alpha \rangle \qquad (D.1)$$

The ^{4}He wavefunction $|\alpha\rangle$ is factorised into a product between a spacial density distribution and a Slater determinant $|\Phi\rangle$ describing the spin and isospin dependence, and which, writing the proton and neutron spin states as $p\uparrow$, $p\downarrow$, $n\uparrow$, $n\downarrow$, may be written as

$$|\Phi\rangle = \begin{pmatrix} p\uparrow(1) & p\uparrow(2) & p\uparrow(3) & p\uparrow(4) \\ p\downarrow(1) & p\downarrow(2) & p\downarrow(3) & p\downarrow(4) \\ n\uparrow(1) & n\uparrow(2) & n\uparrow(3) & n\uparrow(4) \\ n\downarrow(1) & n\downarrow(2) & n\downarrow(3) & n\downarrow(4) \end{pmatrix} \qquad (D.2)$$

The use of the determinant simplifies calculation since the spin and isospin operators $\underline{\sigma}$ and $\underline{\tau}$ alter the rows of the determinant and the elastic scattering condition is easily applied since for two rows equal the determinant becomes zero. A further property of the determinant causes the inclusion of a factor of (-1) for each

transposition of two rows.

For the single scattering term of (D.1), the operation of g^+ and g^- of (6.15) upon (D.2) produce a zero determinant and hence zero coefficients. The remaining terms are obtained by considering the remaining operators acting upon the 4-nucleon state to give

$$\langle \pi^- {}^4\mathrm{He} \mid f^+ - f^-(\theta\tau) \mid \pi^- {}^4\mathrm{He} \rangle = 2 \langle \pi^- p \mid f^+ - f^-(\theta\tau) \mid \pi^- p \rangle + 2 \langle \pi^- n \mid f^+ - f^-(\theta\tau) \mid \pi^- n \rangle \qquad (D.3)$$

Expanding $\underline{\theta}.\underline{\tau}$ in terms of the step-up and step-down operators

$$\theta^{\pm} = \theta_x \pm i\theta_y \qquad \text{and} \qquad \tau^{\pm} = \frac{1}{2}(\tau_x \pm i\tau_y)$$

we get

$$\underline{\theta}.\underline{\tau}_i = \theta_z \tau_{iz} + (\theta^+ \tau_i^- + \theta^- \tau_i^+) \qquad (D.4)$$

For the elastic scattering from the nucleons, only the term $\theta_z \tau_z$ is retained so (D.3) becomes

$$\langle \pi^- {}^4\mathrm{He} \mid f^+ - f^-(\theta\tau) \mid \pi^- {}^4\mathrm{He} \rangle = 2(f^+ - f^-(-1)(+1)) + 2(f^+ - f^-(-1)(-1)) = 4f^+$$

so that the single scattering contribution to (6.21) is of form

$$G^1(\underline{q}_j) = 4 f^+(\underline{q}_j) \qquad (D.5)$$

In calculating the next term, a product of two amplitudes $F_{\pi N}(\underline{q}_j)F_{\pi N}(\underline{q}_k)$ and eliminating those terms linear in g^+ or g^- as before, we obtain

$$F_{\pi N}(\underline{q}_j)F_{\pi N}(\underline{q}_k) = f_j^+f_k^+ + f_j^-f_k^- + g_j^+g_k^+ + g_j^-g_k^- + f_j^+f_k^- + f_j^-f_k^+ \qquad (D.6)$$

Evaluating the coefficients of these operators term by term

$\underline{f_j^+f_k^+}$: The ordering is not important as these operators commute and so the resultant coefficient is given by the number of possible combinations of j and k which is 6, so that

$$\langle \pi^- | \langle \Phi | \; f_j^+f_k^+ \; | \Phi \rangle | \pi^- \rangle = 6 \; f^+(\underline{q}_j)f^+(\underline{q}_k) \qquad (D.7)$$

$\underline{f_j^-f_k^-}$: The operators do not commute so that the ordering is important, giving an element of the form

$$\frac{1}{2} \langle \pi^- | \langle \Phi | \; f_1^-f_2^-(\theta\tau_1)(\theta\tau_2) + f_2^-f_1^-(\theta\tau_2)(\theta\tau_1) + \ldots + f_4^-f_3^-(\theta\tau_4)(\theta\tau_3) \; | \Phi \rangle | \pi^- \rangle \qquad (D.8)$$

and again using the step-up and step-down operators we may expand

$$(\theta\tau_i)(\theta\tau_j) = \theta_z\tau_{i_z}\theta_z\tau_{j_z} + \theta^+\tau_i^-\theta^-\tau_j^+ + \theta^-\tau_i^+\theta^+\tau_j^- + \text{other terms} \qquad (D.9)$$

where the ' other terms ' may be neglected, being removed by the constraint of elasticity. Using the further constraint

$$\theta^- | \pi^- \rangle = 0$$

(D.8) may be written as

$$\frac{1}{2}\langle\pi^-|\langle\Phi|\ f_1^- f_2^-\ 2\theta_z\theta_z\tau_{1_z}\tau_{2_z} + \theta^-\theta^+(\tau_1^+\tau_2^- + \tau_2^+\tau_1^-) + f_1^- f_3^- \ldots\ |\Phi\rangle|\pi^-\rangle \tag{D.10}$$

The pi-meson operators give the factors

$$\langle\pi^-|\ \theta_z^2\ |\pi^-\rangle = (-1)^2 = +1$$

and using the commutation relation

$$\theta^+\theta^- - \theta^-\theta^+ = 2\theta_z$$

$$\theta^-\theta^+ = \theta^+\theta^- - 2\theta_z \tag{D.11}$$

so that

$$\langle\pi^-|\ \theta^-\theta^+\ |\pi^-\rangle = \langle\pi^-|\ \theta^+\theta^- - 2\theta_z\ |\pi^-\rangle$$

$$= -(-2)$$

$$= 2$$

so that (D.10) becomes

$$\frac{1}{2}\langle\pi^-|\langle\Phi|\ f_1^- f_2^-(2\tau_{1_z}\tau_{2_z} + 2(\tau_1^+\tau_2^- + \tau_2^+\tau_1^-)) + \ldots\ |\Phi\rangle|\pi^-\rangle \tag{D.12}$$

To obtain the remaining factors, the relations (D.13) are used

$$\tau^-|p\rangle = \sqrt{\tau(\tau+1) - \tau_z(\tau_z - 1)}\ |n\rangle = |n\rangle$$

$$\tau^+|n\rangle = \sqrt{\tau(\tau+1) - \tau_z(\tau_z + 1)}\ |p\rangle = |p\rangle \tag{D.13}$$

and considering one ordering of the nucleons (the symmetry of the

nucleus providing the others) with

$$1 \longleftrightarrow p\uparrow$$
$$2 \longleftrightarrow n\uparrow$$
$$3 \longleftrightarrow p\downarrow$$
$$4 \longleftrightarrow n\downarrow$$

then from (D.12), and including a factor of (-1) with each interchange of rows of (D.2) we obtain

$$f_{12} + f_{21} \longrightarrow 2x1x(-1) + 2x(0+1)x(-1) = -2 -2 = -4$$
$$f_{13} + f_{31} \longrightarrow +2$$
$$f_{14} + f_{41} \longrightarrow -2$$
$$f_{23} + f_{32} \longrightarrow -2$$
$$f_{24} + f_{42} \longrightarrow +2$$
$$f_{34} + f_{43} \longrightarrow -2 -2 = -4$$

so that

$$\langle \pi^-|\langle \Phi | \; f_j^- f_k^- \; |\Phi\rangle|\pi^-\rangle = -4\, f^-(\underline{q}_j)\, f^-(\underline{q}_k) \qquad (D.14)$$

$\underline{g_j^+ g_k^+}$: This term is evaluated by similar methods to the previous term, by making the assumption that the vectors $\underline{n}_j$, $\underline{n}_k$ are equal, an assumption present in all the spin-dependent parts of the calculation which considers the multiple-scattering to be coplanar, giving the form

$$\frac{1}{2}\langle \pi^-|\langle \Phi | \; g^+(\underline{\sigma}_j.\underline{n})g^+(\underline{\sigma}_k.\underline{n}) + g^+(\underline{\sigma}_k.\underline{n})g^+(\underline{\sigma}_j.\underline{n}) \; |\Phi\rangle|\pi^-\rangle \qquad (D.15)$$

and since we are free to choose axes, $\underline{n}$ is chosen to lie along the y - axis so that (D.15) becomes

$$\frac{1}{2}\langle\pi^-|\langle\Phi|\ g_j^+ g_k^+ (\ \sigma_y^j \sigma_y^k + \sigma_y^k \sigma_y^j\ )\ |\Phi\rangle|\pi^-\rangle \qquad (D.16)$$

and using

$$\sigma_y = i(\sigma^- - \sigma^+) \quad (D.16) \text{ becomes}$$

$$-\frac{1}{2}\langle\pi^-|\langle\Phi|\ g_j^+ g_k^+\ (\sigma_j^- - \sigma_j^+)(\sigma_k^- - \sigma_k^+) + (\sigma_k^- - \sigma_k^+)(\sigma_j^- - \sigma_j^+)\ |\Phi\rangle|\pi^-\rangle$$

which may be reduced to

$$\frac{1}{2}\langle\pi^-|\langle\Phi|\ g_j^+ g_k^+ (\ \sigma_j^+\sigma_k^- + \sigma_j^-\sigma_k^+ + \sigma_k^+\sigma_j^- + \sigma_k^-\sigma_j^+\ )|\Phi\rangle|\ \pi^-\rangle \qquad (D.17)$$

and using the same relations as before and the same ordering of the four nucleons we obtain

$$\begin{aligned} f_{12} + f_{21} &= 0 \\ f_{13} + f_{31} &= -2 \\ f_{14} + f_{41} &= 0 \\ f_{23} + f_{32} &= 0 \\ f_{24} + f_{42} &= -2 \\ f_{34} + f_{43} &= 0 \end{aligned}$$

so that

$$\langle\pi^-|\langle\Phi|\ g_j^+ g_k^+\ |\Phi\rangle|\pi^-\rangle = -2\ g^+(\underline{q}_j)\ g^+(\underline{q}_k) \qquad (D.18)$$

$\underline{g_j^- g_k^-}$: The calculation for this element is simply a combination of the calculations for the preceding two elements and so the contribution of each term is a product of the two corresponding terms. Hence using the same ordering of nucleons, the contributions are

$$f_{12} + f_{21} = (-4)x0 = 0$$
$$f_{13} + f_{31} = 2x(-2) = -4$$
$$f_{14} + f_{41} = 0$$
$$f_{23} + f_{32} = 0$$
$$f_{24} + f_{42} = -4$$
$$f_{34} + f_{43} = 0$$

so that the total contribution is $-8/2 = -4$ and so

$$\langle \pi^- | \langle \Phi | g_j^- g_k^- | \Phi \rangle | \pi^- \rangle = -4\, g^-(\underline{q}_j)\, g^-(\underline{q}_k) \qquad (D.19)$$

$\underline{f_j^+ f_k^-}$: The two terms of this form have zero matrix elements since the operation of $f^-(\theta\tau)$ alone was shown to result in a zero coefficient for single scattering so that the product terms of this type are likewise zero.

Hence from (D.6), $G^2(\underline{q}_j,\underline{q}_k)$ takes the form

$$G^2(\underline{q}_j,\underline{q}_k) = 6\, f^+(\underline{q}_j)f^+(\underline{q}_k) - 4\, f^-(\underline{q}_j)f^-(\underline{q}_k) - 2\, g^+(\underline{q}_j)g^+(\underline{q}_k) - 4\, g^-(\underline{q}_j)g^-(\underline{q}_k)$$

A similar result has been obtained by Querrou[61] using similar arguments but has not been extended beyond the second term. Baier & Samaranayake[64] have evaluated the elements for G^1 - G^4 and a complete list of these is repeated in table D I.

It is also interesting to calculate the same elements for the scattering of positive pions, such calculations obtaining expressions identical with the above. Unfortunately there is as yet no $\pi^{+-}{}^4$He data available and we would suggest that such an experiment would

provide an interesting test of isospin invariance and at small angles would permit measurement of the coulomb effects, this being the sole cause of the difference in differential cross-section between π^- and π^+ scattering.

Table D I The coefficients $G^j(\underline{q}_1,..,\underline{q}_j)$

$$G^1(\underline{q}_j) = 4 f_j^+$$

$$G^2(\underline{q}_j,\underline{q}_k) = 6 f_j^+ f_k^+ - 4 f_j^- f_k^- - 2 g_j^+ g_k^+ - 4 g_j^- g_k^-$$

$$G^3(\underline{q}_i,\underline{q}_j,\underline{q}_k) = 4 f_i^+ f_j^+ f_k^+ - 8 f_i^+ f_j^- f_k^- - 8 f_i^+ g_j^- g_k^- - 4 f_i^+ g_j^+ g_k^+ + 16 f_i^- g_j^+ g_k^-$$

$$G^4(\underline{q}_i,\underline{q}_j,\underline{q}_k,\underline{q}_m) = f_i^+ f_j^+ f_k^+ f_m^+ + \frac{10}{3} f_i^- f_j^- f_k^- f_m^- + g_i^+ g_j^+ g_k^+ g_m^+ + \frac{10}{3} g_i^- g_j^- g_k^- g_m^- - 4 f_i^+ f_j^+ f_k^- f_m^- - 4 g_i^+ g_j^+ g_k^- g_m^- - 2 f_i^+ f_j^+ g_k^+ g_m^+ - \frac{20}{3} f_i^- f_j^- g_k^- g_m^- - 4 f_i^+ f_j^+ g_k^- g_m^- - 4 g_i^+ g_j^+ f_k^- f_m^- + 16 f_i^+ f_j^- g_k^+ g_m^-$$

APPENDIX E Evaluation of the Multiple Integrals

The program DSDT must evaluate a large number of integrals for any of the forms of input described. By describing the most complicated form that the expansion (6.23) may take, the more simple cases encountered may then be obtained by reduction of the resultant expression. As a result this Appendix describes the integral of (6.23) with a completely correlated nuclear density of the form (6.33) and with all parameters taken to be different.

The first integrals required are over the momentum transfers $\underline{q}'_j$, no increased complexity occurs with the increase in j however as these integrals are independent of one another.

For a gaussian input the integrals over momentum transfer are easily performed provided that the limits of $\underline{q}'$ are taken to be infinite, whereas more correctly $q^2 \leq 4k^2$ where $\underline{k}$ is the incident momentum. For rapidly falling gaussians this forms only a small error and permits a simple analytic evaluation of the integral, which then takes the form

$$\begin{aligned} I_q &= \int d^2\underline{q}\; e^{-i\underline{q}.(\underline{b}-\underline{s})}\; e^{-\alpha q^2} \\ &= \int_0^{2k} q\,dq \int_0^{2\pi} d\Phi\; e^{-\alpha q^2}\; e^{-q|\underline{b}-\underline{s}|\cos\Phi} \\ &= 2\pi \int_0^{2k} q\,dq\; e^{-\alpha q^2}\; J_0(q|\underline{b}-\underline{s}|) \end{aligned} \qquad (E.1)$$

and as $2k \longrightarrow \infty$, this becomes

$$I_q = \frac{\pi}{\alpha} \exp\left[-\left| \frac{\underline{b}-\underline{s}}{4\alpha} \right|^2 \right] \qquad (E.2)$$

The following integrals over the spacial co-ordinates are

considerably complicated by the c.m. constraint δ-function which results in more involved forms. To obtain the result for four-fold scattering with full correlations, (E.2) is rewritten with $\gamma_i = \frac{1}{4a_i}$ for particle i to give

$$I_q^i = \frac{\pi}{a_i} \exp\left[-\gamma_i |\underline{b} - \underline{s}_i|^2\right] \qquad (E.3)$$

so that the spacial integral becomes

$$I_s = \int d\underline{r}_1 d\underline{r}_2 d\underline{r}_3 d\underline{r}_4 \; \delta\left(\frac{1}{4}\sum_i \underline{r}_i\right) \exp\left[-a_1^2 r_1^2 - a_2^2 r_2^2 - a_3^2 r_3^2 - a_4^2 r_4^2\right] \quad x$$

$$x \quad \exp\left[-\mu_1^2(\underline{r}_1-\underline{r}_2)^2 - \mu_2^2(\underline{r}_1-\underline{r}_3)^2 - \mu_3^2(\underline{r}_1-\underline{r}_4)^2 - \mu_4^2(\underline{r}_2-\underline{r}_3)^2 - \mu_5^2(\underline{r}_2-\underline{r}_4)^2 - \right.$$

$$\left. - \mu_6^2(\underline{r}_3-\underline{r}_4)^2\right] \exp\left[-\gamma_1|\underline{b}-\underline{s}_1|^2 - \gamma_2|\underline{b}-\underline{s}_2|^2 - \gamma_3|\underline{b}-\underline{s}_3|^2 - \gamma_4|\underline{b}-\underline{s}_4|^2\right]$$

(E.4)

and where the program DSDT is responsible for the different combinations of the values of α, γ, and μ for each case. For an uncorrelated density the result may easily be obtained by putting $\mu_i = 0$, i = 1,..,6 and similarly the lower scattering orders are obtained by setting the relevant $\gamma_j = 0$.

The δ-function in (E.4) may then be included explicitly, by removing $\underline{r}_4$, writing $\underline{r}_4 = -(\underline{r}_1 + \underline{r}_2 + \underline{r}_3)$ so that (E.4) becomes

$$I_s = \int d\underline{r}_1 d\underline{r}_2 d\underline{r}_3 \exp\left[-a_1^2 r_1^2 - a_2^2 r_2^2 - a_3^2 r_3^2 - a_4^2(\underline{r}_1+\underline{r}_2+\underline{r}_3)^2\right] \exp\left[-\mu_1^2(\underline{r}_1-\underline{r}_2)^2 - \right.$$

$$- \mu_2^2(\underline{r}_1-\underline{r}_3)^2 - \mu_3^2(2\underline{r}_1+\underline{r}_2+\underline{r}_3)^2 - \mu_4^2(\underline{r}_2-\underline{r}_3)^2 - \mu_5^2(\underline{r}_1+2\underline{r}_2+\underline{r}_3)^2 -$$

$$\left. - \mu_6^2(\underline{r}_1+\underline{r}_2+2\underline{r}_3)^2\right] \exp\left[-\gamma_1|\underline{b}-\underline{s}_1|^2 - \gamma_2|\underline{b}-\underline{s}_2|^2 - \gamma_3|\underline{b}-\underline{s}_3|^2 - \gamma_4|\underline{b}+\underline{s}_1+\underline{s}_2+\underline{s}_3|^2\right]$$

(E.5)

In the following pages, (E.5) is evaluated using a cartesian frame, since despite the cylindrical nature of the problem, this proved the most convenient frame and all the integrals may be evaluated using the two standard forms

$$\int_{-\infty}^{\infty} dx \exp\left[-q^2 x^2\right] = \frac{\sqrt{\pi}}{q} \qquad (E.6)$$

$$\int_{-\infty}^{\infty} dx \exp\left[-p^2 x^2 \pm q x\right] = \frac{\sqrt{\pi}}{p} \exp\left[q^2/4p^2\right] \qquad (E.7)$$

Rewriting (E.5) in the form

$$I_5 = \int d\underline{r}_1\, d\underline{r}_2\, d\underline{r}_3 \exp\Big[-(\alpha_1^2+\alpha_4^2) r_1^2 - (\alpha_2^2+\alpha_4^2) r_2^2 - (\alpha_3^2+\alpha_4^2) r_3^2 - 2\alpha_4^2 \underline{r}_1\cdot\underline{r}_2 -$$

$$- 2\alpha_4^2 \underline{r}_3\cdot(\underline{r}_1+\underline{r}_2) \Big] \exp\Big[-\gamma_1 |\underline{b}-\underline{s}_1|^2 - \gamma_2 |\underline{b}-\underline{s}_2|^2 - \gamma_3 |\underline{b}-\underline{s}_3|^2 - \gamma_4 |\underline{b}+\underline{s}_1+\underline{s}_2+\underline{s}_3|^2 \Big] \times$$

$$\times \exp\Big[-2\underline{s}_1\cdot\underline{s}_2 (2\mu_3^2 + 2\mu_6^2 + \mu_6^2 - \mu_1^2) - 2\underline{s}_1\cdot\underline{s}_3 (2\mu_3^2 + 2\mu_6^2 + \mu_5^2 - \mu_2^2) -$$

$$- 2\underline{s}_2\cdot\underline{s}_3 (2\mu_3^2 + 2\mu_6^2 + \mu_3^2 - \mu_4^2) \Big] \exp\Big[-(\mu_1^2 + \mu_2^2 + \mu_5^2 + \mu_6^2 + 4\mu_3^2) r_1^2 -$$

$$- (\mu_1^2 + \mu_3^2 + \mu_4^2 + 4\mu_5^2 + \mu_6^2) r_2^2 - (\mu_2^2 + \mu_3^2 + \mu_4^2 + \mu_5^2 + 4\mu_6^2) r_3^2 \Big]$$

and making the substitutions

$$\rho_i^2 = \alpha_i^2 + \gamma_i \qquad i = 1, \ldots, 4 \qquad (E.8)$$

and

$$\delta^2 = \sum_{i=1}^{6} \mu_i^2 \qquad (E.9)$$

this becomes

$$I_5 = \int d\underline{r}_1 d\underline{r}_2 \exp\left[-(\gamma_1+\gamma_2+\gamma_3+\gamma_4)b^2\right] \exp\left[-(\alpha_1^2+\alpha_4^2+\delta^2-\mu_4^2+3\mu_3^2)r_1^2 - \right.$$

$$- (\alpha_2^2+\alpha_4^2+\delta^2-\mu_2^2+3\mu_5^2)r_2^2 - 2\alpha_4^2 \underline{r}_1\cdot\underline{r}_2 - (\gamma_1+\gamma_4)s_1^2 - (\gamma_2+\gamma_4)s_2^2 + 2(\gamma_1-\gamma_4)\underline{b}\cdot\underline{s}_1$$

$$\left. + 2(\gamma_2-\gamma_4)\underline{b}\cdot\underline{s}_2 - 2\gamma_4 \underline{s}_1\cdot\underline{s}_2 - 2\underline{r}_1\cdot\underline{r}_2(2\mu_3^2+2\mu_5^2+\mu_6^2-\mu_1^2)\right] \times$$

$$\times \int d\underline{r}_3 \exp\left[-(\alpha_3^2+\alpha_4^2+\delta^2-\mu_1^2+3\mu_6^2)r_3^2 + (\gamma_3+\gamma_4)s_3^2 - 2\alpha_4^2 \underline{r}_3\cdot(\underline{r}_1+\underline{r}_2) + \right.$$

$$\left. + 2(\gamma_3-\gamma_4)\underline{b}\cdot\underline{s}_3 - 2\gamma_4 \underline{s}_3\cdot(\underline{s}_1+\underline{s}_2) - 2\underline{r}_1\cdot\underline{r}_3(2\mu_3^2+2\mu_6^2+\mu_5^2-\mu_2^2) - 2\underline{r}_2\cdot\underline{r}_3(2\mu_5^2+2\mu_6^2+\mu_3^2-\mu_4^2)\right]$$

and writing

$$\begin{aligned} A_1^2 &= 2\mu_3^2 + 2\mu_5^2 + \mu_6^2 - \mu_1^2 \\ A_2^2 &= 2\mu_3^2 + 2\mu_6^2 + \mu_5^2 - \mu_2^2 \\ A_3^2 &= 2\mu_5^2 + 2\mu_6^2 + \mu_3^2 - \mu_4^2 \end{aligned} \qquad (E.10)$$

the integral over $\underline{r}_3$ in cartesians takes the form

$$I_6^3 = \int dz_3 \exp\left[-(\alpha_3^2+\alpha_4^2+\delta^2-\mu_1^2+3\mu_6^2)z_3^2 - 2z_3\left\{(A_2^2+\alpha_4^2)z_1 + (\alpha_4^2+A_3^2)z_2\right\}\right] \times$$

$$\times \int dx_3 \exp\left[-(\rho_3^2+\rho_4^2+\delta^2-\mu_1^2+3\mu_6^2)x_3^2 - 2x_3\left\{(\rho_4^2+A_2^2)x_1 + (\rho_4^2+A_3^2)x_2\right\} + 2(\gamma_3-\gamma_4)b_x x_3\right] \times$$

$$\times \int dy_3 \quad (x \leftrightarrow y)$$

which using (E.6) and (E.7) becomes

$$I_5^3 = \pi^{1/2}(\alpha_3^2+\alpha_4^2+\delta^2-\mu_1^2+3\mu_6^2)^{-1/2}\pi\,(\rho_3^2+\rho_4^2+\delta^2-\mu_1^2+3\mu_6^2)^{-1} \times$$

$$\times \exp\left[\frac{\left\{(\alpha_4^2+A_2^2)z_1 + (\alpha_4^2+A_3^2)z_2\right\}^2}{\alpha_3^2+\alpha_4^2+\delta^2-\mu_1^2+3\mu_6^2}\right] \times$$

$$\times \exp\left[\frac{\left\{(\rho_4^2+A_2^2)x_1 + (\rho_4^2+A_3^2)x_2 - (\gamma_1-\gamma_4)b_x\right\}^2}{\rho_3^2+\rho_4^2+\delta^2-\mu_1^2+3\mu_6^2}\right] \exp\left[x \leftrightarrow y\right]$$

and for further simplification we may write

$$A^{-2} = \alpha_3^2 + \alpha_4^2 + \delta^2 - \mu_1^2 + 3\mu_6^2$$

$$R^{-2} = \rho_3^2 + \rho_4^2 + \delta^2 - \mu_1^2 + 3\mu_6^2 \qquad (E.11)$$

so that I_5 becomes

$$I_5 = (\pi A^2)^{1/2} \pi R^2 \exp\left[-(\gamma_1+\gamma_2+\gamma_3+\gamma_4)b^2 + R^2(\gamma_3-\gamma_4)^2 b^2\right] \times$$

$$\times \int d\underline{r}_1 \exp\left[-(\alpha_1^2+\alpha_4^2+\delta^2+3\mu_5^2-\mu_4^2)r_1^2 - (\gamma_1+\gamma_4)s_1^2 + 2(\gamma_1-\gamma_4)\underline{b}\cdot\underline{s}_1 + A^2(\alpha_4^2+A_2^2)^2 z_1^2\right.$$

$$\left. + R^2(\rho_4^2+A_2^2)^2 s_1^2 - 2R^2(\gamma_3-\gamma_4)(\rho_4^2+A_2^2)\underline{b}\cdot\underline{s}_1\right] \times \int d\underline{r}_2 \exp\left[-(\alpha_2^2+\alpha_4^2+\delta^2-\mu_2^2+3\mu_5^2)r_2^2 -\right.$$

$$- (\gamma_2-\gamma_4)s_2^2 - 2\alpha_4^2 \underline{r}_1\cdot\underline{r}_2 - 2\gamma_4 \underline{s}_1\cdot\underline{s}_2 - 2A_1^2 \underline{r}_1\cdot\underline{r}_2 + 2(\gamma_2-\gamma_4)\underline{b}\cdot\underline{s}_2 + A^2(\alpha_4^2+A_3^2)^2 z_2^2$$

$$\left. + 2A^2(\alpha_4^2+A_2^2)(\alpha_4^2+A_3^2) z_1 z_2 + R^2(\rho_4^2+A_3^2)^2 s_2^2 + 2R^2(\rho_4^2+A_2^2)(\rho_4^2+A_3^2)\underline{s}_1\cdot\underline{s}_2 -\right.$$

$$\left. - 2R^2(\gamma_3-\gamma_4)(\rho_4^2+A_3^2)\underline{b}\cdot\underline{s}_3\right]$$

The integral over $\underline{r}_2$ may be written as

$$I_5^2 = \int dz_2 \exp\left[-P_1^2 z_2^2 + 2Q_1^2 z_1 z_2\right] \int dx_2 \exp\left[-P_2^2 x_2^2 + 2(Q_2^2 x_1 + Q_3^2 b_x)x_2\right] \times$$

$$\times \int dy_2 \quad (x \leftrightarrow y)$$

where

$$P_1^2 = \left\{(\alpha_2^2+\alpha_4^2+\delta^2-\mu_2^2+3\mu_5^2)(\alpha_3^2+\alpha_4^2+\delta^2-\mu_1^2+3\mu_6^2) - (\alpha_4^2+A_3^2)^2\right\} A^2$$

$$P_2^2 = \left\{(\rho_2^2+\rho_4^2+\delta^2-\mu_2^2+3\mu_5^2)(\rho_2^2+\rho_4^2+\delta^2-\mu_1^2+3\mu_6^2) - (\rho_4^2+A_3^2)^2\right\} R^2$$

$$Q_1^2 = \left\{(\alpha_4^2+A_2^2)(\alpha_4^2+A_3^2) - (\alpha_4^2+A_1^2)(\alpha_3^2+\alpha_4^2+\delta^2-\mu_1^2+3\mu_6^2)\right\} A^2$$

$$Q_2^2 = \{ (\rho_4^2+A_2^2)(\rho_4^2+A_2^2) - (\rho_4^2+A_1^2)(\rho_3^2+\rho_4^2+\delta^2-\mu_1^2+3\mu_6^2) \} R^2$$

$$Q_3^2 = \{ (\gamma_2-\gamma_4)(\rho_3^2+\rho_4^2+\delta^2-\mu_1^2+3\mu_2^2) - (\gamma_3-\gamma_4)(\rho_4^2+A_2^2) \} R^2 \qquad (E.12)$$

so that

$$I_5^2 = \left(\frac{\pi}{P_1^2}\right)^{1/2}\left(\frac{\pi}{P_2^2}\right) \exp\left[\frac{Q_1^4 z_1^2}{P_1^2} + \frac{(Q_2^2 x_1 + Q_3^2 b_x)^2 + (Q_2^2 y_1 + Q_3^2 b_y)^2}{P_2^2} \right]$$

to give for I_5

$$I_5 = \pi^3\left(\frac{A^2}{P_1^2}\right)^{3/2}\left(\frac{R^2}{P_2^2}\right) \exp\left[-(\gamma_1+\gamma_2+\gamma_3+\gamma_4)b^2 + R^2(\gamma_3-\gamma_4)^2 b^2 + Q_3^4/P_2^2 b^2 \right] \times$$

$$\times \int d\underline{r}_1 \exp\left[-(\alpha_1^2+\alpha_4^2+\delta^2-\mu_4^2+3\mu_3^2) r_1^2 + A^2(\alpha_4^2+A_2^2) z_1^2 + \frac{Q_1^4}{P_1^2} z_1^2 - (\gamma_1-\gamma_4)\varepsilon_1^2 + \right.$$

$$\left. + R^2(\rho_4^2+A_2^2)^2 + Q_2^4/P_2^2 \varepsilon_1^2 + 2(\gamma_1-\gamma_4)\underline{b}\cdot\underline{\varepsilon}_1 - 2R^2(\gamma_3-\gamma_4)(\rho_4^2+A_2^2)\underline{b}\cdot\underline{\varepsilon}_1 + \frac{2Q_2^2Q_3^2}{P_2^2}\underline{b}\cdot\underline{\varepsilon}_1 \right]$$

The integral over $\underline{r}_1$ then has the form

$$I_5' = \int dz_1 \exp\left[-\left\{ (\alpha_1^2+\alpha_4^2+\delta^2-\mu_4^2+3\mu_3^2) - A^2(\alpha_4^2+A_2^2)^2 - Q_1^4/P_1^2 \right\} z_1^2 \right] \times$$

$$\times \int dx_1 \exp\left[-\left\{ (\rho_1^2+\rho_4^2+\delta^2-\mu_4^2+3\mu_3^2) - R^2(\rho_4^2+A_2^2)^2 - Q_2^4/P_2^2 \right\} x_1^2 + \right.$$

$$\left. + 2b_x x_1 \left\{ (\gamma_1-\gamma_4) - 2R^2(\gamma_3-\gamma_4)(\rho_4^2+A_2^2) + \frac{Q_2^2Q_3^2}{P_2^2} \right\} \right] \int dy_1 \; (x \leftrightarrow y)$$

so that we finally obtain

$$I_5 = \pi^{9/2} \frac{A}{P_1} \frac{R^2}{P_2^2} \left\{ (\alpha_1^2+\alpha_4^2+\delta^2-\mu_4^2+3\mu_3^2) - A^2(\alpha_4^2+A_2^2)^2 - Q_1^4/P_1^2 \right\}^{-1/2} \left\{ (\rho_1^2+\rho_4^2+\delta^2-\mu_4^2+3\mu_3^2) - \right.$$

$$\left. - R^2(\rho_4^2+A_2^2) - Q_2^4/P_2^2 \right\}^{-1} \exp\left[\left\{ -(\gamma_1+\gamma_2+\gamma_3+\gamma_4) + R^2(\gamma_3-\gamma_4)^2 + Q_3^4/P_2^2 + \right.\right.$$

$$\left.\left. + \frac{\left\{ (\gamma_1-\gamma_4) - 2R^2(\gamma_3-\gamma_4)(\rho_4^2+A_2^2) + Q_2^2Q_3^2/P_2^2 \right\}^2}{\left\{ (\rho_1^2+\rho_4^2+\delta^2-\mu_1^2+3\mu_3^2) - R^2(\rho_4^2+A_2^2)^2 - Q_2^4/P_2^2 \right\}} \right\} b^2 \right] \qquad (E.13)$$

The terms of this expression may be rationalised and shown to possess an overall symmetric form. The final integral over $d^2\underline{b}$ of (6.23) is then performed in a similar manner to that demonstrated for $\underline{q}$ with simply a more complicated argument. A more elegant form of evaluation is given in the Appendix to the classic paper of Bassel and Wilkin[69] who give a more general form for evaluating the resultant terms.

In order to evaluate these, the program DSDT was organised in the following manner. The main routine of DSDT organised the reading of the input, the construction of the multiple scattering amplitudes and the construction of the actual differential cross-sections. In order to calculate each integral a permutation subroutine was first called, which determined the combinations of the parameters of the basic nuclear density and for each of these this then called another subroutine. This next subroutine in turn performed the task of permuting the terms from the correlation series and then in turn this called the final subroutine in which the actual integral was evaluated. Terms lower than the fourth order were obtained by putting the relevant $\gamma_i = 0$ and by means of options within the permutation subroutines the calculations could be performed for any of the nuclear densities employed.

REFERENCES

1) A. Donnachie Scottish Universities Summer School 1966, Ed. T. Priest & L. Vick. Oliver & Boyd.

A. Barbaro-Galtieri Advances in Particle Physics Vol.2, Ed. R. Cool & R. Marshak. Interscience.

C. Lovelace Proc. Heidelberg Int. Conference 1967, Ed. H. Filthuth. North-Holland.

2) E. Mertzbacher P 171, 'Quantum Mechanics', Wiley.

3) Review of Particle Properties Phys.Lett. 39B,1,(1972) and references therein.

4) P. Bareyre, C. Bricman & G. Villet Phys.Rev. 165,1730,(1968)

5) M.H. MacGregor, M.J. Moravcsik & H.P. Stapp Ann. Rev. Nuc. Sci. 10,291,(1960) also see ref.(33)

6) R.K. Roychoudhury, R. Perrin & B.H. Bransden Nuc.Phys.B16,461,(1970)

B.H. Bransden & P.J. Ogden Nuc.Phys. B26, 511, (1971)

R.K. Roychoudhury & B.H. Bransden Nuc.Phys. B27, 125, (1971)

7) P.J. Litchfield Nuc.Phys. B22, 269, (1970)

P.J. Litchfield et al. Nuc.Phys. B30, 125, (1971)

8) M. Jacob & G.C. Wick Ann.Phys. 7, 404, (1959)

M. Goldberger & R.M. Watson 'Collision Theory' , Wiley.

9) N.F. Mott & H.S.W. Massey 'The theory of Atomic Collisions' O.U.P.

10) M.E. Rose 'Theory of Angular Momentum' , Wiley.

11) S. Minami Progr.Theoret.Phys.(Kyoto) 11, 213, (1954)

A. Gersten Nuc.Phys. B12, 537, (1969)

12) R. Armentaros et al. Nuc.Phys. B21, 15, (1970)

13) M.B. Watson,M. Ferro-Luzzi & R.D. Tripp Phys.Rev. 131, 2248, (1963)

14) R.D. Tripp 'Duke Conference on Hyperon Resonances', 95 Durham N.C. (1970)

15) M.H. Alston et al. Phys.Rev.Lett. 6, 698, (1961)
A.D. Martin 'Springer Tracts in Modern Physics', Vol 55 page 142, (1970)

16) R. Levi Setti Lund Conference , Ed. R. Von Dardel (Lund 1969)

17) P. Eberhard et al. Phys.Rev.Lett. 22, 200, (1969)
M. Aguilar-Benitez et al. Phys.Rev.Lett. 25, 58, (1970)
R.D. Estes et al. Duke Conference , 279, Durham N.C. 1970
C. Watal & B.K. Agarwal Lett.al Nuovo Cim. 2, 911, (1971)

18) D.H. Miller Duke Conference , 229 , Duke N,C. 1970

19) J.K. Kim Phys.Rev.Lett. 27, 356, (1971)
Duke Conference , 161 , Durham N.C. 1970

20) R. Armentaros et al. Duke Conference, 123 , Durham N.C. 1970

21) For a review of different analyses and comparison of results see M.L. Gupta et al. to be published in Fortschr. Phys.

22) A. Barbaro-Galtieri 'Advances in Particle Physics' 2, 210

23) W.M. Smart Phys.Rev. 169, 1330, (1968)

24) A.T.Lea, B.R. Martin & G.C. Oades Phys.Rev. 165, 1770, (1968)

25) a) R. Armentaros et al. Nucl. Phys. B8, 195, (1968)
b) R. Armentaros et al. Nucl. Phys. B8, 223, (1968)
c) R. Armentaros et al. Nucl. Phys. B14, 91, (1969)

26) P.J. Litchfield et al. Nuc. Phys. B30, 125, (1971)

27) R.D. Tripp in 'Proc. Int. School of Physics "Enrico Fermi" ' Course 33 , 1966. Academic.

28) R.H. Dalitz & R.G. Moorhouse Proc.Roy.Soc.Lond. A318, 279,(1970)

29) S. Coleman 'Int. School of subnuclear Physics "Ettore Majorana" '

30) G. Breit & E. Wigner Phys. Rev. 49, 519, (1936)

31) E.P. Wigner Phys. Rev. 98, 145, (1955)

32) C. Michael Phys.Lett. 21, 93, (1966)

33) J.M. Blatt & V.F. Weisskopf 'Theoretical Nuclear Physics' N.Y. 1952

34) S.L. Glashow & A.H. Rosenfeld Phys.Rev.Lett. 10, 192, (1963)

35) P.R. Bevington 'Data Reduction and Error Analysis for the Physical Sciences' McGraw-Hill 1969

36) MINUIT - CERN Program Library.

37) J.D. Jackson Nuovo Cim. 34, 1644, (1964)

38) C. Lanczos 'Applied Analysis' Pitman

39) D. Budgen Lett.al Nuovo Cim. 2, 85, (1971)

40) S. Miyashita & L.M. Libby Phys.Rev. 168, 1779, (1968)

41) R. Armentaros et al. Nuc. Phys. B8, 183, (1968)

42) H.S. Wong Nuovo Cim. 2A, 353, (1971)

43) M. Abramowitz & I.A. Stegun 'Handbook of Mathematical Functions' Dover N.Y.

44) D.M. Brink & G.R. Satchler 'Angular Momentum' O.U.P.

45) H.H. Rosenbrock Comp.J. 3, 175, (1960)

46) R.J. Glauber Phys. Rev. 100, 242, (1955)

47) R.J. Glauber 'Lectures in Theoretical Physics' Vol I Ed. W. Brittin & L. Dunham Interscience N.Y. 1959

48) R.J. Glauber 'High-Energy Physics & Nuclear Structure' Ed. G. Alexander North-Holland 1967

R.J. Glauber 'High-Energy Physics & Nuclear Structure' Ed. S.Devons Plenum 1970

49) V.S. Barashenkov & V.D. Toneev Sov.Phys USPEKHI 13,182, (1970)

W. Czyż 'Theory of Nuclear Structure' IAEA - Trieste 1969

50) V. Franco & R.J. Glauber Phys. Rev. 142, 1195, (1966)

51) R.J. Glauber & V. Franco Phys. Rev. 156, 1685, (1967)

52) V. Franco Phys.Rev.Lett. 21, 1360, (1968)

53) G. Alberi & L. Bertocchi Nuovo Cim. 63A, 285, (1969)

54) C. Wilkin Phys.Rev.Lett. 17 , 561 , (1966)

55) C. Michael & C. Wilkin Nuc. Phys. B11 , 99 , (1969)

56) F. Bradamante et al. Lett. al Nuovo Cim. 1 , 894 , (1969)

57) F. Bradamante et al. Phys. Lett. 31B , 87 , (1970)

58) T.T. Chou Phys. Rev. 168 , 1594 , (1968)

59) W. Czyż & L. Leśniak Phys. Lett. 25B , 319 , (1967)

60) J. Hüfner Nuc. Phys. B27 , 260 , (1971)

61) M. Querrou Nuovo Cim. 3A , 670 , (1971)

62) A.H. Cromer Nuc. Phys. B11 , 152 , (1969)

63) W. Czyż & L. Leśniak Phys. Lett. 24B , 227 , (1967)

64) H. Baier & V.K. Samaranayake Nuc. Phys. B24 , 273 , (1970)

65) H. Baier & V.K. Samaranayake Nuc. Phys. B15 , 67 , (1970)

66) J. Combe et al. Nuovo Cim. 3A , 663 , (1971)

67) T. Ekelof et al. Nuc. Phys. B35 , 493 , (1971)

68) R.H. Bassel & C. Wilkin Phys.Rev.Lett. 18 , 871 , (1967)

69) R.H. Bassel & C. Wilkin Phys. Rev. 174 , 1179 , (1968)

70) T. Kohmura Prog.Th.Phys. 46 , 167 , (1971)

71) H. Leśniak & L. Leśniak Nuc. Phys. B25 , 525 , (1971)

72) C. Ciofi Degli Atti & R. Guardiola Phys.Lett. 36B,287,(1971)

73) K. Bjornenak et al. Nuc. Phys. B22 , 179 , (1970)

74) R. Guardiola Nouvo Cim. 3A , 747 , (1971)

75) J.S. Trefil Phys. Rev. 180 , 1366 , 1379 , (1969)

76) J. Rohlin et al. Nuc. Phys. B37 , 461 , (1972)

77) C. Wilkin Lett. al Nuovo Cim. 4 , 491 , (1970)

78) R.J. Glauber & G. Matthaie Nuc. Phys. B21 , 135 , (1970)

79) O. Guisan et al. Nuc. Phys. B32 , 681 , (1971)

80) E.J. Moniz & G.D. Nixon Ann. Phys. 67 , 58 ,(1971)

81) H. Palevsky et al. Phys. Rev. Lett. 18 , 1200 , (1967)

82) I. Ahmad Phys. Lett. 36B , 301 , (1971)

83) L.I. Schiff Phys. Rev. 103 , 443 , (1956)

84) L.I. Schiff Phys. Rev. 176 , 1390 , (1968)

85) D.R. Harrington Phys. Rev. 184 , 1745 , (1969)

86) R. Blankenbecler & M.L. Goldberger Phys. Rev. 126,706,(1962)

87) R.L. Sugar & R. Blankenbecler Phys. Rev. 183 , 1387 , (1970)

88) S.J. Wallace Phys. Rev. Lett. 27 , 622 , (1971)

89) R.J. Moore Phys. Rev. D2 , 313 , (1970)

90) R. Blankenbecler & R.L. Sugar Phys.Rev. D2 , 3024 , (1970)

91) M. Lévy & J. Sucher Phys. Rev. 186 , 1656 , (1969)

92) C.B. Chiu Rev. Mod. Phys. 41 , 640 , (1969)

93) G. Tiktopoulos & S.B. Trieman Phys. Rev. D2 , 805 , (1970)

94) T. A. Osborn Ann. Phys. 58 , 417 , (1970)

95) E.S. Abers et al. Nuovo Cim. 42 , 365 , (1966)

96) J.M. Eisenberg Ann. Phys. 71 , 542 , (1972)

97) B.H. Bransden 'Atomic Collision Theory' Benjamin 1971

98) P.E. Hodgeson Ann. Rev. Nuc. Sci. 17 , 1 , (1967)

99) I. Úlehla, L. Gomolčák & Z. Pluhař
'Optical Model of the Atomic Nucleus' Academic Press 1964

100) C. Wilkin CERN Yellow Report 71-14 (1971)

101) L.S. Kisslinger Phys. Rev. 98 , 761 , (1955)

102) J.P. Maillet et al. Lett. al Nuovo Cim. 1 , 191 , (1971)

103) K.M. Watson Phys. Rev. 89 , 575 , (1953)
Phys. Rev. 105 , 1388 , (1957)

104) N.C. Francis & K.M. Watson Phys. Rev. 92 ,291 , (1953)

105) M. Goldberger & K.M. Watson 'Collision Theory' Wiley

106) S. Gartenhaus & C. Schwartz Phys. Rev. 108 , 482 , (1957)

107) L.J. Tassie & F.C. Barker Phys. Rev. 111 , 940 , (1958)

108) W. Czyż, L. Leśniak & H. Wołek Nuc. Phys. B19 , 125 , (1970)

109) F. Binon et al. Nuc. Phys. B17, 168 , (1970)

110) G. Giacomelli Riv. del Nuovo Cim. 2 , 297 , (1970)

111) C. Wilkin Phys. Rev. Lett. 17 , 561 , (1966)

112) N.N. Dean & J.L Friar Nuc. Phys. B19 , 301 , (1970)

113) M.L. Goldberger in ' Relation de dispersion et particules élémentaires ' Wiley

114) Y.A. Budagov et al. J.E.T.P. 15 , 824 , (1962)

115) R. Hofstadter Ann. Rev. Nuc. Sci. 7 , 231 , (1957)

116) R.J. Jastrow Phys. Rev. 98 , 1479 , (1955)

117) R.F. Frosch et al. Phys. Rev. 160 , 874 , (1967) and Bull. Am. Phys. Soc. 12 , 16 , (1967)

118) T. Stovall & D. Vinciguerra Lett. al Nuovo Cim. 1 , 100 , (1969)

119) A. Małecki & P. Picchi Phys. Rev. Lett. 21 , 1395 , (1968)

120) S. Fantoni et al. Nuovo Cim. 69A, 88 , (1970)

121) C. Ciofi Degli Atti Nuc. Phys. A129 , 350 , (1969)

122) F. Binon et al. '4-th Int. Conf. on H.E. Physics and Nuclear structure '

123) C. Schmit Lett. al Nuovo Cim. 4 , 454 , (1970)

124) C. Wilkin Lett. al Nuovo Cim. 4 , 491 , (1970)

125) G. Fäldt Phys. Rev. C5 , 400 , (1972)

126) I am grateful to Dr. P.J. Ogden for supplying these phase-shifts

127) H.K. Lee & H. McManus Nuc. Phys. A167 , 257 , (1971)

128) D. Budgen Lett. al Nuovo Cim. 5 , 160 , (1972)

129) Private Communication from T. Ekelof

130) K.J. Foley et al. Phys. Rev. 181 , 1775 , (1969) and Phys. Rev. Lett. 19 , 330 , (1967)

131) D. Harting et al. Nuovo Cim. 38 , 60 , (1965)

132) D.M. Brink 'Proc. Int. School of Physics " Enrico Fermi " ' XXXVI Academic Press 1966

133) K. Wildermuth & Th. Kanellopoulos CERN Yellow Report 59-23

134) D.M. Brink et al. Phys. Lett. 33B , 143 , (1970)
H. Friedrich & A. Weiguny Phys. Lett. 35B , 105 , (1971)

135) There are a number of printing errors in this paper, generally of signs a particular example being the transformation used in evaluating the double scattering terms which is in error.

136) E.V. Inopin et al. Sov. J. Nuc. Phys. 2 , 573 , (1966)

137) S.J. Biel Proc. Phys. Soc. A70 , 866 , (1957)

138) J.A. Wheeler Phys. Rev. 52 , 1083 , (1937)